UNIVERSITY of ROME "TOR VERGATA"

Faculty of Engineering

Ph. D. in

MATERIALS FOR ENVIRONMENT AND ENERGY

(XXI Cycle)

Hybrid Polymer Electrolytes for Proton Exchange Membrane Fuel Cells: Synthesis and Applications

Catia de Bonis

A.A. 2008/2009

Advisor: Prof. Silvia Licoccia

Coordinator: Prof. Enrico Traversa

Acknowledgements

I would like to thank:

Prof. Silvia Licoccia for her guidance, the insightful discussions and for the great possibility she offered me. This experience was really important for my professional and personal training.

Prof. Enrico Traversa for giving me this opportunity and for freedom in conducting research.

Dr. Alessandra D'Epifanio and Dr. Barbara Mecheri for their assistance and helpful advice.

Mrs. Cadia D'Ottavi for her valuable technical assistance.

Dr. M. Luisa Di Vona for her collaboration to this work.

Prof. Marcella Trombetta of the University "Campus Bio-Medico" of Rome, for her contribution to this work.

All members of the Chemistry and Engineering group of Tor Vergata University: Fang, Alma, Antonio, Laure, Chiara, Zakarya, Sherif, Alessandro, Nella, Emanuela, Andrea, Michele, Elisabetta, Debora, Vincenzo, Francesco, Corrado, Emiliana, Alessia, Simone, Milan, Alberto, Stefano and Marco, for their support and the enjoyable time we spent together.

My family and Emanuele for their patience, encouragement, and support.

This work has been financed by MIUR (FISR 2001 NUME Project Development of composite protonic membranes and innovative electrode configurations for Polymer Electrolyte Fuel Cells).

Abstract

Proton exchange membrane fuel cells (PEMFCs) are promising power sources emerging among alternative energy conversion systems, because they can operate at relatively low temperature and offer numerous benefits, such as high efficiency, high power density and low polluting emissions.

The present dissertation deals with the development of new proton conducting membranes having good conductivity, chemical and thermal stability, low methanol permeability and low cost.

The main strategy used in this work was the preparation of sulfonated and silylated polyetheretherketone (PEEK) and polyphenylsulfone (PPSU) as membrane materials, because this synthetic approach represents a powerful tool to modulate the proton conductivity and hydrolytic stability of the electrolyte by the dosage of sulfonic acid groups and inorganic moieties covalently bound to the aromatic chains.

Several types of proton exchange membranes were studied. Sulfonated and silylated PEEK and/or PPSU were used to prepare systems where two components resulted crosslinked by physical interactions or covalent bonds, obtaining the synergic effect of polymers having different conductivity and mechanical properties.

- Sulfonated and silylated polyetheretherketone $PhSi_{0.1}S_{0.9}PEEK$ (degree of sulfonation DS=0.9, and degree of silylation DSi=0.1) was synthesized *via* (i) sulfonation of PEEK, (ii) conversion of sulfonated polyetheretherketone ($S_{0.9}PEEK$) into sulfonyl chlorinated derivative (PEEKSO2Cl), (iii) lithiation of PEEKSO2Cl and subsequent addition of $PhSiCl_3$, followed by hydrolysis. The solubility of PEEKSO2Cl in organic solvent allows the silylation reaction to be carried out in homogeneous conditions. The structural characterization of the products by ^{1}H and ^{13}C NMR and ATR/FTIR spectroscopies highlighted the success of the synthetic pathway. The thermogravimetric analysis of PEEK derivatives indicated that the presence of the inorganic moieties stabilizes the aromatic matrix of the sulfonated polyetheretherketone. Blends of $PhSi_{0.1}S_{0.9}PEEK$ and $S_{0.5}PEEK$ (DS=0.5) were prepared using different weight ratios of the two polymers. The membranes were characterized by water uptake measurements and electrochemical impedance spectroscopy (EIS). The results converge

to indicate that the developed materials are promising electrolytes for PEMFC application.

- Silylated and sulfonated polyphenylsulfone $PhSi_{0.2}S_2PPSU$ (DS=2.0 and DSi=0.2) was synthesized *via* (i) lithiation of PPSU and subsequent addition of $PhSiCl_3$, followed by hydrolysis, (ii) sulfonation by reaction with concentrated sulphuric acid. The chemical structure of polymers was investigated by ^1H and ^{13}C NMR, and ATR/FTIR, verifying the success of the developed synthetic route.

Blends of $PhSi_{0.2}S_2PPSU$ and $S_{0.5}PEEK$ were prepared, obtaining electrolytes with higher hydrolytic stability and increased proton conductivity with respect to those of pure $S_{0.5}PEEK$ membrane. Blend membranes showed also better performance in DMFC, where a reduced methanol permeability and adequately high power density values were observed, at temperature values as high as 100°C. All these features identify the prepared blend membranes as promising electrolytes for DMFC operating at intermediate temperatures.

- Two silylated and sulfonated PPSU derivatives: $Si_{0.2}S_2PPSU$ (DS=2.0 and DSi=0.2) and $Si_{0.03}S_{0.05}PPSU$ (DS=0.05 and DSi=0.03) were synthesized following two different routes. In the first one, PPSU was silylated by reaction with $SiCl_4$, then sulfonated by reaction with concentrated sulphuric acid, and $Si_{0.2}S_2PPSU$ was obtained. In the second route, the use of the mild sulfonating agent $ClSO_3Si(CH3)_3$ allowed a careful control of the degree of sulfonation, and PPSU with a lower DS was obtained. Subsequent silylation by reaction with $SiCl_4$ led to the final product $Si_{0.03}S_{0.05}PPSU$.

An organic-inorganic hybrid polymer HSiSPPSU was synthesized by non-hydrolytic sol–gel reaction of $Si_{0.2}S_2PPSU$ and $Si_{0.03}S_{0.05}PPSU$. The condensation between the silanol groups of the two polymers led to the formation of Si-O-Si bonds, as highlighted by analysis of ATR/FTIR spectra.

The electrochemical characterization of HSiSPPSU membranes by EIS showed adequately high conductivity values to make the hybrid polymer a suitable candidate for application in PEMFCs operating at $T > 100$°C.

The strategies followed in this work seems to be an effective way to overcome some drawbacks related to conventional polymer membranes currently used, demonstrating the relevant role played by synthesis in the preparation of electrolytes for PEMFCs.

Table of Contents

1 Introduction

1.1 Power Generation from an Environmental Sustainability Perspective

Throughout the world, the need of the hour is power generation coupled with environmental protection because energy use from traditional sources, such as burning fossil fuels, poses serious challenges to human health, energy security and sustainability of natural resources.

Since the last century, alternative energy sources economy has been proposed as alternative to the current fossil-fuel economy. This alternative economy is based on fuel cells and other renewable sources like photovoltaic, hydro electric and wind power.

Fuel cells are one of the most important devices because they convert the chemical energy of the fuel into electrical energy with high efficiency, minimal environmental pollution and low maintenance costs.

They are one of the oldest electrical energy conversion technologies known to man because fuel cell experiments were performed by Sir William Grove as early as in 1842. Unfortunately, fuel cells were forgotten until the middle of the 20th century due to the invention of the combustion engine. They exhibited some renaissances in the 1960's, in the US Apollo space program, and during the first oil crisis in 1973, when especially the interest for large power plants based on high-temperature fuel cells increased.

In the last decades, the focus on environmental and pollution problems has made the world search for cleaner energy technology, and fuel cells have experienced increasing interest from governments and industry.

Among the different type of fuel cells, Proton Exchange Membrane Fuel Cells (PEMFCs), offer great promise as a clean and efficient technology for energy generation and provide significant environmental benefits. Since PEMFCs are modular and have a simple design, they can be scaled up in size to suit the demands of a variety of applications. They have the potential to revolutionize transportation, which consumes 60% of the worldwide production of oil, improve stationary power generation, thereby reducing dependence on the electrical grid, and provide reliable portable power for our ever-increasing array of personal electronic devices.

Conventional proton exchange membranes (PEM) are based on polymers in their protonated form. These materials are typically phase separated into a percolating network of hydrophilic nano-pores embedded in a hydrophobic polymer-rich phase domain. The hydrophilic nano-pores contain the acidic moieties which ensure the proton conductivity. The hydrophobic phase domain provides mechanical strength by stabilizing the morphology of the membrane.

Nowadays, Nafion is the most widely used polymer electrolyte for PEMFCs due to its excellent oxidative stability, high proton conductivity and good mechanical strength within the operating environment of the cell.

However, Nafion and similar perfluorinated polymers have relevant drawbacks, including decrease of conductivity at temperature over 80 °C, high methanol permeability, and high cost that is incommensurate with potential mass markets.

Consequently, a major trend in the present research activities is the preparation of alternative membrane materials which performance would be less affected by humidification, temperature and fuel crossover to overcome the barriers in the wide commercialization of PEMFCs.

Among the different materials alternative to Nafion that are investigated, aromatic polymers are considered to have the proper features as membrane materials. They are low-cost polymers with good oxidative and thermal resistance and their chemical structure opens up a wide window of chemical modification opportunities, including the introduction of sulfonic moieties to obtain proton-conducting materials.

In fact, the synthesis of functionalized polymers represents a very promising way to obtain electrolytes having the desired features because it allows to prepare tailored materials for specific applications.

1.2 Research Objective

The purpose of the present dissertation is to develop new polymer electrolytes with good proton conductivity and the required chemical and morphological stability for PEMFCs applications.

The aromatic polymers *Polyetheretherketone* (PEEK) and *Polyphenylsulfone* (PPSU) were chosen as starting materials due to their promising features as membrane materials. These polymers show excellent chemical resistance, high thermo-oxidative stability, good mechanical properties, ease of direct functionalization and low cost.

However, in these systems the high degree of sulfonation required to attain proper conductivity values leads to highly swollen or even water soluble products, lowering mechanical and morphological properties.

Hence, several approaches were followed to modulate the ratio between hydrophilic and hydrophobic domains: such ratio, in fact, determines hydrolytic stability and conductivity, which balance will, eventually, be responsible of the electrolyte performance under fuel cell operating conditions.

Different systems were thus studied:

- Derivatives of PEEK and PPSU with silicon-containing moieties covalently linked to the aromatic chain were synthesized. The used synthetic strategies allowed to tailor the molecular structures controlling the amount of inorganic moieties to obtain polymers with high sulfonation degree and hydrolytic stability.
- Blend membranes where the microstructure of sulfonated PEEK, the major component, was modified by physical cross-linking with silylated and sulfonated PPSU or PEEK.
- Polymer systems where two derivatives of PPSU having different degrees of sulfonation and silylation were cross-linked through Si-O-Si moieties.

In all cases, good membrane performance were obtained due to the interactions between the different components that avoided the degradation of highly sulfonated polymers, maintaining good proton conductivity.

2 Proton Exchange Membrane Fuel Cells

2.1 Fuel Cell Classification

A Fuel Cell is an electrochemical device similar to a battery; it transforms the chemical energy in Direct electric Current (DC) which can be used to power vehicles or to run household appliances. The main difference with respect to a conventional battery is that in the battery the charge is consumed during the discharge and restored with the recharges. The fuel cell functions continuously until there is the fuel (reactants on the electrodes) as a standard combustion motor, because the power is assured by the chemical reaction between the reactants (fuel and oxidant).

Fuel cells are classified primarily by the kind of used electrolyte. This determines the chemical reactions that take place in the cell, the used fuel, the kind of catalysts required, the temperature range in which the cell operates, and other factors.

A second grouping can be done considering the operating temperature of the fuel cells. Low-temperature fuel cells operate below about 250 °C and include Proton Exchange Membrane Fuel Cells, Alkaline Fuel Cells and Phosphoric Acid Fuel Cells. High-temperature fuel cells operate in the range 600-1000 °C and include Solid Oxide Fuel Cells and Molten Carbonate Fuel Cells.[1]

These characteristics affect the applications for which these cells are most suitable. Each fuel cell currently under development has its own advantages, limitations and potential applications.

An overview of the fuel cell types is given in **Table 2.1**.

	AFC (Alkaline)	PEMFC (Polymer Electrolyte Membrane)	DMFC (Direct Methanol)	PAFC (Phosphoric Acid)	MCFC (Molten Carbonate)	SOFC (Solid Oxide)
Operating temperature (°C)	< 100°C	60-120	60-120	160-220	600-800	**600-1000**
Anode Reaction	$H_2 + 2OH^- \rightarrow 2H_2O + 2e^-$	$H_2 \rightarrow 2H^+ + 2e^-$	$CH_3OH + H_2O \rightarrow CO_2 + 6H^+ + 6e^-$	$H_2 \rightarrow 2H^+ + 2e^-$	$H_2 + CO_3^{2-} \rightarrow H_2O + CO_2 + 2e^-$	$H_2 + O^{2-} \rightarrow H_2O + 2e^-$
Cathode Reaction	$\frac{1}{2} O_2 + H_2O + 2e^- \rightarrow 2OH^-$	$\frac{1}{2} O_2 + 2H^+ + 2e^- \rightarrow H_2O$	$3/2\ O_2 + 6H^+ + 6e^- \rightarrow 3H_2O$	$\frac{1}{2} O_2 + 2H^+ + 2e^- \rightarrow H_2O$	$\frac{1}{2} O_2 + CO_2 + 2e^- \rightarrow CO_3^{2-}$	$\frac{1}{2} O_2 + 2e^- \rightarrow O^{2-}$
Application	Transportation Space Energy storage system			Combined heat and power for decentral stationary power systems	**Combined heat and power for stationary decentralised systems and for transportation (trains, boats,...)**	
Charge Carrier	OH^-	H^+	H^+	H^+	CO_3^{2-}	O^{2-}

Table 2.1 - Fuel Cell Classification.

2.1.1 Polymer Electrolyte Membrane Fuel Cells

Proton exchange membrane fuel cells (PEMFCs) use a solid polymer as electrolyte and porous carbon electrodes containing a platinum catalyst. Low operating temperature allows PEMFCs to start quickly and results in low wear on system components.

Depending on the fuel, a PEMFC can be classified as direct H_2-PEMFC that is directly fed with hydrogen, indirect reformate PEMFC where the hydrogen fuel is produced by steam reforming, and direct methanol fuel cell (DMFC) that uses methanol as fuel.

H_2-PEMFC

H_2-PEMFCs are used to power automobiles, scooters, buses, backup power generators, boats and underwater vehicles.

This kind of PEMFC uses hydrogen as fuel and oxygen as an oxidant, giving only water as waste product, but whereas oxygen can be taken from the surrounding air, the availability of hydrogen presents a challenge.

Most fuel cell vehicles powered by pure hydrogen must store the hydrogen onboard as a compressed gas in pressurized tanks. Due to the low energy density of hydrogen, it is difficult to store enough hydrogen onboard to allow vehicles to travel the same distance as gasoline-powered vehicles before refuelling, typically 300-400 miles.[2] Alternatively, cryogenic hydrogen (liquid) can be stored; this process would reduce the low-density problem, but the liquefaction uses about 30% of the inherent energy.[3]

Reformate Fuel Cell

The problem of storage and transportation of hydrogen can be solved by producing it from a steam reforming process or by a partial oxidation of liquid fuels such as methanol, ethanol, by using a fuel processor placed onboard the fuel cell powered vehicle.

Basically, all organic molecules are potential candidates for a direct electrochemical conversion. However, due to undesired side reactions and high activation overpotentials, the rate of electrochemical conversion is often very poor.

The steam reforming reactions for the methanol are shown below:

Methanol Steam Reforming:	$CH_3OH_{(g)} + H_2O \rightarrow CO_{2(g)} + 3\ H_{2(g)}$	*(Eq. 2.1)*
Water Gas Shift Reaction:	$CO + H_2O \rightarrow CO_2 + H_2$	*(Eq. 2.2)*
Selective Oxidation of CO:	$CO + ½\ O_2 \rightarrow CO_2$	*(Eq. 2.3)*

The main problem connected to use of a reformed fuel is the platinum catalyst poisoning by CO, which causes a decrease of the electrocatalytic activity of the noble metal. Moreover, the reformer also releases carbon dioxide (a greenhouse gas), though less than that emitted from current gasoline-powered engines.[4]

DMFC

In direct methanol fuel cells the liquid fuel is directly oxidized at the anode, so that these devices have the advantage of being simpler power systems in comparison to fuel cells using H_2 derived from methanol reforming.

Compared with an H_2-PEMFC, a DMFC shows a larger efficiency decrease due to greater polarization losses and high methanol permeability of the polymer electrolyte (up to 50% methanol crossover).[5]

DMFCs have potential application in portable devices, such as laptops, mobile phones and MP3 players that require low current density and small system size.

2.1.2 Alkaline Fuel Cells

Alkaline fuel cells (AFCs) were among the first fuel cell technologies developed, and the first type widely used in the USA space program to produce electrical energy and water onboard spacecrafts.

AFCs use a solution of potassium hydroxide in water as the electrolyte and can use a variety of non-precious metals as catalysts at the anode and cathode.

The disadvantage of this fuel cell type is that it is easily poisoned by carbon dioxide. In fact, even the small amount of CO_2 in the air can affect the operation and lifetime of the cell, adding to cost.[6]

2.1.3 Phosphoric Acid Fuel Cells

Phosphoric acid fuel cells (PAFCs) are typically used for stationary power generation, but some of them have been used to power large vehicles such as city buses.

This type of fuel cells use liquid phosphoric acid as electrolyte and porous carbon electrodes containing a platinum catalyst.

PAFCs are more tolerant of impurities in fossil fuels that have been reformed into hydrogen than PEMFCs, but are less powerful than other fuel cells, given the same weight and volume. As a result, these fuel cells are typically large and heavy.[6]

2.1.4 Molten Carbonate Fuel Cells

Molten carbonate fuel cells (MCFCs) are currently being developed for industrial and military applications.

They are high-temperature fuel cells that use an electrolyte composed of a molten carbonate salt mixture suspended in a porous, chemically inert ceramic lithium aluminium oxide matrix. Since they operate at extremely high temperatures, non-precious metals can be used as catalysts at the anode and cathode, reducing costs.

The primary disadvantage of current MCFC technology is durability. The high temperatures at which these cells operate and the corrosive electrolyte used accelerate component breakdown and corrosion, decreasing cell life.[6]

2.1.5 Solid Oxide Fuel Cells

Solid oxide fuel cells (SOFCs) are suitable for stationary applications as well as for auxiliary power units used in vehicles to power electronics.

They use a hard, non-porous ceramic compound as electrolyte. High operating temperature removes the need for precious-metal catalyst and allows SOFCs to reform fuels internally, reducing cost.

However, high-temperature operation results in a slow start-up and requires significant thermal shielding to retain heat and protect personnel.[6]

2.2 Operating Principle of PEMFC

2.2.1 H_2-PEMFC

Proton exchange membrane fuel cell consists of two porous carbon electrodes, the anode and the cathode, separated by a polymer electrolyte, the proton conducting membrane. The electrodes are connected to an external load circuit and integrated between each electrode and the membrane is a thin layer of platinum catalyst. A schematic representation of H_2-PEMFC is shown in **Figure 2.1**. [4]

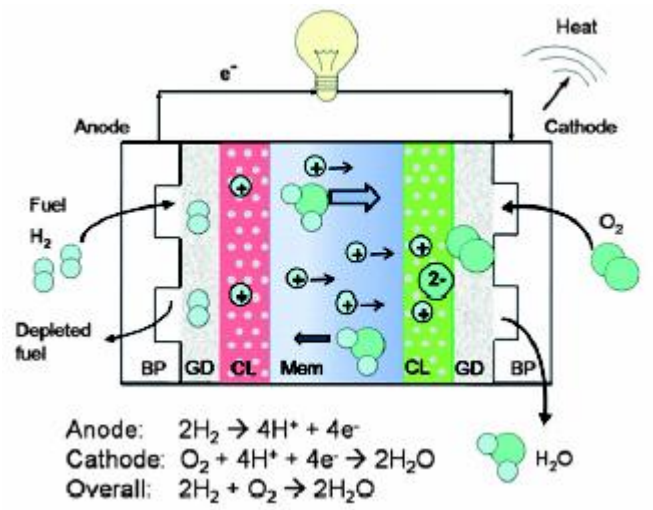

Figure 2.1 - Schematic diagram of H_2-PEMFC.

On the anode side, hydrogen diffuses to the anode catalyst where it dissociates into protons and electrons. The protons are conducted through the membrane to the cathode, while the electrons are forced to travel in an external supplying power circuit because the membrane is electrically insulating. On the cathode catalyst, oxygen molecules react with the electrons and protons to form water, the only waste product.[7]

Hydrogen Oxidation

The overall reaction of hydrogen oxidation is:

$$H_2 \rightarrow 2\,H^+ + 2\,e^- \qquad \textit{(Eq. 2.4)}$$

The mechanism of H_2 electro-oxidation on Pt in acid electrolytes is thought to proceed by the absorption of the gas onto the catalyst surface, followed by charge transfer which gives hydrogen ions, as follows:

$$H_2 + 2\ Pt \rightarrow 2\ Pt\text{-}H_{ads} \qquad \textit{(Eq. 2.5)}$$

$$2\ Pt\text{-}H_{ads} \rightarrow 2\ Pt + 2\ H^+ + 2\ e^- \qquad \textit{(Eq. 2.6)}$$

When pure hydrogen is used as fuel the performance of the anode is excellent with pure Pt. Unfortunately in most practical systems the fuel stream contains traces of elements or compounds, such as CO, S, and NH_3, that can poison the anode catalysts. In particular, CO is one of the major poisons in low temperature fuel cells, due to its absorption to the active sites of the platinum based catalysts so that no, or virtually no, sites are available for reaction with H_2.[8]

Oxygen Reduction

Each oxygen molecule requires the transfer of four electrons for complete reduction:

$$O_2 + 4\ H^+ + 4\ e^- \rightarrow 2\ H_2O \qquad \textit{(Eq. 2.7)}$$

The simultaneous transfer of these electrons is highly unlikely, in fact, partial electron transfer takes place leading to the formation of intermediates such as superoxide.
The application of a platinum electrocatalyst allows the stabilization of these intermediates and the reaction then proceeds at a reasonable and useful rate.
The mechanism is believed to take place through the following sequence: [5]

$$O_2 + Pt \rightarrow Pt\text{-}O_2 \qquad \textit{(Eq. 2.8)}$$

$$Pt\text{-}O_2 + H^+ + e^- \rightarrow Pt\text{-}HO_2 \qquad \textit{(Eq. 2.9)}$$

$$Pt\text{-}HO_2 + Pt \rightarrow Pt\text{-}OH + Pt\text{-}O \qquad \textit{(Eq. 2.10)}$$

$$Pt\text{-}OH + Pt\text{-}O + 3\ H^+ + 3\ e^- \rightarrow 2\ Pt + 2\ H_2O \qquad \textit{(Eq. 2.11)}$$

Although a huge variety of catalysts have been investigated, at present, Pt based catalysts are the most widely used cathode materials in low temperature fuel cells, due to their intrinsic activity and stability in acidic solutions.

2.2.2 DMFC

In DMFC, methanol and water electrochemically react at the anode to produce carbon dioxide, proton and electrons. The protons are conducted through the membrane to the cathode, while the electrons travel through the external circuit where they can be made to do useful work, such as powering an electric motor.[9]

On the cathode catalyst, oxygen molecules react with the electrons and protons to form water, analogously to that which occurs in a H_2-PEMFC *(Eq. 2.7)*.

Methanol Oxidation

The electro-oxidation of methanol to carbon dioxide involves the transfer of six electrons:

$$CH_3OH + H_2O \rightarrow CO_2 + 6\,H^+ + 6\,e^- \qquad (Eq.\ 2.12)$$

Few materials are able to electrosorb methanol, and in acidic electrolytes, only platinum-based electrocatalysts have shown the required activity and chemical stability.[10]

The adsorption mechanism is believed to take place through the sequence of step shown in **Figure 2.2**.

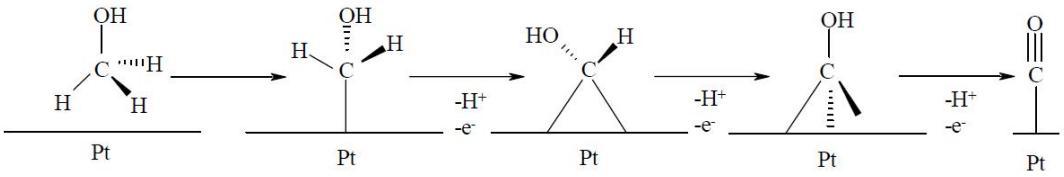

Figure 2.2 - Scheme of methanol electrosorption mechanism on pure Pt surface.

The mechanism shows the electrosorption of methanol on the surface of platinum with sequential proton and electron stripping, leading to the main catalyst poison, linearly bonded carbon monoxide (Pt-CO). Subsequent reactions are believed to involve oxygen transfer to the Pt-CO species to produces CO_2.[11]

Much research is being rendered on catalysts for methanol oxidation to find a catalyst which can avoid the poisoning effect of the CO species. Several promoters, such as Ru, Sn, W, have been found to increase the activity of the Pt catalyst. At the present, the most active methanol electro-oxidation catalysts are bimetallic alloys consisting of Pt and Ru supported on carbon.[12]

2.3 Performance

2.3.1 Ideal Performance

A fuel cell is a galvanic cell which converts the chemical energy of the reaction directly into the electrical energy. The maximum electrical work (W_{el}) obtainable in a fuel cell operating at constant temperature and pressure is given by the change in Gibbs free energy (ΔG) of the electrochemical reaction:

$$W_{el} = \Delta G = - nFE \qquad \textit{(Eq. 2.13)}$$

where n is the number of electrons involved in the reaction, F is the Faraday's constant and E is the ideal potential.

The thermodynamic equilibrium potential E represents the ideal performance of the cell and is described by the Nernst equation:

$$E = E^{\circ} + \frac{RT}{nF} \ln \frac{\Pi[\text{reactant activity}]}{\Pi[\text{product activity}]} \qquad \textit{(Eq. 2.14)}$$

where E° is the ideal potential at standard conditions (298.15 K and 1 atm), resulting from the difference between the potentials of cathode and anode.

For H_2-PEMFC, the standard ideal potential is 1.23 volts (V) with liquid water as product and 1.18 V with gaseous water as product: [13]

$2\ H_2 \rightarrow 4\ H^+ + 4\ e^-$ ($E°_{anode} = 0.00$ V) *(Eq. 2.15)*

$O_2 + 4\ H^+ + 4\ e^- \rightarrow 2\ H_2O_{(l)}$ ($E°_{cathode} = 1.23$ V) *(Eq. 2.16)*

$2\ H_2 + O_2 \rightarrow 2\ H_2O_{(l)}$ ($E° = 1.23$ V) *(Eq. 2.17)*

For DMFC, the standard ideal potential corresponds to 1.18 volts:

$CH_3OH + H_2O \rightarrow CO_2 + 6\ H^+ + 6\ e^-$ ($E°_{anode} = 0.05$ V) *(Eq. 2.18)*

$3/2\ O_2 + 6\ H^+ + 6\ e^- \rightarrow 3\ H_2O_{(l)}$ ($E°_{cathode} = 1.23$ V) *(Eq. 2.19)*

$CH_3OH + 3/2\ O_2 \rightarrow CO_2 + 2\ H_2O_{(l)}$ ($E° = 1.18$ V) *(Eq. 2.20)*

2.3.2 Actual Performance

When current flows in the cell, the actual potential (*V*) is decreased from its ideal value (*E*) because of irreversible losses, called polarization or overpotential (η):

$$V = E - \eta \qquad \textit{(Eq. 2.21)}$$

These losses originate primarily from three sources:
(1) activation polarization (η_{act}), related to the rates of electrochemical reactions;
(2) ohmic polarization (η_{ohm}), due to resistance of the cell components and interconnects;
(3) concentration polarization (η_{conc}), arising from the depletion of reactants at catalyst sites under high loads.

As can be seen in **Figure 2.3**, the activation polarization loss (η_{act}) is dominant at low current density, giving the characteristic logarithmic shape to the polarization curve. It is present when the rate of an electrochemical reaction at an electrode surface is controlled by sluggish electrode kinetics. In other words, activation polarization is directly related to the rates of electrochemical reactions and therefore to the activation barriers that must be overcome by the reacting species prior to current and ion flow.

Ohmic losses (η_{ohm}) occur because of resistance to the flow of ions in the electrolyte and resistance to flow of electrons through the electrode materials. Because both the electrolyte and electrodes obey Ohm's law, the ohmic losses can be expressed by the equation:

$$h_{ohm} = i \times R \qquad \textit{(Eq. 2.22)}$$

where i is the current flowing through the cell, and R is the overall resistance of the cell (protonic, electronic and contact resistance).

Ohmic polarization varies directly with current, increasing over the whole range of current because cell resistance remains essentially constant.

The ohmic losses through the electrolyte can be reduced by decreasing the electrode separation, that is by reducing membrane thickness, and enhancing the ionic conductivity of the electrolyte.

The concentration losses (η_{conc}) occur over the entire range of current density, but these losses become prominent at high limiting currents where it becomes difficult to provide enough reactant flow to the cell reaction sites.

The slow transport of reactants and products to and from the electrochemical reaction sites causes a loss of potential due to the inability of the surrounding material to maintain the initial concentration of the bulk fluid.

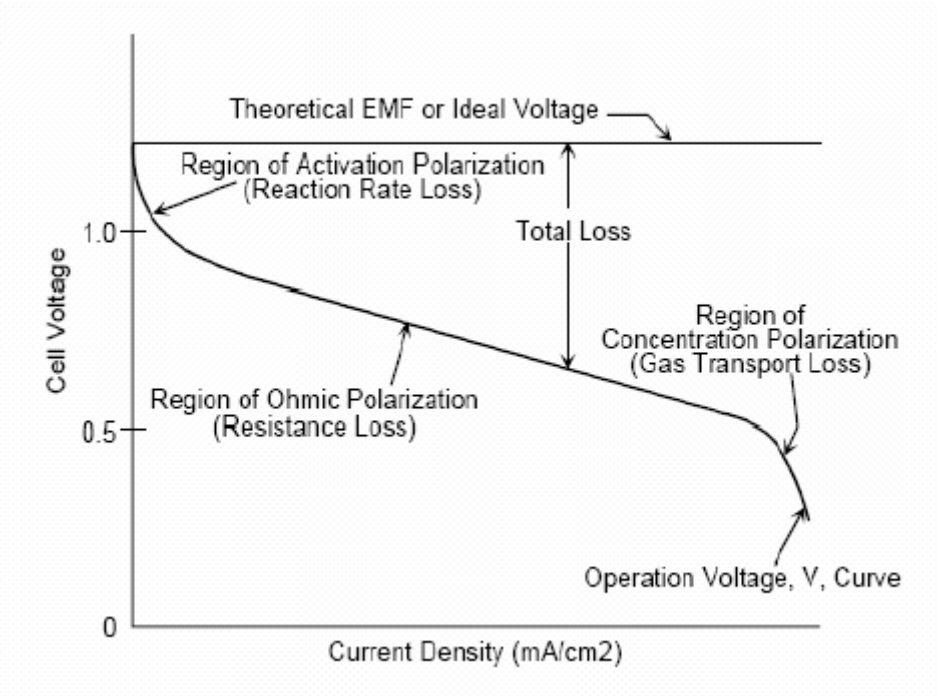

Figure 2.3 - Ideal and Actual fuel cell Voltage/Current density characteristic.

Moreover, when no current is drawn from the cell, the actual cell potential, *i.e.* open circuit voltage (OCV), does not reach the thermodynamic potential value *E* because of parasitic electrochemical processes. Some voltage loss at the OCV is due to crossover of some hydrogen or methanol through the membrane to the cathode where some hydrogen or methanol oxidation competes with oxygen reduction, causing a mixed potential.

2.3.3 Efficiency

The thermal efficiency ($\varepsilon_{\text{thermal}}$) of an energy conversion device is defined as the amount of useful energy produced relative to the change in stored chemical energy (commonly referred to as thermal energy) that is released when a fuel is reacted with an oxidant:

$$e_{thermal} = \frac{useful\ energy}{\Delta H} \qquad \textit{(Eq. 2.23)}$$

In order to compare fuel cells with other systems, such as internal combustion engines, an evaluation of the system efficiency is necessary.

In the internal combustion engines the conversion of chemical energy into electricity is not a direct process, since chemical energy is firstly converted into mechanical energy, and then transformed into electrical energy:

Chemical energy → Heat → Mechanical energy → Electrical energy

The combustion of a hydrocarbon (chemical energy) is accompanied by a rise in temperature as these reactions are exothermic and the reaction products are usually gases. The heat increase causes an expansion of the formed gases, which in turn can produce mechanical work that be transformed into electrical energy by means of a rotating generator.

The maximum thermal efficiency for such conversion systems is determined by Carnot's law and it is written as follows:

$$e_{thermal} = \frac{-W_r}{\Delta H} = 1 - \frac{T_2}{T_1} \qquad \textit{(Eq. 2.24)}$$

where W_r is the reversible work performed, ΔH is the enthalpy change of reaction, T_1 is the higher temperature of the heat source and T_2 is the lower temperature, e.g. at the gas outlet. In general, these efficiencies are not surpassing 40 % for the most efficient engines.

Fuel cells represent an attractive alternative as their efficiency is not limited by the Carnot cycle and most of the chemical energy stored in the reactants can be converted into electricity:

Chemical energy → Electrical energy

For a fuel cell, the ideal efficiency (ε_{ideal}) can be calculated from the Gibbs free energy change (ΔG) and the enthalpy change (ΔH) of the electrochemical reaction. It describes the ratio between the maximum electric work that can be drawn from a fuel cell (W_{el}), and the overall quantity of energy that can be transformed into heat (ΔH). Ideally, the free energy of the reaction can be completely converted into electrical energy and the efficiency is given by:

$$e_{ideal} = \frac{-W_{el}}{\Delta H} = \frac{\Delta G}{\Delta H} \qquad \textit{(Eq. 2.25)}$$

Thus, the efficiency of an ideal fuel cell operating reversibly on pure hydrogen and oxygen at standard conditions (1 atm pressure and 25 ºC) would be 0.83.

The efficiency of an actual fuel cell (ε_{actual}), can be expressed in terms of the ratio of the operating cell voltage (V) to the ideal cell voltage (E), according to the equation report below:

$$e_{actual} = \frac{0.83 \times V}{E} \qquad \textit{(Eq. 2.26)}$$

where the actual cell voltage is less than the ideal cell voltage because of the losses due to electrode overpotentials and the electrolyte resistance.

A fuel cell can be operated at different current densities and the corresponding cell voltage then determines the actual efficiency. A typical H_2-PEMFC running at 0.7 V has an actual efficiency of about 0.5, meaning that 50% of the energy content of the hydrogen is converted into electrical energy and the remaining 50% will be converted into heat.

2.4 PEMFC System

2.4.1 Components

The electrodes and membrane together form the membrane electrode assembly (MEA). A single cell is realized when bipolar flow field plates, with gas channels grated into their surface, are placed on each side of the MEA, as shown in **Figure 2.4**.

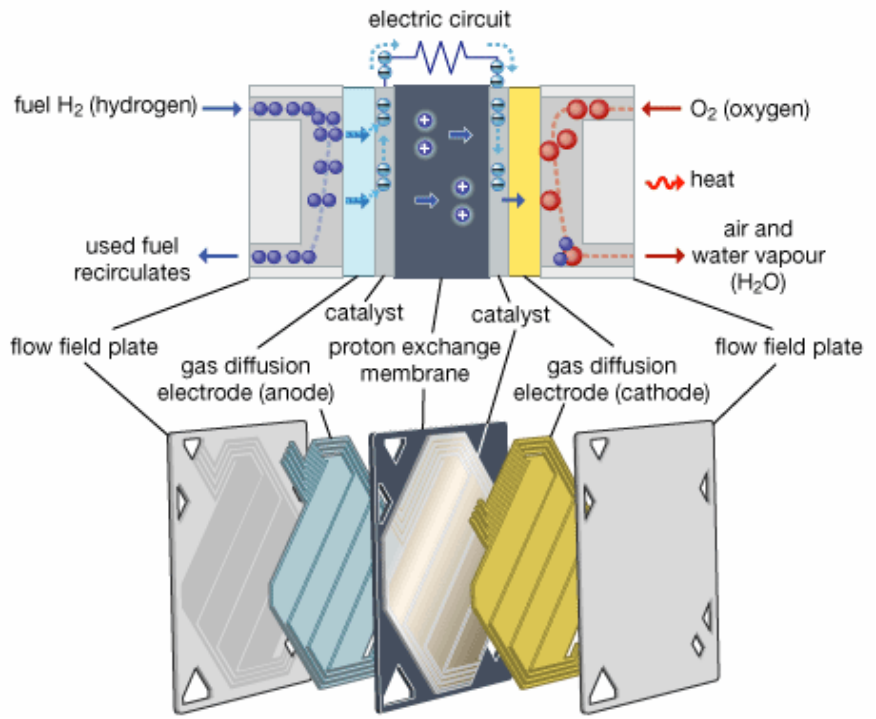

Figure 2.4 - Scheme of a single PEMFC.

The anode and cathode are thin sheets of porous carbon paper or carbon cloth having a catalyst layer pressed onto one side of them (typically Pt or Pt/Ru alloys) and wet-proofed with Teflon. The side containing the catalyst is placed in contact with the proton exchange membrane.

Polymer Electrolyte

Solid polymer electrolytes form a thin but sound electronic insulator and gas barrier between the two electrodes while allowing rapid proton transport and high current densities.

The reduction of the membrane thickness can lead to the greatest improvement in fuel cell performance. The advantages gained with this simple strategy include lower membrane resistance, lower material utilization, and improved hydration of the entire membrane.

However, the extent to which a membrane can be thinned is limited because of difficulties with durability and reactant crossover. This is especially true for direct methanol fuel cells, where excessive methanol transport occurs, reducing power density.[14]

The essential requirements of polymer electrolyte membranes include: good proton conductivity, chemical and thermal stability, low methanol crossover (in DMFCs), and low cost.[15]

A detailed discussion on electrolyte features and membrane materials has been developed in *Chapter 3*.

Electrodes

Electrodes for PEMFCs are generally porous gas diffusion electrodes to ensure the supply of the reactant gases to the active zones where the noble metal catalyst is in contact with the ionic and electronic conductor.

The main requirement of a good electrode is a three-phase boundary between the gas supply on the one hand, and the catalyst particle and the ionic conductor, on the other hand. **Figure 2.5** shows a detailed scheme of a typical electrode, which displays three layers: (*i*) teflonized substrate (typically carbon cloth); (*ii*) a diffusion layer, generally formed by carbon particles of about 0.1 μm size along with Teflon and (*iii*) an active layer, where Pt catalyst grains (dimensions 2-4 nm) are supported on carbon particles (Pt load usually 0.4 mg/cm^2 or less) with or without Teflon; a proton conducting membrane phase partly penetrates the pores in this layer.[16]

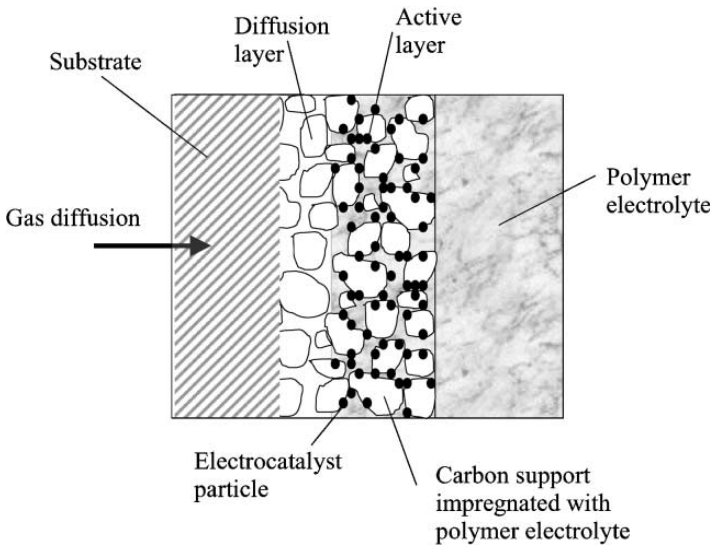

Figure 2.5 - Scheme of a typical electrode.

The catalyst particles must be in direct contact with an electronic conductor to ensure that the electrons are supplied to or taken away from the reaction site. Electronic conductivity is usually provided by carbon particles. To enhance the three-phase boundary and to obtain a maximum utilization of the highly dispersed electrocatalyst, additional ionomer (usually liquid Nafion) is impregnated into the active layer. This ensures a wide access of the H^+ ions within the catalyst layer.

When using humidified gases or a methanol/water mixture (for DMFC) the catalyst layer must be sufficiently hydrophobic to prevent the pores from flooding. This hydrophobicity can be provided by introducing polytetrafluoroethylene (PTFE) as a binder, in combination with Nafion that is hydrophilic.[17]

Additional Components

Bipolar plates supply the reactants through the flow channels to the electrodes and serve the purpose of electronically connecting one cell to another in the electrochemical cell stack. Their essential requirements are: high values of electronic conductivity, high mechanical strength, impermeability to reactants, resistance to corrosion and low cost of automated production.[18]

Generally, bipolar plates are made up of graphite and gas channels are grated into their surface in a parallel flow configuration. Both the material of the flow field plates and the design of the flow field are subject to several development projects considering volume, weight, pressure loss etc.[19]

2.4.2 Water Management

Water is carried into the fuel cell via humidified gas streams and methanol/water mixture (for DMFCs) entering gas diffusion electrodes. An additional source of water is the oxygen reduction reaction occurring at the cathode.

Water transport across the membrane takes place by three different processes: electro-osmotic drag, diffusion and hydraulic permeation, which are schematically depicted in **Figure 2.6**.[20]

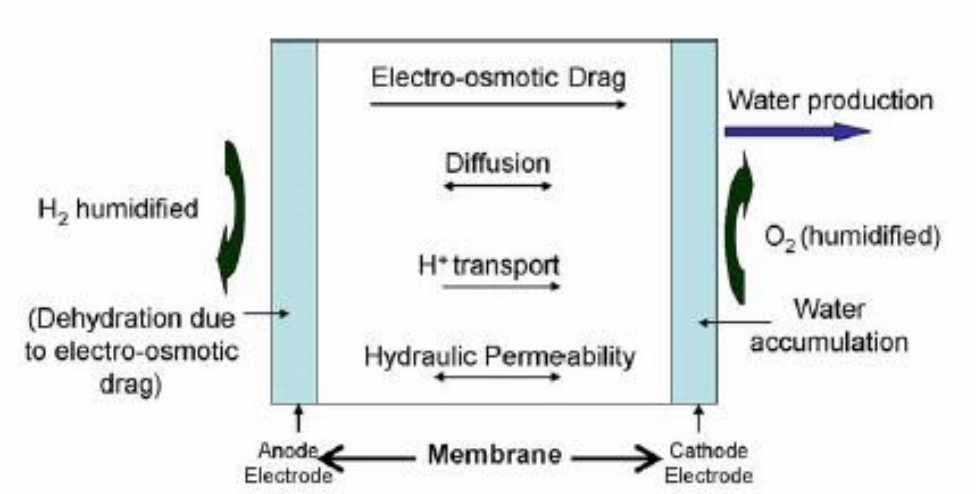

Figure 2.6 - Scheme illustrating the modes of water transport in an operating PEMFC.

The electro-osmotic drag is due protons that migrate across the membrane from the anode to cathode carrying water molecules with them.

The production of water by the oxygen reduction reaction together with the electro-osmotic drag creates an excess of water at the cathode. This gradient of water content across the membrane may results in back diffusion of water from cathode to anode.[21] If a differential pressure exists across the membrane, a hydraulic permeation can also contribute to the water transport.

In the absence of the latter, the net water flux across the membrane is a combination of diffusion and electro-osmotic drag and two specific water transport parameters have then a direct impact on cell performance: the water self-diffusion coefficient (D_{H_2O}) that is a measure of the average mobility of water in the membrane, and the electro-osmotic drag coefficient (K_{drag}) that represents the average number of water molecules that are carried through the membrane per proton conducted.

In PEMFC, the membrane to be well humidified because the proton conducting process relies on water content of membrane. Operating at high current density, the anode side must be humidified by pre-humidifying the hydrogen to avoid dehydration due to the electro-osmotic drag. Moreover, the cathode side needs to remove water to prevent slow oxygen diffusion due to flooding of the catalytic layer.

Water removal conditions should be carefully controlled. In fact, if water is removed too quickly, the membrane dries and resistance across it increases, whilst, if the water is removed too slowly, the cathode will flood preventing the oxygen from reaching the catalyst and stopping the reaction.

2.4.3 Heat Management

Increase in operating temperature of fuel cell is attractive for a number of reasons: (*i*) improved tolerance of the electrodes to carbon monoxide, which enables the use of hydrogen produced by reforming of natural gas, methanol or gasoline; (*ii*) simplification of the cooling system; (*iii*) increased proton conductivity; and (*iv*) in DMFC, improved kinetics of the methanol oxidation reaction at the anode.[22]

However, increase in temperature confers the restraints. Because in the most of proton exchange polymer materials the conduction occurs through a water-assisted mechanism, they exhibit the highest proton conductivity when fully hydrated. This requires humidification of gas feeds before entering the fuel cell and the application of pressure to maintain adequate relative humidity.

2.4.4 Methanol Crossover

The methanol crossover consists of the protonic drag of methanol through the membrane of the DMFC, similar to electro-osmotic drag of water. In fact, due to the similar properties of water, such as dipole moment, methanol molecules are transported to the cathode by the electro-osmotic drag as well as diffusion.

The effects of methanol crossover on DMFC performance consist of (*i*) limited activity of the anode catalyst, (*ii*) lowering of methanol utilization, resulting of methanol/oxygen recombination at the cathode catalyst, and (*iii*) the deleterious effects of methanol penetrating the cathode on the performance of the cathode itself. [5]

Methanol crossover depends on several factors: the membrane permeability, the concentration of methanol in the fuel feed, the operating temperature and the performance of the anode itself.

The nature of the membrane is a very important factor and great efforts have been made to vary the membranes morphological features in order to reduce their methanol permeability.[23]

The crossover is also dependent on the methanol concentration in the feed. A higher concentration as well as a higher temperature in the cell increase the diffusion of methanol through the membrane, lowering the cell performance. This factor can be controlled to a certain extent by strictly correlating methanol feed concentration with the actual current demand of the cell. An optimum concentration of methanol was considered to be around 1-2 M methanol in water.[24]

Finally, if the anode is sufficiently active to oxidize methanol at a rate comparable or higher than the rate of methanol supply, the concentration at interface could decrease to zero preventing methanol to cross through the membrane. The anode activity can be promoted by the use of suitable Pt/Ru catalysts.[25] Slight activity improvements can be found by the use of multinary catalysts.[26]

2.5 References

1) L. Carrette, K.A. Friedrich, U. Stimming, *Fuel Cells* **2001**, 1, 5.

2) F. Barbir, *PEM Fuel Cells: Theory and Practice*, Elsevier Academic Press, New York, **2005**.

3) K. Kordesch, G. Simader, *Fuel Cells and their Application*, 1st ed., VCH, Weinheim, **1996**.

4) R. Devanathan, *Energy Environ. Sci.* **2008**, 1, 101.

5) A.S. Aricò, S. Srinivasan, V. Antonucci, *Fuel Cells* **2001**, 1, 133.

6) C. Song, *Catalysis Today* **2002**, 77, 17.

7) P.R. Pathapati, X. Xue, J. Tang, *Renewable Energy* **2005**, 30, 1.

8) P. Futerko, I.M. Hsing, *Electrochim. Acta* **2000**, 45, 1741.

9) M. Hogarth, *Fuel Cell Technology Handbook: Prospects of the Direct Methanol Fuel Cell*, CRC Press LLC, **2003**.

10) R. Parson, T. Vandernoot, *J. Electroanal. Chem.* **1988**, 257, 9.

11) P.A. Christensen, A. Hamnett, R.J. Potter, Ber. *Bunsenges. Phys. Chem.* **1990**, 94, 1034.

12) A.S. Aricò, V. Baglio, A. Di Blasi, E. Modica, P.L. Antonucci, V. Antonucci, *J. Electroanal. Chem.* **2003**, 557, 167.

13) P.W. Atkins, *Physical Chemistry*, 3rd ed., W.H. Freeman and Company, New York, NY, **1986**.

14) K. Prater, *J. Power Sources* **1990**, 29, 239.

15) M. Hickner, H. Ghassemi, Y.S. Kim, B.R. Einsla, J.E. McGrath, *Chem. Rev.* **2004**, 104, 4587.

16) P. Costamagna, S. Srinivasan, *J. Power Sources* **2001**, 102, 253.

17) R. Dillon, S. Srinivasan, A.S. Aricò, V. Antonucci, *J. Power Sources* **2004**, 127, 112.

18) G. Hoogers, *Fuel Cell Technology Handbook: Fuel Cell Components and Their Impact on Performance*, CRC Press LLC, **2003**.

19) P.L. Hentall, J.B. Lakeman, G.O. Mepsted, P.L. Adcock, J.M. Moore, *J. Power Sources* **1999**, 80, 235.

20) J. Zhang, Z. Xie, J. Zhang, Y. Tang, C. Song, T. Navessin, Z. Shi, D. Song, H. Wang, D.P. Wilkinson, Z.-S. Liu, S. Holdcroft, *J. Power Source* **2006**, 160, 872.

21) T.A. Zawodzinski, C. Derouin, S. Radzinski, R.J. Sherman, V.T. Smith, T.E. Springer, S. Gottesfeld, *J. Electrochem. Soc.* **1993**, 140, 1041.

22) S. Cleghon, J. Kolde, W. Liu, *Handbook of Fuel Cells-Fundamentals, Technology and Application*, J. Wiley and Sons, Ltd, Chichester, **2003**.

23) V. Baglio, A. Di Blasi, A.S. Aricò, V. Antonucci, P.L. Antonucci, C. Traknprapai, V. Esposito, S. Licoccia, E. Traversa, *J. Electrochem. Soc.* **2005**, 152, A1373.

24) X. Ren, T.E. Sprinter, S. Gottesfeld, *J. Electrochem. Soc.* **2000**, 147, 92.

25) B.D. McNicol, D.A.J. Rand, K.R. Williams, *J. Power Sources* **1999**, 83, 15.

26) A.S. Aricò, Z. Poltarzeski, H. Kim, A. Morana, N. Giordano, V. Antonucci, *J. Power Sources* **1995**, 55, 159.

3 Proton Exchange Membranes

3.1 Polymer Membrane Properties

The membrane is the core component of PEMFCs. Its function is twofold: proton conduction from the anode to the cathode, and effective separation of the electrode reactants.[1]

To achieve good cell performance, the membrane must possess the following features:[2]

- high proton conductivity, greater than 10^{-2} S cm^{-1} for a fully hydrated polymer;
- low permeability to reactants;
- chemical and electrochemical stability under operating conditions;
- mechanical properties (strength, flexibility and processability);
- production costs compatible with intended application.

To focus on the relevant properties of polymer electrolytes, it is useful to categorize them in tuneable parameters, structural features and transport properties, as summarized in **Table 3.1**.[3]

Tuneable Parameters	Structural Features	Transport Properties
Backbone Characteristics	Water Domain Size, Shape, Interface	Proton Conductivity
Acid Group Characteristics	Interanionic Distance	Water Transport Properties
Ion Exchange Capacity	Water Uptake	Reactant Permeability
Processing	Tortuosity	

Table 3.1 - Relevant membrane properties.

3.1.1 Tuneable Parameters

The tuneable parameters represent the characteristics that can be controlled or modified in the preparation of the electrolyte. They include backbone and acid group characteristics, ion exchange capacity and processing conditions.

Backbone characteristics offer perhaps the greatest number of controllable variables due to the extreme versatility of chemical synthetic processes. The nature of the polymer backbone is extremely important in determining its flexibility, strength and processability, oxidation and thermal resistance.[4]

The acid group is another modifiable component of the polymer. Most polymer electrolytes have acid groups covalently bound to the polymer backbone, either through a side chain or directly through a chemical bond. In the case of side chains, features such as the length of the side chain, its flexibility, and its hydrophobicity are also important.[5]

Ion-exchange capacity (IEC) indicates the density of ionizable hydrophilic groups in the membrane matrix, which are responsible for the ionic conductivity. IEC is probably the simplest quantity to control from a synthetic standpoint.[6]

Processing of polymer electrolyte includes methods of preparation and treatment of membrane. Processing conditions affect polymer matrix morphology and hence characteristics of membrane such as water uptake, mechanical properties and proton conductivity.[7]

3.1.2 Structural Features

The structural features that determine the behaviour of water within the membrane are correlated to the water domain size, shape and the nature of the domain interface.

Interanionic distances among the sulfonate sites are a contributing factor to water domain features and primarily affect the proton conductivity of the membrane. The energy barriers associated with proton transport are also dependent on the distance between anionic sites, so that the greater the distance between sites the greater the resistive losses associated with transport.[8]

Tortuosity or continuity of the phases is important for both transport properties and mechanical stability. Tortuosity affects transport properties by describing the path

length over which transport occurs and mechanical properties, because tortuosity also addresses the architecture of the structural phase.

3.1.3 Transport Properties

Proton conductivity is fundamental for any fuel cell electrolyte and is usually the first characteristic considered when evaluating membranes for potential use. It is well know that for these systems proton conductivity is strongly dependent on water content, and performance improvements are needed in the area of increased conduction at low water content, particularly for higher temperature applications.[4]

Cell performance depends also on two specific water transport parameters, the water self-diffusion coefficient (D_{H_2O}) and the electro-osmotic drag coefficient (K_{drag}). The first coefficient is a measure of the average mobility of water in the membrane and the latter is a measure of the number of water molecules that are carried through the membrane per proton conducted. These coefficients are particularly important for water management both on a local and global scale. On a local scale, they affect hydration of the electrolyte and the electrodes which influences conductivity, electrode kinetics and mass transport, due to flooding. On a global scale, they affect feed gas flow rates, operating pressures, and humidification and cooling requirements.

Reactant permeability is another important transport property in these materials. While hydrogen and oxygen permeability in polymer electrolyte membranes are typically low, methanol permeability represents a significant problem in DMFCs. In such fuel cells, methanol permeability leads to significant performance losses due to crossover, impacting the cathode kinetics and overall fuel efficiency.[9]

3.2 Nafion and Sulfonated Aromatic Polymers

Nafion® was developed 40 years ago by DuPont Inc.[10] It consists of a polytetrafluoroethylene (PTFE) backbone, which gives it high chemical inertness. The side chains consist of perfluorinated vinyl polyether ending in sulfonic acid groups - SO_3H that give proton exchange capability to the polymer. The chemical structure of Nafion is shown in **Figure 3.1**, where the values of n, x and y can be varied to produce materials with different equivalent weights.

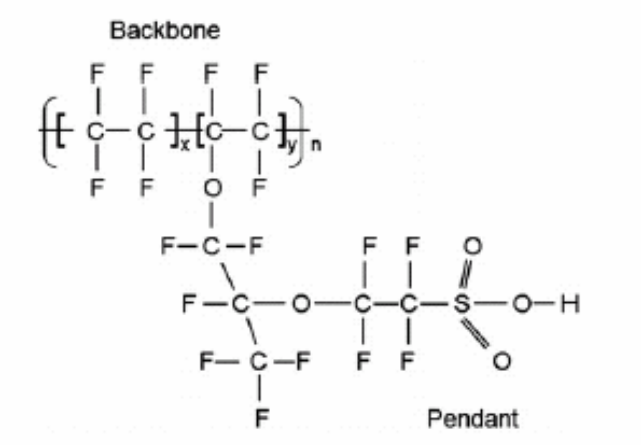

Figure 3.1 - Chemical structure of Nafion.

Among non-fluorinated polymers alternative to Nafion, arylene main-chain polymers can provide some definitive advantages. Such polymers are inexpensive and open up a wide window of chemical modification opportunities. Their aromatic structure offers the possibility of electrophilic as well as nucleophilic substitution, allowing to obtain material with desired features for PEMFC applications.[11,12] In particular, the most important modification regards the introduction of sulfonic moieties to obtain proton-conducting materials.

Commercial polymers from the aromatic family are often of the type *poly-p-phenylene* shown in **Figure 3.2a**, where X is an atom or group of atoms, giving the polymer chains a certain degree of flexibility and hence processability.[13]

Most simply, X is a single atom such as S in *polyphenylene sulfide* (PPS) (**Figure 3.2b)** or O in *polyphenylene oxide* (PPO) **(Figure 3.2c)**. In particular, ether links provide a very good choice of functional groups as the -C-O-C- link itself is very flexible and also is highly resistant to thermal oxidation. In the development of polymer electrolyte membranes, modifications of the aromatic polymers containing ether links, such as *polyetheretherketone* (PEEK) (**Figure 3.2d)**, have been widely investigated.[14,15]

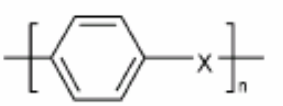

(a) Poly-*p*-phenylene

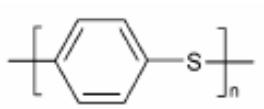

(b) Polyphenylene sulfide

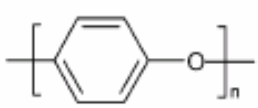

(c) Polyphenylene oxide

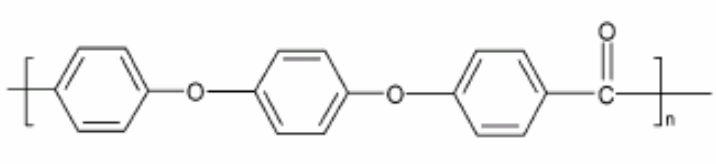

(d) Polyetheretherketone

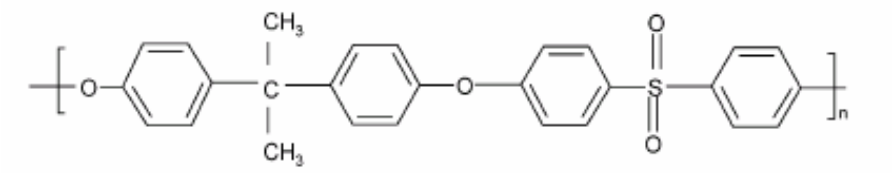

(e) Udel Polysulfone

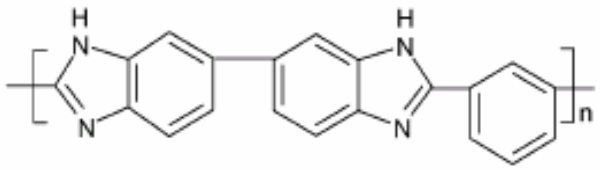

(f) Poly(2,2'-*m*-(phenylene)-5,5'-bibenzimidazole)

Figure 3.2 - Polymer structures of interest.

More commonly, X is a simple functional group such as SO_2 in polysulfone, NHCO in polyamides, COO in polyesters, and CO in polyketones.

Modifications of polymers of the polysulfones (PSUs) family, such as Udel *Polysulfone* shown in **Figure 3.2e**, have been widely studied by several research groups.[16,17]

The polybenzimidazoles represent another group of high performance aryl polymers. One of these is the *poly(2,2'-m-(phenylene)-5,5'-bibenzimidazole)* (PBI) whose structure is reported in **Figure 3.2f**. Non-modified PBI shows some tendency to take up water but its proton conductivity is very low. Hence, it is necessary to dope the polymer with sulphuric or phosphoric acid to increase its proton conductivity.[18,19]

3.3 Membrane Structure as function of Water Content

Modeling of water sorption and effect on the membrane structure is important since proton conductivity is strongly dependent on the water content. To examine the processes that take place, it is useful to focus on Nafion, for which data are more readily available. A comparison with sulfonated polyetherketones membranes is then reported.

The general structure of Nafion membrane as a function of water content has been the topic of many studies, such as swelling, infrared, X-ray and microscopy studies, just to name a few.[20,21] These have shown that a hydrated membrane contains two phases, an ionic phase that is associated with the hydrated sulfonic acid groups, and a non-ionic phase that is the perfluorinated matrix. The actual form of the phases depends on the water content.

Several models have been proposed since the early 1970s, to predict ionic transport properties of Nafion describing the way in which ionic groups aggregate. These models include the Mauritz-Hopfinger Model,[22] the Yeager Three Phase Model and the Gierke Cluster Network Model.

The Yeager Model is based on a three-phase clustered system with interconnecting channels within the polymer. The three regions consist of (A) a fluorocarbon backbone, (B) an interfacial region and (C) the clustered regions, as shown in **Figure 3.3**.

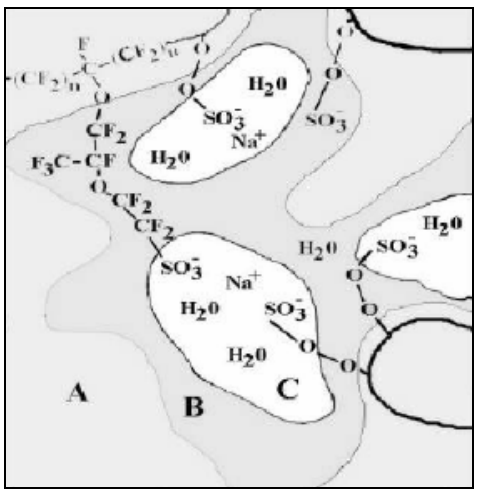

Figure 3.3 - Yeager's model of Nafion membranes: fluorocarbon region (A), interfacial zone (B), ionic cluster region (C).

The hydrophobic region (A) contains the CF_2-CF_2-CF_2 units. The interface region (B) contains the side chains O-CF_2-O-CF_2-CF_2-CF_2 binding (A) and (C) regions and some water and counter ions which are not in clusters. The hydrophilic region (C) consists of clusters containing most of the ionic exchange sites, counter ions and absorbed water.[23]

In the cluster network model proposed by Gierke and Hsu, the structure is an inverted micelle in which the ion-exchange sites are separated from the fluorocarbon backbone thus forming spherical clusters, connected by short narrow channels.[24]
When the membrane is dry, an average cluster has a radius of about 1.8 nm. In the swollen state the diameter increases to about 4 nm, each cluster being filled with about 1000 water molecules and the connecting channels have a diameter and a length of about 1 nm, as shown in **Figure 3.4**.

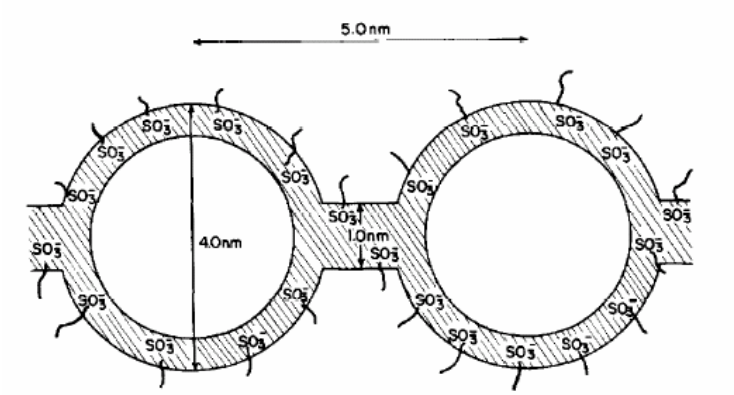

Figure 3.4 - Gierke's cluster network model of Nafion membranes.

Thus, with increasing water content the clusters grow and form transitory interconnections with each other. This network of collapsed channels leads to a percolation-type phenomenon.

Gierke and Hsu also used the percolation theory to correlate the electrical conductivity with the water content of the membrane, expressed as λ, i.e. the number of water molecules per sulfonic group. According to this theory, there is a critical amount of water available in the membrane, below which ion transport is extremely difficult due to the absence of extended pathways.[25] The percolation threshold in Nafion is around $\lambda = 2$, as shown from conductivity data.[22]

Figure 3.5 shows a schematic representation of the hydration states for Nafion membrane. At low hydration level, i.e. λ in the range 1-2, it is reasonable to consider that all water molecules absorbed by Nafion membrane are associated with the sulfonate heads because of the hydrophobic nature of the backbone and the hydrophilic nature of the sulfonic groups. Moreover, the hydronium ions will be localized on the sulfonate heads and the conductivity will be extremely low being the amount of water absorbed insufficient for the formation of a continuous water phase.[26]

For λ in the range 3-5, the counterion clusters continue to grow and, as λ approaches 5, the membrane becomes more conductive because some counterion clusters may connect, but there is still insufficient water for all clusters to coalesce.
Molecular dynamics simulations indicate that 5 water molecules form the primary hydration shell for the sulfonic groups and any additional water molecules are not as strongly bound and thus form a free phase.[27]

For $\lambda \geq 6$, counterion clusters coalesce to form larger clusters and eventually a continuous phase is formed, and the conductivity threshold is overcome.

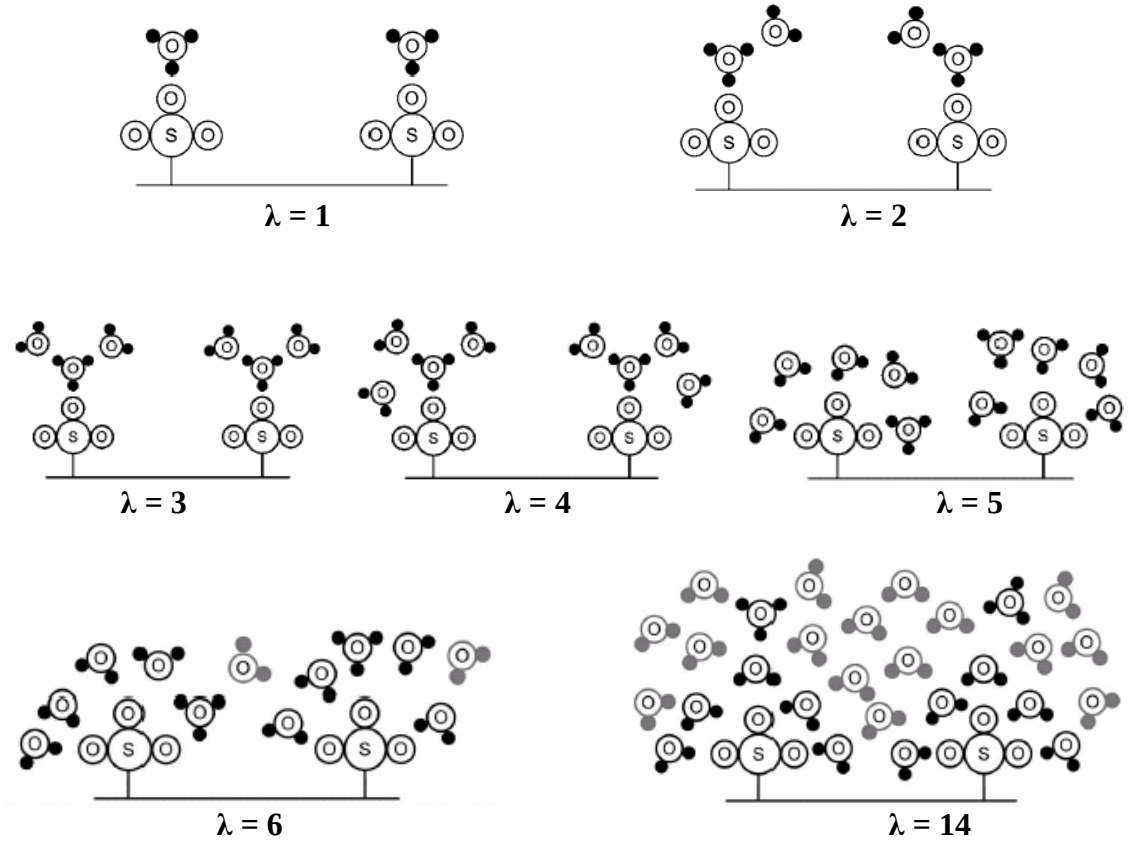

Figure 3.5 - Schematic hydration diagram for Nafion.

Some variations on this hydration scheme are expected for the sulfonated polyetherketones membranes. Among other factors, the number of water molecules in the primary hydration shell will vary according to the strength of the sulfonic acid groups, and the distance between sulfonate heads will affect the conductivity threshold, which will vary with the amount of water needed to connect the clusters.

Sulfonated polyetherketones have less pronounced hydrophobic/hydrophilic separation with respect to Nafion because their backbone are less hydrophobic and flexible and their sulfonic acid groups are less acidic and therefore, also less polar. As a consequence, in sulfonated polyetherketones microstructure narrower channels and a less-connected network of clusters are present, resulting in a higher dependence of the transport properties on water content due to percolation concepts.[28]

A schematic representation of the microstructure of sulfonated polyetherketone compared with that of Nafion is reported in **Figure 3.6**.

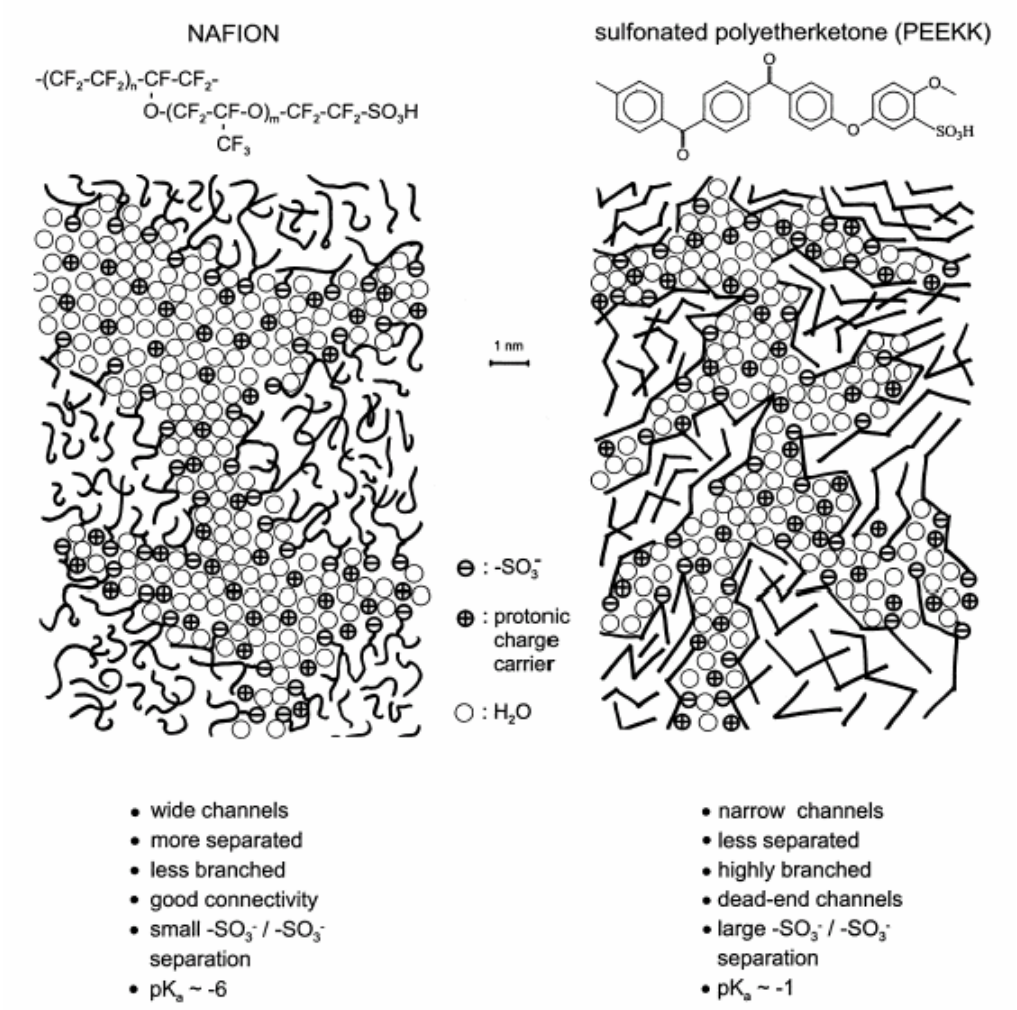

Figure 3.6 - Schematic representation of the microstructures of Nafion and a sulfonated polyetherketone.

Both Nafion and sulfonated polyetherketones membranes exhibit Schroeder's paradox, an observed difference in the amount of water absorbed by a liquid-equilibrated membrane and a saturated vapour equilibrated membrane, with both reservoirs at the same temperature and pressure.[29]

Schroeder's paradox can be explained by models showing the structural changes of Nafion membrane as a function of water content, as shown in **Figure 3.7**.

For saturated vapour water-equilibrated membrane ($\lambda = 14$), the water vapour does not have enough energy to condense in the channels due to their hydrophobicity.

Conversely, the water uptake increases for the liquid water-equilibrated membrane (λ = 22) because the liquid water has enough pressure and energy to infiltrate and expand the channels.

Thus, the reason for the difference in water uptake is due to the filling and expansion of the channels connecting the clusters. It is essentially a structural, not an equilibrium, issue.[30]

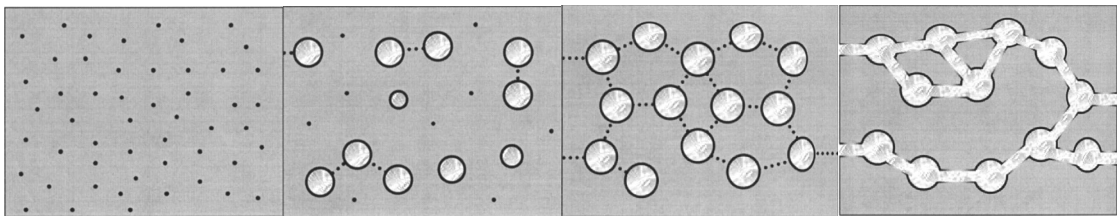

Figure 3.7 - Evolution of the membrane structure as a function of water content. The gray area is the fluorocarbon matrix, the black is the polymer side-chain, the light gray is the liquid water, and the dotted line is a collapsed channel.

3.4 Proton Transport

3.4.1 Proton Conduction Mechanisms

Proton transport proceeds through the membrane following two main mechanisms.[31]

The first is the *vehicle mechanism* where the proton diffuses together with the vehicle water. The counter diffusion of unprotonated water allows the net transport of protons.[32] Therefore, the observed conductivity depends on the rate of vehicle diffusion and it can be expressed as a function of water self-diffusion coefficient (D_{H2O}) that represents a measure of the average mobility of water in the membrane.

The other principal mechanism is known as *Grotthuss mechanism* or "proton hopping" or "structure diffusion". In this process, the water molecules show pronounced local dynamics but reside on their sites. The process consists of two steps: (1) proton transfer from one water molecule to the other by hydrogen bonds; (2) consequent reorientation of water dipoles that results in the formation of an uninterrupted trajectory for proton migration.

The schematic description of two typical proton conduction mechanisms is shown in **Figure 3.8**. [33]

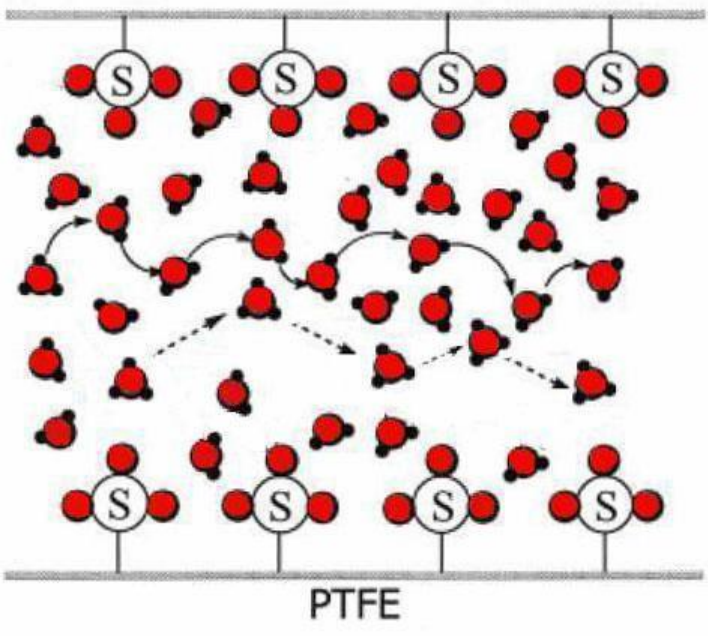

Figure 3.8 – Simplified scheme of the proton transfer in Nafion by the Grotthuss mechanism (solid lines) and the vehicle mechanism (dotted lines).

The prevalence of one or the other mechanism depends on the hydration level of the membrane.[8] At low water content, (in Nafion λ = 2-3), the relative population of hydrogen bonds is low as well and the conductivity follows the vehicle mechanism.

3.4.2 Proton Conductivity and Water Diffusion

Proton conductivity (σ) is related to proton mobility (D_σ) by the Nernst–Einstein equation:

$$s = \frac{cF^2}{RT} D_s \qquad \textit{(Eq. 3.1)}$$

where c is the proton concentration; F is Faraday's constant; R is the universal gas constant and T is the thermodynamic temperature.[34]

Moreover, proton conductivity is strongly dependent on the membrane water content because proton displacement occurs through water-assisted mechanisms, hence the water self-diffusion coefficient (D_{H_2O}) must be also considered.

At high water content, the proton mobility (D_σ) is higher than D_{H2O} and this difference increases with increasing water content, for both Nafion and sulfonated polyetherketones. The gap between the two coefficients indicates that some intermolecular proton transfer is involved in the mobility of protonic charge carriers via Grotthuss mechanism.[35]

At very low hydration levels, the decrement of dissociation degree of the sulfonic acid groups leads to a stronger decrease of D_σ compared to D_{H2O} with decreasing of water content. This effect is more pronounced in sulfonated polyetherketones as a consequence of their less acidic sulfonic groups with respect to Nafion. Hence, the proton conductivity, that is related to D_σ (Eq. 3.1), decreases much more severely with decreasing hydration level in sulfonated aromatic polymers than in Nafion.[27]

Another phenomenon linked to membrane conductivity is electro-osmotic drag, the process whereby a certain number of water molecules associated with a proton are dragged through the liquid phase of the membrane. The electro-osmotic drag coefficient (K_{drag}) represents the number of water molecules dragged per proton and depends on the type of complex that water forms with a proton.

At low degrees of hydration, the only complex that can form and be transported is the hydronium ion (H_3O^+), that corresponds to an electro-osmotic drag coefficient of 1.[36] Thus, the conductivity and the electro-osmotic flow are due to H_3O^+ that displaces

from acid site to acid site through the clusters and across the collapsed channels, as schematically shown in **Figure 3.9**.[30]

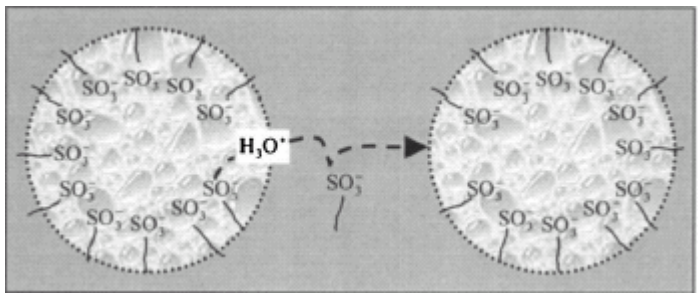

Figure 3.9 - Scheme of the transport mechanism at low water content.

When the water content increases, the channels form continuous water pathways from cluster to cluster and from one side of the membrane to the other. The K_{drag} increases with increasing hydration level because larger structures, such as Zundel ($H_5O_2^+$) and Eigen ($H_9O_4^+$) ions, can form.[37] These ions diffuse through the well interconnected liquid phase of membrane, and more water molecules are dragged per proton. The transport occurs by continuous formation of hydrogen bonds between the proton, its environments and water molecules, as schematically shown in **Figure 3.10**.

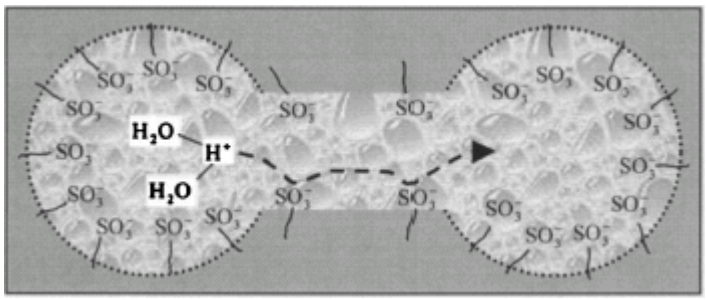

Figure 3.10 - Scheme of the transport mechanism at high water content.

For a given water content, sulfonated polyetherketones show a lower electro-osmotic drag coefficient than Nafion, due to their narrower water channels.[38] As important consequence, their lower K_{drag} facilitate the water management under cell operating conditions and their lower water and methanol crossover is advantageous with respect to that of Nafion, for DMFC applications.[39,40,41]

3.4.3 Activation Energy

Proton conduction in a polymer membrane is a thermally activated process. At temperatures below and close to the glass transition temperature (T_g) of the polymer, the conductivity (σ) obeys an Arrhenius-type law:

$$s = A \times e^{\frac{-E_a}{RT}} \qquad \textit{(Eq. 3.2)}$$

where A is a constant proportional to the number of charge carriers; E_a is the activation energy; R is the universal gas constant; T is the absolute temperature.[42]

Activation energy represents the minimum energy required for proton transport through the membrane and it can be determined experimentally via Arrhenius plots for proton conductivity.

Activation energy value depends on membrane water content, occurring the proton displacement through water-assisted mechanisms.

For Nafion in a dry state, that is containing only residual water molecules, E_a falls in the range 0.4–0.5 eV. In the highly swollen membrane, the activation energy is 0.1 eV, which is close to the bulk water value. At intermediate degrees of wetting, the activation energy varies between these two values.[43]

3.5 Synthetic Approaches

The synthesis of functionalized polymers represents a very promising way to obtain proton-conducting membranes having the desired features for fuel cell applications because it allows to prepare tailored materials for specific applications.[44,45,46]

Several methods have been developed to prepare proton-conducting electrolytes, including total synthesis from monomer building blocks, direct sulfonation of a polymer backbone, and grafting of functional groups onto a polymer main chain. A schematic diagram is shown in **Figure 3.11**.[47]

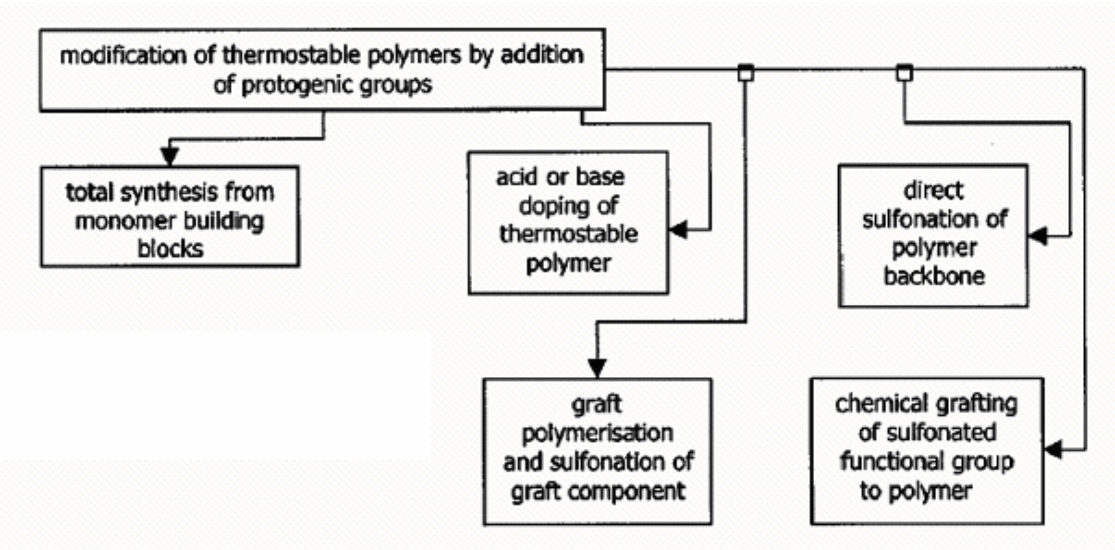

Figure 3.11 - Development of proton-conducting membranes by the modification of thermostable polymers.

Good tailoring of polymer composition is possible by the direct synthesis of a new polymer from monomer building blocks.[48,49] Control of the position, number, and distribution of protogenic functions along the polymer backbone could allow tuning of the microstructure and correlated properties such as conductivity and degree of swelling. However, the range of polymers that can be produced is limited by the commercial availability or the ease of preparation of the corresponding monomers.

Moreover, multistage syntheses could increase costs rendering the polymer less attractive for industrial use than one prepared by direct sulfonation.

Consequently, there is a great interest in using arylene main-chain polymers, such as poly(ether ketone)s (PEK), polysulfones (PSU) and polyimides (PI), because they are high-performance and low-cost materials that can be sulfonated by direct reaction with an appropriate reagent.

In the last years, a large number of these polymers have been sulfonated to obtain proton-conducting electrolytes.[50,51,52] Some of these sulfonated polymers are shown in **Figure 3.12**. The most attractive site for sulfonation depends both on the polymer structure and the directing effect of substituent groups, and advantages of simplicity and reproducibility of the sulfonation reaction are associated with this inherent reactivity.

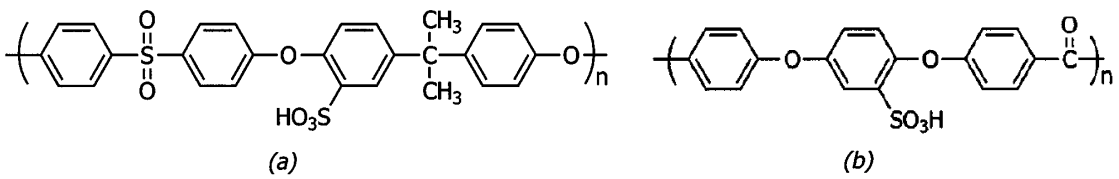

Figure 3.12 - a) Sulfonated polysulfone; b) Sulfonated polyetheretherketone.

A general problem with use of the sulfonated polymers, having the sulfonic groups bound directly to the aromatic chain, is the undesirable swelling of membrane when a certain degree of sulfonation is exceeded.

Several strategies have been used to overcome these problems, including the separation of polymer main chain and sulfonic acid groups by placing the protogenic groups on short pendant side chains,[53,54] and the synthesis of aromatic polymer chains cross-linked covalently by organic spacers.[55]

An emerging strategy is the development of hybrid materials in which organic and inorganic components are combined at molecular level. The nanostructure, the degree of organization and the properties that can be obtained for such materials certainly depend on the chemical nature of their components, but they also rely on the synergy between them.

The nature of the interface between the organic and inorganic components has been used to classify the hybrids into two different classes:[56]

- **Class I** corresponds to systems where there are no covalent bonds between the organic and inorganic components, but only exchange interactions such as van der Waals forces, hydrogen bonding or electrostatic forces.

These hybrids are also called composites and will be discussed in detail in *Section 3.6*.

- **Class II** corresponds to systems where the organic and inorganic components are linked through covalent bonds.

These hybrids are called nanocomposites and can be composed of structural units, which span the whole range from inorganic glass type to compositions with a high content of organic network similar to carbon based polymers, as can be seen in **Figure 3.13**.[57]

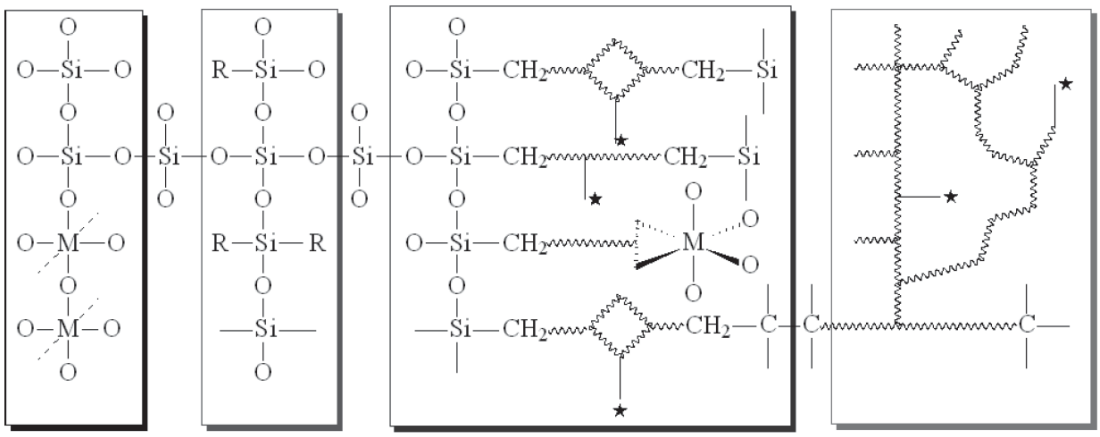

Figure 3.13 - Structural units of Class II hybrids.

Two types of Class II hybrids can be further distinguished:[58]

- **Organic-Inorganic Polymers** (OIPs) that have carbon atoms in the main chain/network and inorganic groups linked to the organic structures.
- **Inorganic-Organic Polymers** (IOPs) that have inorganic elements in the main chain/network and organic side groups.

The organic-inorganic polymers open very broad and promising horizons to obtain proton-conducting electrolytes with the desired features.

The functionalization of organic polymers, where inorganic moieties are grafted onto backbone by strong covalent bonds, represents an interesting synthetic methodology to tailor molecular structures controlling the dosage and dispersion of inorganic clusters.

Among the possible functionalizations, the introduction of silicon-containing moieties appears to be extremely interesting to improve water management in PEMFCs operating at high temperatures.

In these structures additional inorganic crosslinking, due to Si-O-Si bonds, can be achieved by sol-gel process.[59] **Figure 3.14** shows an OIP, where aromatic chains of poly(ether ether sulfone)-co-(ether sulfone) (PEES-PES) are cross-linked via SiO_4 bridges.

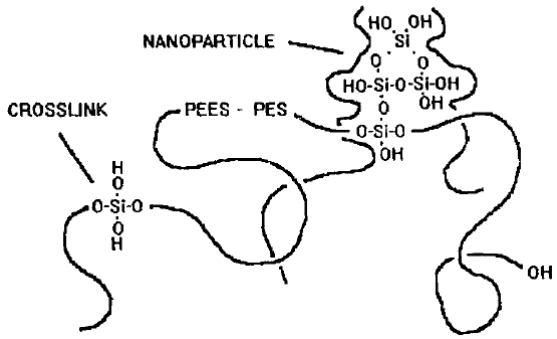

Figure 3.14 - Depiction of PEES-PES chains that are cross-linked through the end groups via SiO_4 bridges.

Over the last decade, numerous studies were also performed for designing inorganic-organic polymers for different applications. [60,61,62]

When the organic groups of IOPs are reactive, additional organic crosslinking/polymerization is possible. If classical sol-gel processing of modified metal alkoxides is followed by organic polymerization or crosslinking, the resulting hybrid materials are called organically modified ceramics (ORMOCERs).

An interesting type of these materials are organic-modified silicates (ORMOSILs) that show good thermal and mechanical stability due to the high Si-O bond strength, making them suitable for PEMFC applications. [63,64]

An ORMOSIL with siloxane backbone and aryl-containing side chains is shown in **Figure 3.15**.

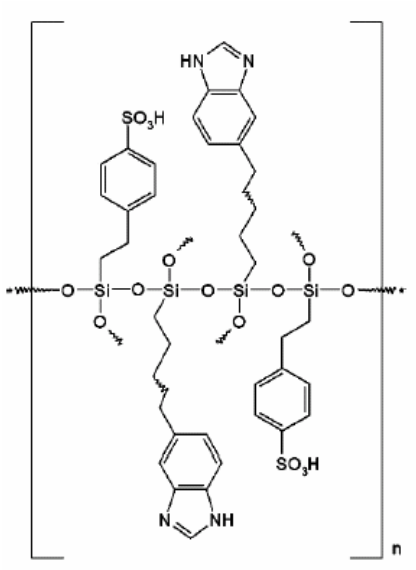

Figure 3.15 - Organically Modified Silicate.

The basic idea of both OIPs and IOPs is to obtain a synergic effect between inorganic and organic phases, not achievable by physical mixing of organic and inorganic materials, as usually made in classical composites (Class I hybrids).

The building principle of these polymers is based on different types of precursor molecules that can be classified by their network forming or modifying. This field of materials research mainly arises from chemists' skills and demonstrates the major role played by chemistry in the preparation of membrane materials for fuel cell applications.

3.6 Composite and Blend Approaches

An effective way to achieve low-humidity and high-temperature operating electrolytes is to prepare composite membranes (Class I hybrids) by casting the polymer solution with an inorganic component. The solid inorganic compounds include hygroscopic oxides, ***e.g.*** silica (SiO_2) and titania (TiO_2), and inorganic proton conductors, such as zirconium phosphates and heteropolyacids.[4]

The growth of inorganic particles ***in situ*** in a polymer solution provide a means of modifying the polymer microstructure because the membrane structure reforms at the same time as the precipitation of the inorganic and/or organic components.

Several approaches have been used to generate organic-inorganic composite membranes, such as: (1) casting a bulk mixture of powder or colloidal inorganic components with a polymer solution, or (2) ***in situ*** formation of inorganic components in a polymer solution.

To prepare uniform and nonporous membranes, size and dispersion of the solid particles are of special importance. For bulk mixing, the use of colloidal suspension of inorganic component enable the nanosized particles to be dispersed in the formed membranes.[65]

On the other hand, the formation of inorganic components ***in situ*** in a polymer matrix can provide many advantages, such as a homogeneous dispersion and a careful morphological control.

This second approach was extensively studied by Mauritz et al. that used a hydrolytic sol-gel route to generate the inorganic network inside the polymer phase. Core of the preparation process using sol-gel techniques is the hydrolysis of an element or metalorganic precursor compound in the matrix of the polymer, yielding an inorganic oxide or oxide/hydroxide network in the polymer phase.[66,67]

Composite membranes containing hygroscopic oxide particles, such as SiO_2,[68,69] TiO_2,[70,71] SnO_2,[72] and ZrO_2,[73] have been investigated by several research groups. Inclusion of these compounds in polymer matrix lead to increase of membrane hydration, due to the water adsorption on the oxide surface, and therefore electrolytes with reduced conduction losses at low-humidity operating conditions can be obtained.

Moreover, composites membranes containing inorganic proton conductors were widely studied.[74,75] Inclusion of these bifunctional particles, that are both proton

conducting and hydrophilic compounds, in the polymer matrix creates additional pathways for the proton conduction and provides hydrogen bonding sites for water in the membrane.[76]

Among the solid proton conductors, zirconium phosphates are of special interest for developing high temperature composite membrane because they exhibit good proton conductivity in a temperature range up to 300 °C. These compounds have been incorporated into polymeric membranes, obtaining electrolytes with good mechanical strength and stability of proton conductivity.[77, 78]

Therefore, several advantages can be obtained by using composite membranes, such as: *i)* improving the self-humidification of the membrane at the anode side; *ii)* suppressing the fuel crossover, *e.g.* methanol in DMFC; *iii)* improving the mechanical strength of membranes without excessively sacrificing proton conductivity.[79]

The main disadvantage of such composite systems is related to the fact that it is very hard to obtain homogenous systems, where the inorganic particles are well dispersed in the polymeric matrix.

Polymer blending represents another versatile and inexpensive way to obtain proton exchange membranes with certain targeted properties for fuel cell application.

Blend membranes are prepared by mixing together two or more organic polymers with different microstructural, thermal, mechanical and conductivity properties to obtain a synergic effect among different components.

Ionomer membrane types have been developed which show the different types of interaction forces between the blend components, such as van der Waals interactions, hydrogen bridge, and dipole-dipole interactions, as schematically shown in **Figure 3.16**.[80]

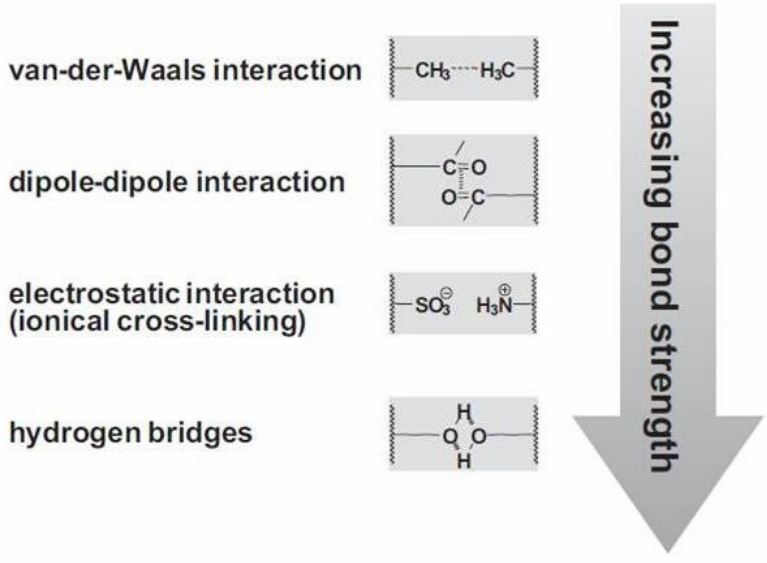

Figure 3.16 - Specific interaction between macromolecules.

Polymer blends, in which van der Waals/dipole-dipole interactions occured between two components, have been prepared starting from a variety of ion-exchange materials, such as sulfonated polysulfone (SPSF), sulfonated polyphenyleneoxide (SPPO) and sulfonated polyetheretherketone (SPEEK) with other materials, such as polyethersulfone (PES) and polysulfone (PSF). [81,82] The basic idea for this membrane type was to reinforce the sulfonated polymer membrane with unmodified polymer, due to the fact that polymers lose much of their mechanical strength by sulfonation.

Blend membranes with increased bond strength between two components have been prepared by mixing silylated and sulfonated polyphenylsulfone (SiSPPSU) and SPEEK. Due to the similar aromatic structure of two polymer, π–π interactions occurred between blend components, together with electrostatic interactions connected with hydrogen bridge and dipole-dipole interactions. These electrolytes have shown good proton conductivity and mechanical strength.[83,84]

Other types of blend membranes, with hydrogen bridge interactions between two polymers, have been prepared starting from polyetherimide (PEI) and SPEEK or sulfonated polyetherketoneketone (SPEKK), obtaining electrolytes with good proton conductivity.[85,86]

An interesting class of proton-conducting membranes is made up of ionically cross-linked acid-base blends. The interaction forces between the acidic and the basic

components include electrostatic and hydrogen bridge interactions. The structure of acid-base blend membranes is depicted schematically in **Figure 3.17**.

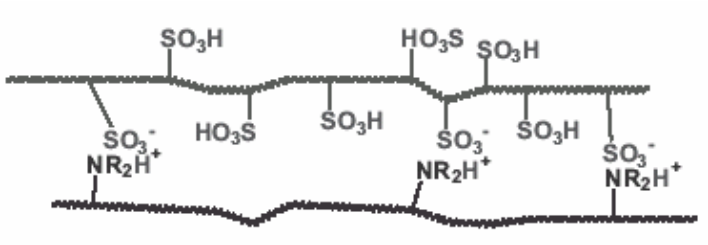

Figure 3.17 - Scheme of Ionically cross-linked acid-base blend membranes.

Several types of ionically cross-linked acid-base blends have been investigated.[87,88] The used acidic polymers are sulfonated polysulfone (SPSF), sulfonated polyethersulfone (SPES), or sulfonated polyetheretherketone (SPEEK). Some basic polymers are commercially available, such as PBI, polyethyleneimine (PEI), and poly(4-vinylpyridine) (P4-VP). New basic polymers have been synthesized by modifying the PSF backbones with amino ($-NH_2$) or dimethylamino ($-N(CH_3)_2$) groups.[89]

Combinations of SPEEK/PBI, SPEEK/P4VP, SPEEK/PSF$(NH_2)_2$, SPSF/PBI, and SPSF/P4VP have been also explored.[90, 91]

3.7 References

1) J. Larminie, A. Dicks, *Fuel Cell Systems Explained*, John Wiley & Sons Ltd, Ontario, **2000**.

2) M. Doyle, G. Rajendran, *Handbook of Fuel Cells, vol. 3,* W. Vielstich, A. Lamm, H.A. Gasteiger (Eds.), Wiley, Chichester, England, **2003**.

3) M.A. Hickner, B.S. Pivovar, *Fuel Cells* **2005**, 5, 213.

4) L. Qingfeng, H. Ronghuan, J.O. Jensen, N.J. Bjerrum, *Chem. Mater.* **2003**, 15, 4896.

5) L.P. Hammett, *Physical Organic Chemistry,* 2nd Ed., McGraw-Hill Ltd, Kogakusha, Tokyo, **1970**.

6) M. Hickner, H. Ghassemi, Y.S. Kim, B.R. Einsla, J.E. McGrath, *Chem. Rev.* **2004**, 104, 4587.

7) G. Alberti, R. Narducci, M. Sganappa, *J. Power Sources* **2008**, 178, 575.

8) K.D. Kreuer, S. Paddison, E. Spohr, M. Schuster, *Chem. Rev.* **2004**, 104, 4637.

9) A.S. Aricò, S. Srinivasan, V. Antonucci, *Fuel Cells* **2001**, 1, 133.

10) W. G. Grot, US Pat., 3718627, **1968**.

11) B. Smitha, S. Sridhar, A.A. Khan, *J. Membr. Sci.* **2005**, 259, 10.

12) O. Savadogo, *J. Power Sources* **2004**, 127, 135.

13) R.W. Dyson, *Ed. Specialty Polymers,* Blackie Academic & Professional London, **1998**.

14) P. Xing, G.P. Robertson, M.D. Guiver, S.D. Mikhailenko, K. Wang, S. Kaliaguine, *J. Membr. Sci.* **2004**, 229, 95.

15) T. Fu, Z. Cui, S. Zhong, Y. Shi, C. Zhao, G. Zhang, K. Shao, H. Na, W. Xing, *J. Power Sources* **2008**, 185, 32.

16) J. Kerres, *Fuel Cells* **2006**, 3, 251.

17) B. Lafitte, L.E. Karlsson, P. Jannasch, *Macromol. Rapid Commun.* **2002**, 23, 896.

18) C.S. Karthikeyan, S.P. Nunes, K. Schulte, *Adv. Engineering Mater.* **2006**, 8, 1010.

19) P. Mustarelli, E. Quartarone, S. Grandi, A. Carollo, A. Magistris, *Adv. Mater.* **2008**, 20, 1339.

20) J. Divisek, M. Eikerling, V. Mazin, H. Schmitz, U. Stimming, Y.M. Volfkovich, *J. Electrochem. Soc.* **1998**, 145, 2677.

21) R.S. McLean, M. Doyle, B.B. Sauer, *Macromolecules* **2000**, 33, 6541.

22) K.A. Mauritz, C.J. Hora, A.J. Hopfinger, *Ions in Polymers*; Ed. A. Eisenberg, ACS Advances in Chemistry Ser. No. 187, American Chemical Society: Washington, DC, **1980**.

23) H.L Yeager, A. Steck,. *J. Electrochem. Soc.* **1981**, 128, 1880.

24) W.Y. Hsu, T.D. Gierket, *Macromolecules* **1982**, 15, 101.

25) W.Y Hsu, T.D. Gierke, *J. Membr. Sci.* **1983**, 13, 307.

26) J. Fimrite, H. Struchtrup, N. Djilali, *J. Electrochemical Soc.* **2005**, 152, A1804.

27) J. Elliot, S. Hanna, A.M.S. Elliot, G.E. Cooley, *Phys. Chem. Chem. Phys.* **1999**, 1, 4855.

28) K.D. Kreuer, *J. Membr. Sci.* **2001**, 185, 29.

29) T.A. Zawodzinski, T.E. Springer, J. Davey, R. Jestel, C. Lopez, J. Valerio, S. Gottesfeld, *J. Electrochem. Soc.* **1993**, 140, 1981.

30) A.Z. Weber, J. Newman, *J. Electrochem. Soc.* **2003**, 150, A1008.

31) K.D. Kreuer, *Chem. Mater.* **1996,** 8, 610.

32) K.D. Kreuer, W. Weppner, A. Rabenau, *Angew. Chem., Int. Ed. Engl.* **1982**, 21, 208.

33) P. Choi, N.H. Jalani, T.M. Thampan, R. Datta, *J. Polym. Sci: Part B: Polym. Phys.* **2006**, 44, 2183.

34) P.G. Bruce, *Solid State Electrochemistry*, Cambridge University Press, **1995**.

35) N. Agmon, *Chem. Phys. Lett.* **1995**, 244, 456.

36) T.A. Zawodzinski, J. Davey, J. Valerio, S. Gottesfeld, *Electrochim. Acta* **1995**, 40, 297.

37) K.D. Kreuer, *Solid State Ionics* **2000**, 136, 149.

38) M. Ise, K.D. Kreuer, J. Maier, *Solid State Ionics* **1999**, 125, 213.

39) M. Eikerling, Y.I. Kharkats, A.A. Kornyshev, Y.M. Volfkovich, *J. Electrochem. Soc.* **1998,** 145, 2684.

40) T. Okada, G. Xie, M. Meeg, *Electrochim. Acta* **1998**, 43, 2141.

41) X.M. Ren, W. Henderson, S. Gottesfeld, *J. Electrochem. Soc.* **1997**, 144, L267.

42) Y. Sone, P. Ekdunge, D. Simonsson, *J. Electrochem. Soc.* **1996**, 143, 1254.

43) M. Eikerling, A.A. Kornyshev, *J. Electroanal. Chem.* **2001**, 502, 1.

44) B. Smitha, S. Sridhar, A.A. Khan, *J. Membr. Sci.* **2005**, 259, 10.

45) M. Ulbricht, *Polymer* **2006**, 47, 2217.

46) Y. Yang, S. Holdcroft, *Fuel Cells* **2005**, 5, 171.

47) J. Rozière, D.J. Jones, *Annu. Rev. Mater. Res.* **2003**, 33, 503.

48) F. Wang, M. Hickner, Y.S. Kim, T.A. Zawodzinski, J.E. McGrath, *J. Membr. Sci.* **2002**, 197, 231.

49) G. Maier, C-K Shin, G.G. Scherer. In *1st Eur. PEFC Conference*, ed. FN Büchi, GG Scherer, A Wokaun, Lucerne, Switerland: European Fuel Cell Forum, **2001**.

50) J.A. Kerres, *J. Membr. Sci.* **2001**, 185, 3.

51) A. Dyck, D. Fritsch, S.P. Nunes, *J. Appl. Polym. Sci.* **2002**, 86, 2820.

52) S. Kaliaguine, S.D. Mikhailenko, K.P. Wang, P. Xing, G. Robertson, M. Guiver, *Catalysis Today* **2003**, 82, 213.

53) L.E. Karlsson, P. Jannasch, *Electrochim. Acta* **2005**, 50, 1939.

54) J.M. Bae, I. Honma, M. Murata, T. Yamamoto, M. Rikukawa, N. Ogata, *Solid State Ionics* **2002**, 147, 189.

55) W. Zhang, V. Gogel, K. Friedrich, J. Kerres, *J. Power Sources* **2006**, 155, 3.

56) C. Sanchez, F. Ribot, *New J. Chem.* **1994**, 18, 1007.

57) K.H. Haas, K. Rose, *Rev. Adv. Mater. Sci.* **2003**, 5, 47.

58) H.L. Allcock, *Adv. Mater.* **1994**, 6, 106.

59) C.H. Brinker, G. Scherer, *Sol-gel Science*, Academic Press, London, **1990**.

60) C. Sanchez, B. Lebeau, F. Chaput, J.P. Boilot, *Adv. Mater.* **2003**, 15, 1969.

61) R. Houbertz, L. Fröhlich, M. Popall, U. Streppel, P. Dannberg, A. Bräuer, J. Serbin, B. N. Chichkov, *Adv. Engineering Mater.* **2003**, 5, 551.

62) L.C. Klein,Y. Daiko, M. Aparicio, F. Damay, *Polymer* **2005**, 46, 4504.

63) D. Gomes, I. Buder, S.P. Nunes, *J. Polym. Sci: Part B: Polym. Phys.* **2006**, 44, 2278.

64) M. Jeske, C. Soltmann, C. Ellenberg, M.Wilhelm, D. Koch, G. Grathwohl, *Fuel Cells* **2007**, 1, 40.

65) G. Alberti, M. Casciola, U. Costantino, R. Vivani, *Adv. Mater.* **1996**, 8, 291.

66) K.A. Mauritz, J.T. Payne, *J. Membr. Sci.* **2000**, 168, 39.

67) S.P. Nunes, B. Ruffmann, E. Rikowski, S. Vetter, K. Richau, *J. Membr. Sci.* **2002**, 203, 215.

68) B. Bonnet, D.J. Jones, J. Rozière, L. Tchicaya, G. Alberti, M. Casciola, L. Massinelli, B. Bauer, A. Peraio, E. Ramunni, *J. New Mat. Electrochem. Systems* **2000**, 3, 87.

69) K.T. Adjemian, S.J. Lee, S. Srinivasan, J. Benziger, A.B. Bocarslya, *J. Electrochem. Soc.* **2002**, 149, A256.

70) M. Watanabe, H. Uchida, Y. Seki, M. Emori, *J. Electrochem. Soc.* **1996**, 143, 3847.

71) M.L. Di Vona, Z. Ahmed, S. Bellitto, A. Lenci, E. Traversa, S. Licoccia, *J. Membr. Sci.* **2007**, 296, 156.

72) B. Mecheri, A. D'Epifanio, E. Traversa, S. Licoccia, *J. Power Sources* **2008**, 178, 554.

73) K.A. Mauritz, *Mat. Sci. Eng.* **1998**, C6, 121.

74) P. Staiti, A.S. Arico, V. Baglio, F. Lufrano, E. Passalacqua, V. Antonucci, *Solid State Ionics* **2001**, 145, 101.

75) P. Costamagna, C. Yang, A.B. Bocarsly, S. Srinivasan, *Electrochim. Acta* **2002**, 47, 1023.

76) K.T. Adjemian, S. Srinivasan, J.Benziger, A.B. Bocarsly, *J. Power Sources* **2002**, 109, 356.

77) G. Alberti, M. Casciola, D. Capitani, A. Donnadio, R. Narducci, M. Pica, M. Sganappa, *Electrochim. Acta* **2007**, 52, 8125.

78) L. Tchicaya-Bouckary, D.J. Jones, J. Rozière, *Fuel Cells* **2002**, 2, 40.

79) G. Alberti, M. Casciola, *Annu. Rev. Mater. Res.* **2003**, 33, 129.

80) J. A. Kerres, *Fuel Cells* **2005**, 5, 230.

81) V. Deimede, G.A. Voyiatzis, J.K. Kallitsis, Q. Li, N.J. Bjerrum, *Macromolecules* **2000**, 33, 7609.

82) J. Kerres, A. Ulrich, F. Meier, T. Haring, *Solid State Ionics* **1999**, 125, 243.

83) M. L. Di Vona, A. D'Epifanio, D. Marani, M. Trombetta, E. Traversa, S. Licoccia, *J. Membr. Sci.* **2006**, 279, 186.

84) E. Sgreccia, M. Khadhraoui, C. de Bonis, S. Licoccia, M. L. Di Vona, P. Knauth, *J. Power Sources* **2008**, 178, 667.

85) S.D. Mikhailenko, S.M.J. Zaidi, S. Kaliaguine, *J. Polym. Sci. Polym. Phys.* **2000**, 38, 1386.

86) S. Swier, M.T. Shaw, R.A. Weiss, *J. Membr. Sci.* **2006**, 270, 22.

87) J.A. Kerres, *J. Membr. Sci*. **2001**, 185, 3.

88) J. Kerres, W. Zhang, L. Jörissen, V. Gogel, *J. New Mat. Electrochem. Systems* **2002**, 5, 97.

89) M.D. Guiver, G.P. Robertson, S. Foley, *Macromolecules* **1995**, 28, 7612.

90) L. Jorissen, V. Gogel, J. Kerres, J. Garche, *J. Power Sources* **2002**, 105, 267.

91) C. Hasiotis, V. Deimede, C. Kontoyannis, *Electrochim. Acta* **2001**, 46, 2401.

4 Experimental

4.1 Materials and Methods

This section presents a description of the starting materials and characterization methods of the polymers and membranes.

4.1.1 Starting Materials

Polyetheretherketone (Victrex, PEEK, 450 P, MW = 38300 g/mol, 132 repeat units per mol), Polyphenylsulfone (Solvay, PPSU-RADEL R®, 5100 P, MW = 46173 g/mol, 115 repeat units per mol) and all other chemicals (Aldrich) were used as-received.

Anhydrous tetrahydrofuran (THF) and dichloromethane (CH_2Cl_2) were prepared according to literature procedures.[1]

PEEK

Polyetheretherketone is a semicrystalline thermoplastic with the glass transition temperature (T_g) of 150°C. It shows extraordinary mechanical properties and exhibits good chemical resistance in many environments, including alkalis, aromatic hydrocarbons and alcohols.

PEEK consists of alternating hydroquinone and diphenyl carbonyl segments, as shown in **Figure 4.1**.

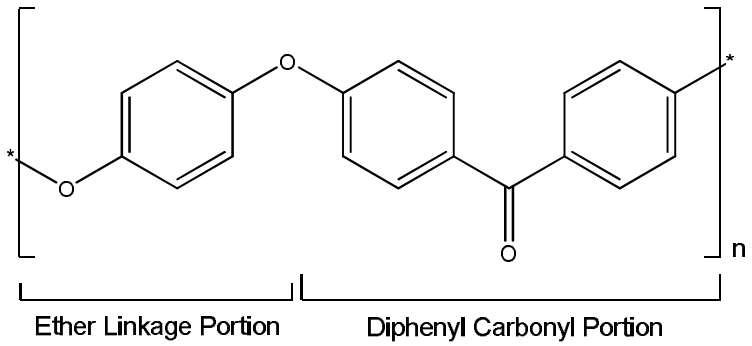

Figure 4.1 - Monomeric repeat unit of PEEK.

Aromatic electrophilic substitution may occur easily on the hydroquinone unit due to the presence of activating and *ortho*-directing ether groups, in contrast with the diphenyl carbonyl portion which has a low electron density, due to the electron-withdrawing effect of carbonyl group.

PPSU

Polyphenylsulfone is an amorphous polymer with a glass transition temperature (T_g) of 220°C. It shows good oxidative resistance and is among the most heat resistant of current commercial thermoplastics.[2]

PPSU consists of alternating bisphenol and diphenyl sulfone segments, as shown in **Figure 4.2**.

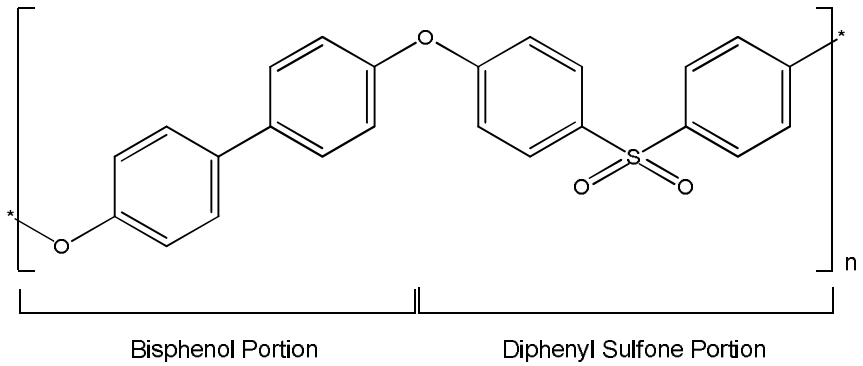

Figure 4.2 - Monomeric repeat unit of PPSU.

The strong electron-withdrawing effect of the sulfone units gives an acidic character to the aromatic hydrogens in the *ortho* position. Thus, the carbons at these sites may be metalized by the use of a strong base.

On the other hand, the electron-donating effect of the ether linkages activates the phenylene rings of the bisphenol part towards electrophilic substitution.[3]

Thus, for both PEEK and PPSU several functionalizations are possible since their chemical structure offers the possibility of electrophilic as well as nucleophilic substitution, increasing their application areas. In particular, both polymers show proton conductivity when sulfonated, thus being potential electrolytes for PEMFCs.[4]

4.1.2 Methods

The chemical structure of synthesized polymers was investigated by nuclear magnetic resonance (NMR) and attenuated total reflectance Fourier transform infrared (ATR/FTIR) spectroscopies, and their thermal stability was evaluated by thermogravimetric analysis (TGA).

Membranes features were investigated by water uptake (W.U.) measurements, electrochemical impedance spectroscopy (EIS) and tests in a prototype fuel cell.

Nuclear Magnetic Resonance Spectroscopy

^{1}H and ^{13}C NMR spectra were recorded with a Bruker Avance 300 spectrometer operating at 300 and 75.4 MHz, respectively, using DMSO-d6 as solvent. Chemical shifts (ppm) were referenced to tetramethylsilane (TMS).

ATR/FTIR Spectroscopy

Infrared spectra were collected in the range 4000–500 cm^{-1}, on a Nicolet 8700 E.S.P. with a Golden Gate MK2 Diamond Specac cell. Spectra were recorded positioning the samples on cell platform operating at room temperature (32 scans, 2 cm^{-1} resolution).

Thermogravimetric Analysis

Thermogravimetric analyses were carried out using a Netzsch STA 409 thermobalance, in air flow (80 mL/min) with a heating rate of 2 °C/min in the range 100-800 °C, using platinum sample holders.

Differential Scanning Calorimetry

The measurements were carried out by using DSC 7 Perkin-Elmer Differential Scanning Calorimeter. Thermograms were recorded under N_2 flow (20 mL/min), placing the samples in aluminum pans. The samples were preheated from 10°C to 160°C at 20 °C/min to remove moisture, then cooled to 90°C, and reheated from that temperature to 250°C at 20 °C/min.

Membranes preparation

Literature conductivity values of proton exchange membranes with similar composition show large discrepancies suggesting that the preparation procedure has a significant influence on the electrical properties of these electrolytes.

Membranes made up of sulfonated PEEK and/or PPSU are usually obtained by casting the polymer solution on a flat surface. The solvents commonly used to prepare the solution are: N,N-dimethylacetamide (DMAc), dimethylformamide (DMF), dimethyl sulfoxide (DMSO) and N-methyl-2-pyrrolidone (NMP). [5]

However, it must be considered that NMP and DMSO are solvents with higher boiling temperature (202°C and 189°C, respectively) compared with DMF (153°C) and DMAc (166°C). As a consequence, it is particularly difficult to dry the NMP or DMSO cast membranes.

On the other hand, amide-based solvents, *i.e.* DMAc and DMF, can form strong hydrogen-bonds with the sulfonic acid groups of the polymer and these interactions may significantly decrease the number and/or mobility of protons, reducing membrane conductivity.

In this work, DMAc was chosen as solvent because it has relatively low boiling point and forms hydrogen-bonds with sulfonic acid groups only above 140 °C.[6]

In a typical experiment for the preparation of the membranes of sulfonated PEEK ($S_{0.5}$PEEK) or hybrid polyphenylsulfone derivative (HSiSPPSU), 400 mg of polymer was dissolved in DMAc (20 mL).

For the preparation of the blend membranes, 400 mg of $S_{0.5}$PEEK was dissolved in DMAc (20 mL) and the appropriate weight of silylated and sulfonated PEEK ($PhSi_{0.1}S_{0.9}$PEEK) or PPSU ($PhSi_{0.2}S_2$PPSU) was dissolved in the same solvent (10 mL), then the two solutions were mixed.

In all cases, the resulting mixture was heated under stirring until the volume was reduced to 5 mL, then cast onto a Petri plate (5.5 cm of diameter) and heated to 80°C for 24 hours. The thickness of the membranes was in the range 140-160 µm.

The membranes were activated by reflux in 0.5 M H_2SO_4 for 1 hour and in distilled water for 1 hour. Before measurements, the samples were equilibrated at RT, at ambient humidity (~ 50%) for 48h.

The activation of the membranes in sulphuric acid was needed to remove the protonated casting solvent, and the subsequent treatment with boiling water was carried out to remove residual sulphuric acid and to promote the water uptake of membranes.
In fact, it is well known that an adequate water uptake is required for good proton conductivity, since proton transport occurs through a water-assisted mechanism.

Solvent uptake

Water and methanol uptake measurements were performed on the membranes to evaluate their hydration behavior and methanol affinity.
Disks were cut from the membranes, dried overnight at 80 °C and immediately weighted to obtain the dry weights (W_{dry}).
Two different procedures were then carried out to measure the water uptake, at 100% relative humidity (RH).

- In the first one, dry disks were immersed in distilled water, at room temperature, for 24 hours. The samples were then rapidly dried with adsorbent paper and weighted.
- In the second procedure, dry samples were exposed at saturated water vapour pressure at room temperature, overnight, and then weighted.

Water uptake values, expressed in percentage units, (W.U.%) were calculated using the following equation: [7]

$$W.U.\% = \left(\frac{W_{wet}}{W_{dry}} - 1 \right) \times 100 \qquad \textit{(Eq. 4.1)}$$

where W_{dry} and W_{wet} are the dry and wet weights, respectively.

Methanol uptake measurements were also carried out. Dry disks were immersed in absolute methanol, at room temperature, for 24h. The samples were then rapidly dried with adsorbent paper and weighted to obtain the wet weights (W_{wet}).

Conductivity Measurements

Proton conductivity of the membranes was measured by electrochemical impedance spectroscopy (EIS) using a Multichannel Potentiostat VMP3 (Princeton Applied Research). An applied voltage of 20 mV and a frequency range of 500 KHz to 10 Hz were used.

Membranes were sandwiched between commercial electrodes (E-Tek ELAT HT 140E-W with a platinum loading of 5 g m^{-2}), as shown in **Figure 4.3**. A teflon ring was used as spacer to avoid the short circuit between the electrodes.

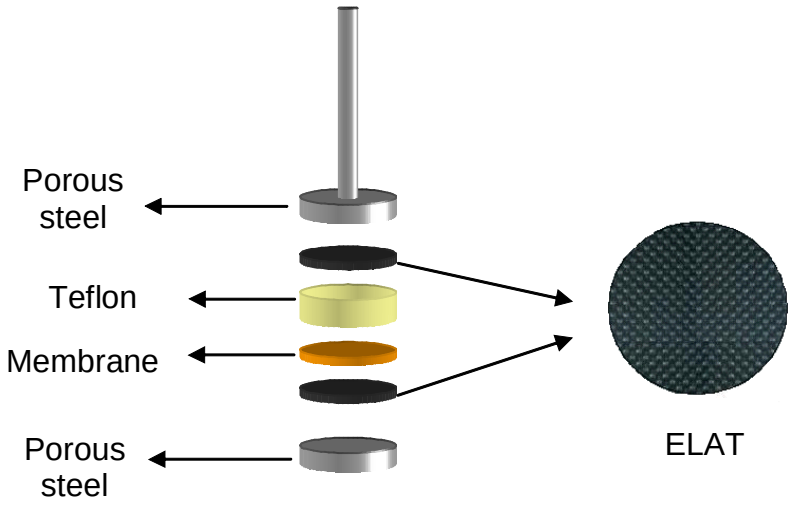

Figure 4.3 - Electrodes and membrane assembly for EIS measurements.

Proton conductivity of the membranes was measured as a function of temperature, at 100% relative humidity (RH). Before measurements, the samples were kept overnight at room temperature (RT) and at 100% RH, and conductivity values were then obtained in the range 20-100°C, at saturated water vapour pressure.

Proton conductivity of the membranes was also measured as a function of RH, at a fixed temperature. Controlled RH environments were obtained using the homemade apparatus that is schematically shown in **Figure 4.4**. [8]

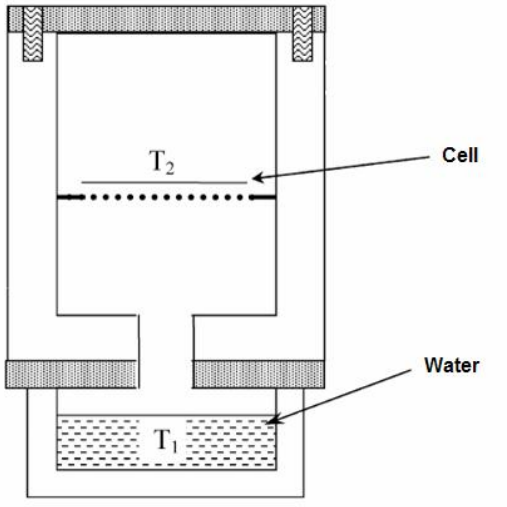

Figure 4.4 - Scheme of the double chamber apparatus.

It is constituted of two compartments one for the lodging of the test cell and the other containing water. The relative humidity was controlled by the different temperature between the two compartments, T_1 and T_2, where $T_1 \leq T_2$, because water vapour pressure depends on temperature and RH% is expressed by the following equation:

$$RH\% = \frac{P^{o}_{H_2O}(T_1)}{P^{o}_{H_2O}(T_2)} \times 100 \qquad \textit{(Eq. 4.2)}$$

where $P°_{H_2O}(T_1)$ is the saturated water vapour pressure at the temperature of the water-containing compartment, while $P°_{H_2O}(T_2)$ is the saturated water vapour pressure at the temperature of the cell-containing compartment.

Electrical heaters were used to control the two temperatures, where T_2 was kept constant, whereas T_1 was varied to achieve different RH% values that were monitored by a humidity sensor (Vaisala HMP237) in the 20 –100% range.

The resistance of the membranes was calculated by a linear fit of the Nyquist plots in their linear portion. Conductivity values (σ) were obtained from the resistance values (R), the thickness of the membrane (l) and the electrode area (A), using the following equation:

$$s = \frac{l}{R \times A} \qquad \textit{(Eq. 4.3)}$$

Direct Methanol Fuel Cell Testing

Membrane electrode assemblies (MEAs) were fabricated using commercial electrodes E-TEK, A-6 ELAT/SS/PtRu60-3-30PTFE/0.8N, custom 3 mg cm^{-2} loading using 60% HP Pt:Ru Alloy (1:1) on Vulcan, 30 wt % PTFE with 0.8 mg cm^{-2} Nafion (anode), and A-6 ELAT/SS/Pt40-2-30PTFE/0.8N custom 2 mg cm^{-2} loading using 40% HP Pt on Vulcan, 30 wt % PTFE with 0.8 mg cm^{-2} Nafion (cathode).

MEAs were prepared by hot pressing using an SPECAC hot press. Membrane and anodic electrode were placed in a teflon sheet and pressed for 1 min at 80 °C under a load of 0.62 MPa. After that, the cathode was put on the other side of the membrane. Proper interfacial adhesion in the electrode/membrane/electrode was achieved pressing the sandwich at 80 °C under a load of 0.62 MPa for 5 min.

Figure 4.5 shows a picture of one of the prepared MEAs.

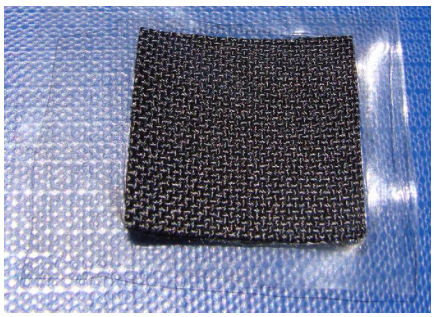

Figure 4.5 - A typical MEA.

Fuel cell experiments were carried out in a 5 cm^2 single cell (ElectroChem) using a homemade fuel cell test station. The test station was equipped for the independent temperature control of the reactant gas (O_2), methanol solution and single cell. Flow rate of the gas was regulated using mass-flow controller (MKS PR4000, 300 sccm), the total pressure of the gas was controlled using a back-pressure regulator. Flow rate of methanol solution (2 M) was monitored by a KNF's Model FEM 1.08 Liquid Metering Pump with control board (1 mL min^{-1}). All experiments were performed fixing at 0.2 MPa the total pressure in the cell and at 100 °C the cell temperature. Polarization data were recorded using a Multichannel Potentiostat VMP3 (Princeton Applied Research).

4.1.3 References

1) B.S. Furniss, A.J. Hannaford, P.W.G. Smith, A.R. Tatchell, *Textbook of Practical Organic Chemistry*, Vogel's Longaman Scientific & Technical, **1989**.

2) R.J. Cotter, *Engineering Plastics: Handbook of Polyaryl Ether*, Gordon and Breach Publishers, USA, **1995**.

3) M.D. Guiver, J. W. ApSimon, O. Kutowy, *J. Polym. Sci. Part C: Polym. Lett.* **1988**, 26, 123.

4) A. Dick, D. Fritsch, S.P. Nunes, *J. Appl. Polym. Sci.* **2002**, 86, 2820.

5) J. Rozière, D.J. Jones, *Annu. Rev. Mater. Res.* **2003**, 33, 503.

6) G.P. Robertson, S.D. Mikhailenko, K. Wang, P. Xing, M.D. Guiver, S. Kaliaguine, *J. Membr. Sci.* **2003**, 219, 113.

7) S.M.J. Zaidi, S.D. Mikhailenko, G.P. Robertson, M.D. Guiver, S. Kaliaguine, *J. Membr. Sci.* **2000**, 173, 17.

8) G. Alberti, M. Casciola, L. Massinelli, B. Bauer, *J. Membr. Sci.* **2001**, 185, 73.

4.2 $PhSi_{0.1}S_{0.9}PEEK$ / $S_{0.5}PEEK$ Blend

Literature data show that the use of highly sulfonated polyetheretherketone (SPEEK) is desirable for high proton conductivity, but the polymer tends to important swelling and, eventually becomes water-soluble, with increasing of degree of sulfonation (DS). [1]

The correct balance between the hydrophilic and hydrophobic domains of the polymer matrix is one of main microstructural features of a good membrane material because the hydrophilic domain is responsible of the proton transport, and the hydrophobic domain provides the morphological stability, avoiding the membrane dissolution in water. [2]

For this reason, in our group, several synthetic routes have been developed to prepare derivatives of polyetheretherketone (PEEK), where the ratio between hydrophilic and hydrophobic domains can be modulated by the introduction of a controlled amount of sulfonic acid groups and silicon-containing substituents covalently bound to the aromatic chain.

Silylated and sulfonated PEEK (SiSPEEK) was synthesized by sulfonation up to DS=0.9 and subsequent silylation with tetrachlorosilane ($SiCl_4$). The introduction of the silanol moieties ($-Si(OH)_3$), covalently bound to the aromatic chain, allowed to achieve membranes with reduced swelling and thermal stability. [3]

Moreover, silylated and crosslinked sulfonated PEEK (SOSiPEEK), with DS=0.8, was prepared. The introduction of sulfonic acid groups and the covalent crosslinking through SO_2 bridging moieties were obtained by reaction of PEEK with chlorosulfonic acid (HSO_3Cl). The subsequent silylation with $SiCl_4$ led to silanol groups covalently bound to the aromatic chain. The presence of inorganic moieties allowed to obtain membranes with good thermal and hydrolytic stability, maintaining adequate conductivity values for PEMFC applications. [4,5]

However, these developed synthetic pathways resulted to be rather complex to obtain always reproducible results and to modulate the hydrophilic/hydrophobic ratio in the polymer matrix by the dosage of sulfonic acid groups and inorganic moieties.

In this work, an efficient, highly reproducible and versatile synthetic pathway was developed to obtain a derivative of polyetheretherketone ($PhSi_{0.1}S_{0.9}PEEK$, DS=0.9 and

degree of silylation DSi=0.1), having sulfonic acid groups and phenylsilanol moieties covalently bound to the aromatic chain.

In this new route, phenylsilanol instead of silanol moieties were covalently bound to the backbone of highly sulfonated PEEK because the presence of hydrophobic phenyl group onto the silicon allows further control on the hydrophilic/hydrophobic ratio, allowing the use of a lower amount of electrophilic reactant.

4.2.1 Polymers Synthesis

The synthesis of silylated and sulfonated polyetheretherketone ($PhSi_{0.1}S_{0.9}PEEK$) was carried out following the synthetic steps shown in **Scheme 4.1**: *i*) sulfonation of PEEK by reaction with concentrated sulfuric acid; *ii*) conversion in sulfonyl chlorinated derivative; *iii*) metalation reaction with butyllithium and subsequent substitution by phenyltrichlorosilane; *iv*) hydrolysis.

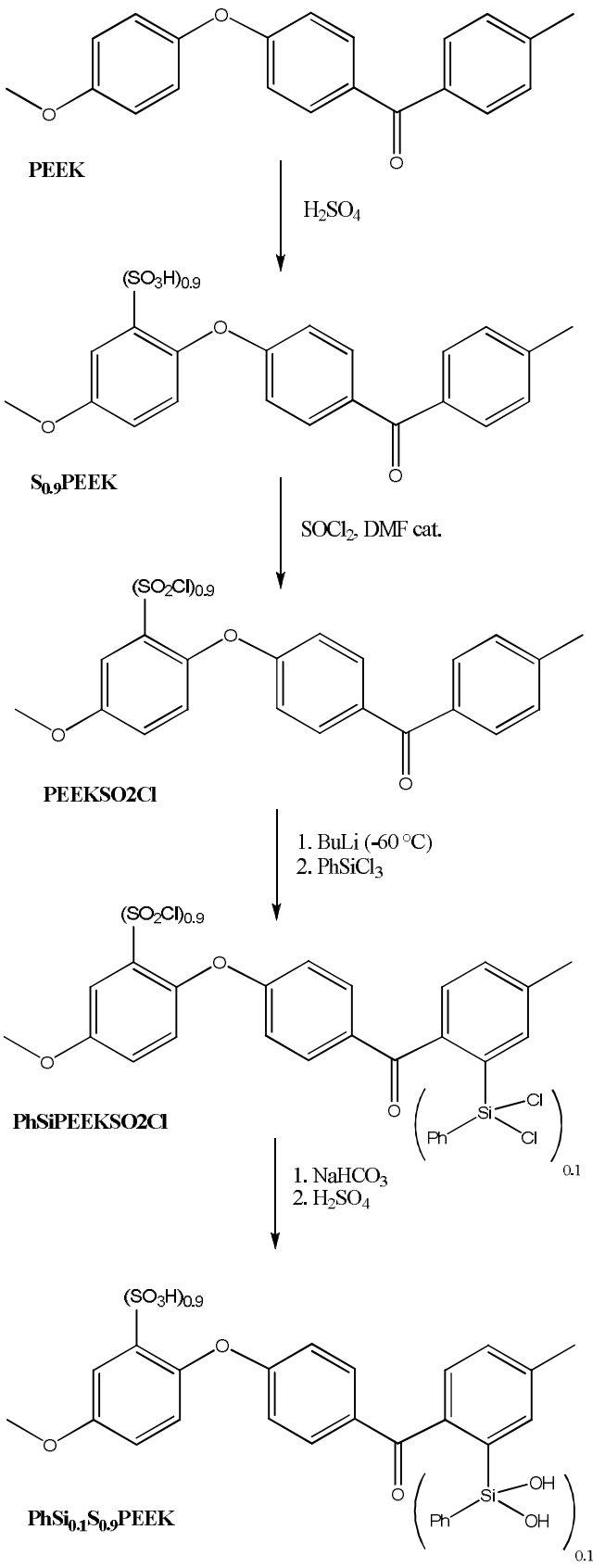

Scheme 4.1 - Synthesis of silylated and sulfonated PEEK.

Synthesis of $S_{0.9}$PEEK

PEEK (20 g, 69 meq) was dissolved in H_2SO_4 96% (1 L) and stirred at 50 °C for 5 days. The solution was poured in a large excess of ice-cold water under continuous stirring, obtaining a white precipitate. After standing overnight, the precipitate was filtered and washed several times with cold water to neutral pH. The sulfonated polymer was then dried under vacuum for 5 h at room temperature.[3] The yield of the reaction was 79%.

The DS of the product was evaluated by ^{1}H NMR spectroscopy and resulted to be 0.9.

Synthesis of PEEKSO2Cl

Sulfonated polyetheretherketone $S_{0.9}$PEEK (1 g, 2.8 meq) was poured, under nitrogen atmosphere, in thionylchloride ($SOCl_2$, 20 mL). A volume of 0.3 mL of N,N-dimethylformamide (DMF) was added and the mixture was stirred at 60°C for 3 h, getting a homogenous solution.[6]

The solution was cooled at room temperature and the $SOCl_2$ was distilled off under reduced pressure. The polymer was dissolved in tetrahydrofuran (THF, 15 mL) and recovered by adding of isopropanol (30 mL) to the solution and subsequent filtration. Again, the polymer was dissolved in THF (10 mL), precipitated by addition of isopropanol (20 mL) and filter. Finally, the purified product was dried under vacuum at room temperature for 4h. The yield of the reaction was 77%.

Synthesis of $PhSi_{0.1}S_{0.9}$PEEK

PEEKSO2Cl (1 g, 2.6 meq) was dissolved at room temperature, in anhydrous THF (150 mL), under nitrogen atmosphere. Then, the solution was cooled to -60°C and N,N,N',N'-tetramethylethylenediamine (TMEDA, ≥99%, 1.6 mL, 10.4 mmol) and Butyllithium (2.5 M BuLi in hexane, 4.2 mL, 10.4 mmol) were added. The solution was stirred for 4h at -60 °C to complete the deprotonation of the aromatic repeating units. Subsequently, a solution of phenyltrichlorosilane ($PhSiCl_3$, ≥97%, 0.04 mL, 0.26 meq) in anhydrous THF (3 mL) was introduced into the reaction flask *via* a syringe. The mixture was warmed up to room temperature and then kept under reflux for 12h. After cooling to room temperature, the product PhSiPEEKSO2Cl was recovered by filtration.

Subsequently, PhSiPEEKSO2Cl was suspended in a saturated aqueous solution of $NaHCO_3$ (70 mL) and stirred under reflux, for 5 h. An aqueous solution of H_2SO_4 (5 M) was then added dropwise to the mixture until complete precipitation of polymer (pH=2). The final product $PhSi_{0.1}S_{0.9}PEEK$ was filtered off, washed with distilled water to neutral pH and dried under vacuum for 6 h at room temperature. The silicon content was determined by Elemental Analysis and was %Si = 0.75±0.05. The yield of the reaction was 69%.

Synthesis of $S_{0.5}$PEEK

Sulfonated polyetheretherketone was synthesized by reaction of PEEK (5 g, 17.3 meq) with H_2SO_4 96% (250 mL) at 25°C for 55 hours. The solution was then poured in a large excess of ice-cold water under continuous stirring, obtaining a white precipitate. After standing overnight, the precipitate was filtered off and washed several times with cold water to neutral pH. The sulfonated polymer was dried under vacuum for 5 h at room temperature. The yield of the reaction was 86%.
The DS of the product was evaluated by ^1H NMR and resulted to be 0.5.

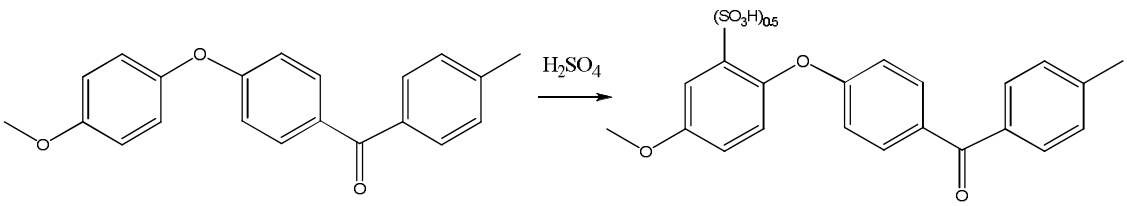

Scheme 4.2 - Synthesis of $S_{0.5}$PEEK.

4.2.2 Results and Discussion

The synthesis of the polymer $PhSi_{0.1}S_{0.9}PEEK$ was carried out starting from PEEK and following the synthetic route shown in **Scheme 4.1**.

The first step consisted of sulfonation of PEEK up to DS = 0.9. This reaction can be carried out choosing among several sulfonating agents, such as sulphur trioxide, sulphuric acid and chlorosulfonic acid. [7] We used concentrated sulphuric acid because it allows to obtain SPEEK with the desired DS, controlling the temperature and time of

reaction, avoiding the formation of degradation products or the occurring of cross-linking reactions which take place using other sulfonating agents.[8,4]

Since sulfonated PEEK is not soluble in solvents commonly used in metalation reaction, $S_{0.9}$PEEK was converted in PEEKSO2Cl by reaction with $SOCl_2$ in the presence of DMF used as catalyst.[9] Sulfonyl chlorinated PEEK was soluble in THF allowing to carry out the subsequent silylation reaction in homogenous conditions and without using of a large excess of BuLi that is necessary in presence of sulfonic acid groups, obtaining an experimental advantage with respect to the previous work, where heterogeneous reaction conditions were used. [3]

Thus, a controlled amount of the electrophile $PhSiCl_3$ was added to achieve the desired amount of phenylsilanol groups bound to the aromatic backbone. Finally, the subsequent hydrolysis led to the conversion of phenylchlorosilyl ($–Si(Cl)_2Ph$) in phenylsilanol ($–Si(OH)_2Ph$) moieties and chlorosulfonyl ($–SO_2Cl$) in sulfonic acid ($–SO_3H$) groups, obtaining the final product $PhSi_{0.1}S_{0.9}$PEEK.

The above described synthetic route allowed to synthesize the PEEK derivative having the desired amount of sulfonic and phenylsilanol groups covalently bound to the backbone, in homogenous and reproducible reaction conditions. Moreover, this pathway represents a versatile tool for synthetic purposes because the ratio between hydrophilic and hydrophobic domains, that determines hydrolytic stability and conductivity of the electrolyte, could be modulated by varying the phenylsilanol groups amount and/or the type of silicon-containing substituent covalently bond to the aromatic chain of sulfonated PEEK.

NMR and ATR/FTIR analysis of the synthesized polymers were carried out to obtain the structural characterization of products, thus verifying the success of the developed synthetic route. The numbering of protons and carbons in $S_{0.9}$PEEK and PEEKSO2Cl repeat units are shown in **Figure 4.6**.

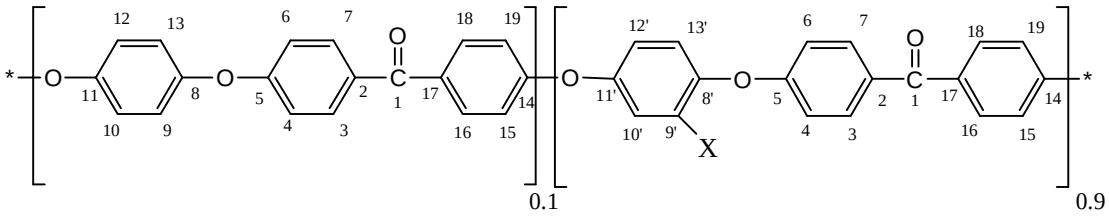

X=SO_3H for $S_{0.9}$PEEK

X=SO_2Cl for PEEKSO2Cl

Figure 4.6 - Assignment of the aromatic protons and carbons of $S_{0.9}$PEEK and PEEKSO2Cl.

Figure 4.7 reports the ^1H NMR spectra of both PEEK derivatives that showed similar chemical shifts. The two protons H4 and H6 in modified PEEK repeat units were a doublet centered at about 7.0 ppm, shifted upfield because of the shielding effect of the sulfonic acid $–SO_3H$ or the chlorosulfonyl $–SO_2Cl$ groups.

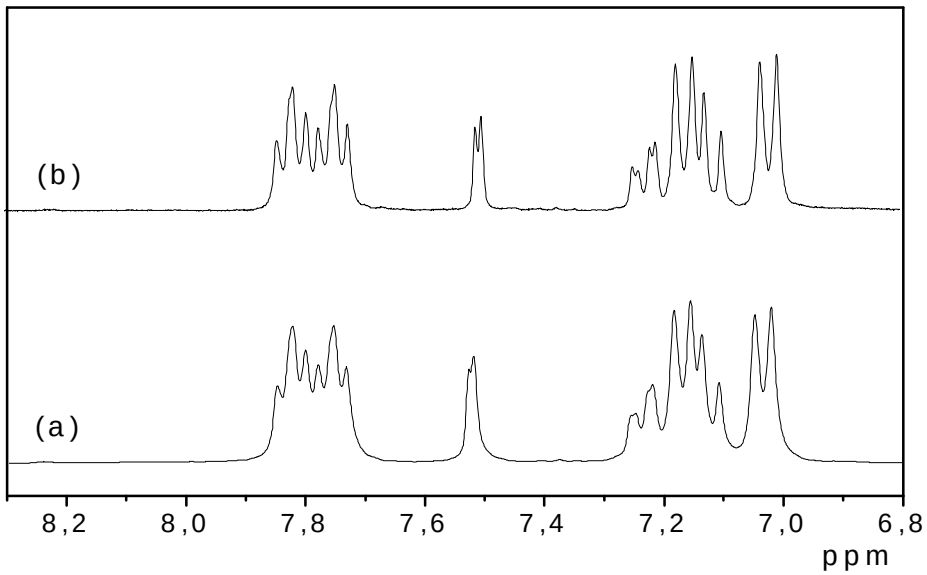

Figure 4.7 - ^1H NMR spectra of (a) $S_{0.9}$PEEK and (b) PEEKSO2Cl.

The H10' proton showed a 0.25 ppm downfield shift with respect to the other protons in the substituted hydroquinone ring of PEEK derivatives because of the deshielding effect of the sulfonic acid or the chlorosulfonyl groups in *ortho* position.

Thus, the H10' proton was used as reference to evaluate the DS of sulfonated PEEK, in according to the following equation: [7]

$$\frac{DS}{12-12\times DS}=\frac{A_{H10'}}{\sum A_H} \qquad \textit{(Eq. 4.4)}$$

where $A_{H10'}$ is the peak area of the distinct H10' signal and A_H the integrated peak area of the signals corresponding to all the other aromatic hydrogens.

Figure 4.8 shows the ^{13}C NMR spectra of $S_{0.9}$PEEK and PEEKSO2Cl. The spectrum of $S_{0.9}$PEEK confirmed that sulfonation occurred only on the hydroquinone segment and the resonance values were in agreement with the literature data.[8]

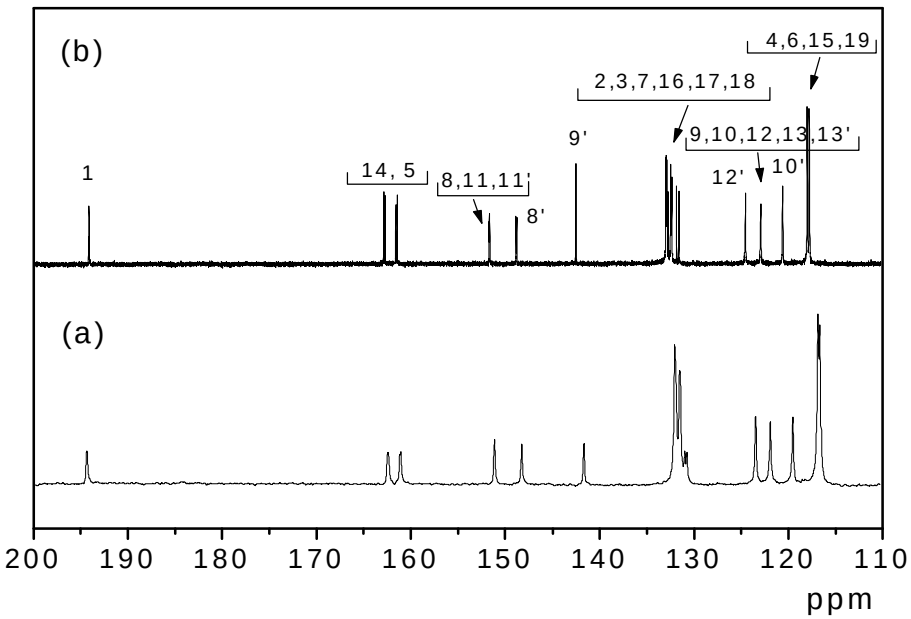

Figure 4.8 - ^{13}C NMR spectra of (a) $S_{0.9}$PEEK and (b) PEEKSO2Cl.

Comparison of the two spectra allowed to assign all the resonances in the spectrum of PEEKSO2Cl according to the structure shown in **Figure 4.6**. The carbon

atoms assignments in PEEKSO2Cl repeat unit and the correspondent resonance values are reported in **Table 4.1**.

These data show that no degradation of the polymer structure occurred during the sulfonyl chlorination reaction. Moreover, the lack of the signals characteristic of the formation of SO_2 bridging moieties, that fall at 8.2 ppm in the ^{1}H NMR spectrum (**Figure 4.7b**) and at about 141.0 and 127.5 ppm in the ^{13}C NMR spectrum,[4] indicates that no cross-linking reactions of sulfonic groups occurred.

δ (ppm)	Carbon designation	δ (ppm)	Carbon designation
117.38 - 118.00	4,6,15,19	148.53	8’
120.40	10’	151.41	8, 11, 11’
122.72	9,10,12,13,13’	161.18	5
124.32	12’	162.48	14
131.33 - 132.98	2,3,7,16,17,18	193.68	1
142.25	9’		

Table 4.1 - ^{13}C NMR data of PEEKSO2Cl.

The chemical structure of the polymers was also investigated by ATR/FTIR spectroscopy. **Figure 4.9** shows the spectra of PEEK, $S_{0.9}$PEEK and PEEKSO2Cl (traces a-c). All samples showed the characteristic bands of PEEK: 1650 cm^{-1} ν_{sym} (C=O), 1220 cm^{-1} ν_{asym} (Ph-CO-Ph), 1015 cm^{-1} ν (C-O-C) and 930 cm^{-1} ν_{sym} (Ph-CO-Ph).

To highlight the signals characteristic of sulfonic groups, the subtraction of the spectrum of PEEK from that of $S_{0.9}$PEEK is shown in **Figure 4.9d**. The bands due to the aromatic sulfonic groups are clearly observed at 1035 cm^{-1} ν_{sym} ($-SO_3H$), 1170 cm^{-1} ν_{asym} ($-SO_3H$), and 930 cm^{-1} δ ($-SO_3H$). [10]

Moreover, the shift of the signal of PEEK from 1485 cm^{-1}, typical of ring stretching vibrations of *para*-substituted compounds, to 1475 cm^{-1} supports the occurrence of sulfonation.

The subtraction of the spectrum of $S_{0.9}$PEEK from that of PEEKSO2Cl is shown in **Figure 4.9e** to highlight the conversion of sulfonated PEEK into its sulfonyl chlorinated derivative. This spectrum shows the bands characteristic of aromatic sulfonyl and sulfinyl moieties: 1200 cm^{-1} ν_{asym} (SO_2), 1065 cm^{-1} (tail) ν_{sym} (SO_2), 1165 and 935 cm^{-1} ν_{sym} (S=O). [11,12]

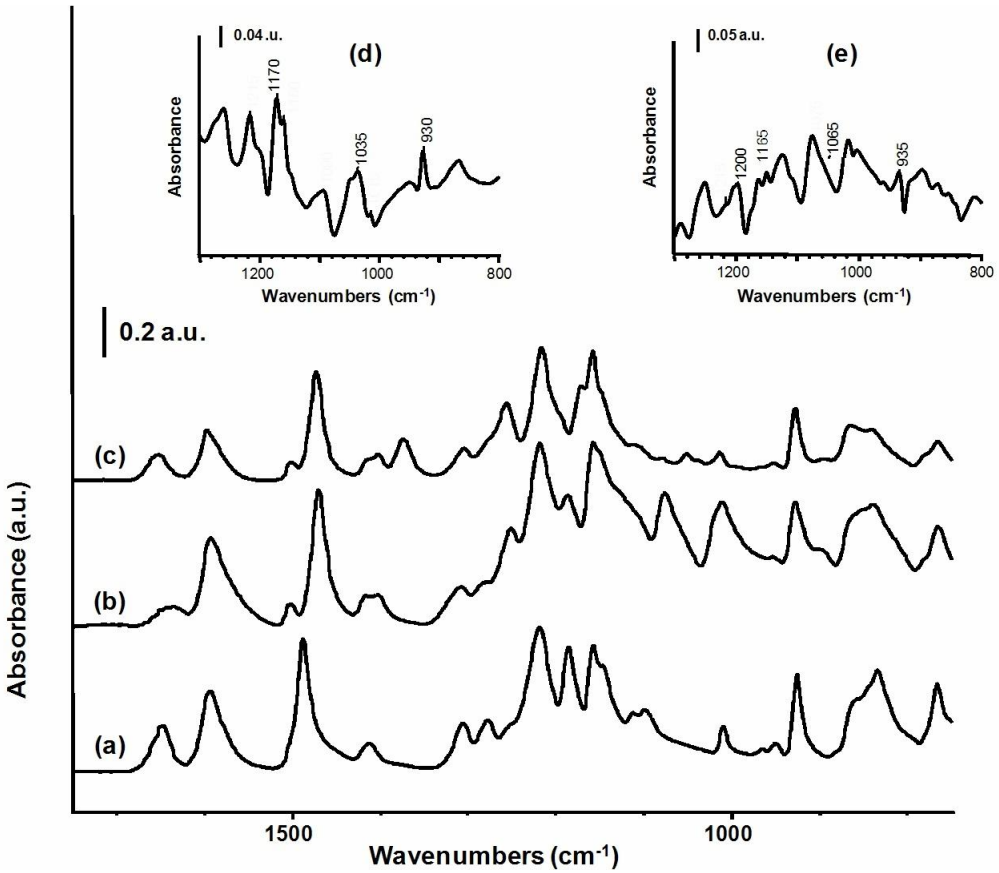

Figure 4.9 - ATR/FTIR spectra of (a) PEEK, (b) $S_{0.9}$PEEK, (c) PEEKSO2Cl and (d, e) subtraction results (d) = (b)-(a) and (e) = (c)-(b).

Figure 4.10 shows the spectra of PEEKSO2Cl, PhSiPEEKSO2Cl and $PhSi_{0.1}S_{0.9}$PEEK (traces a-c). Also in this case, all spectra are dominated by PEEK signals, slightly shifted at lower frequencies respect to reference data due to the presence of 1,2,4- substituted species.

To highlight the signals characteristic of the silylation, the subtraction of the spectrum of PEEKSO2Cl from that of PhSiPEEKSO2Cl is shown in **Figure 4.10d**. The presence of a component at 1625 cm^{-1} is typical of aryl-silicon compounds. The bands at 1435 and 1120 cm^{-1} are attributed to the deformations of the ring with some contribution from the stretching of Si-C bond. [13,14]

Figure 4.10e shows the spectrum obtained subtracting the spectrum of PhSiPEEKSO2Cl from that of $PhSi_{0.1}S_{0.9}PEEK$. The bands due to aromatic sulfonic groups are clearly observed at 1015 cm^{-1} ν_{sym} ($-SO_3H$), 1180 cm^{-1} ν_{asym} ($-SO_3H$), and 990 cm^{-1} δ ($-SO_3H$).[15] The signals at 920 and 880 cm^{-1} are typical of aromatic silanols. No bands due to Si–O–Si bonds were observed.[9] These results confirmed the occurrence of hydrolysis.

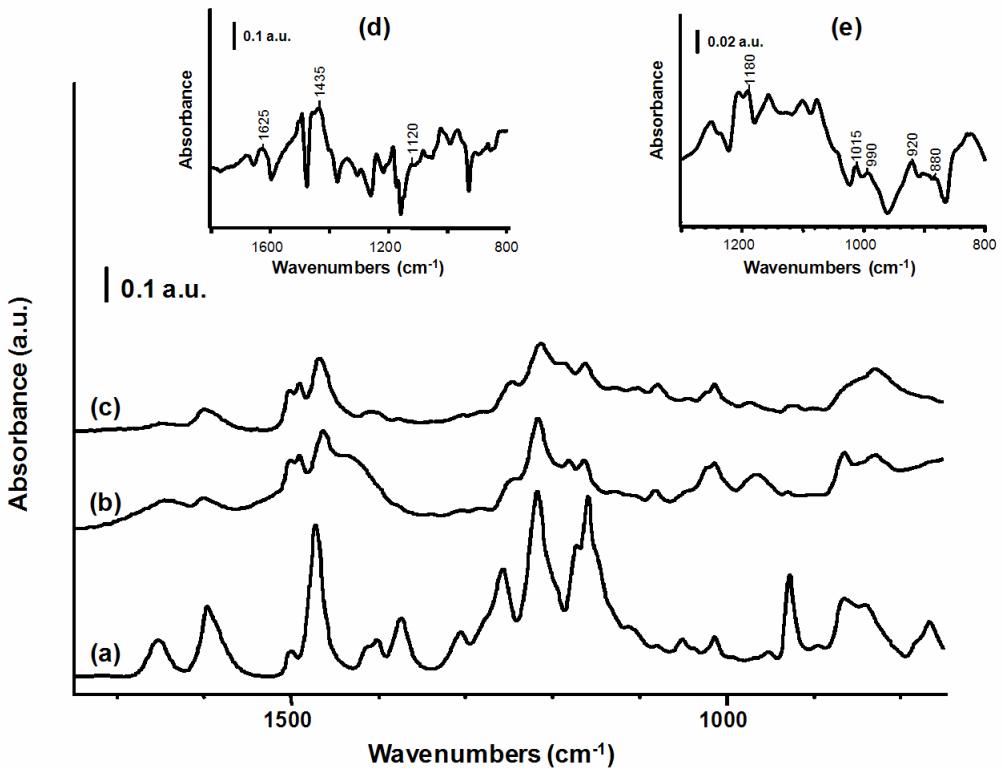

Figure 4.10 - ATR/FTIR spectra of (a) PEEKSO2Cl, (b) PhSiPEEKSO2Cl, (c) $PhSi_{0.1}S_{0.9}PEEK$ and (d, e) subtraction results (d) = (b)-(a) and (e) = (c)-(b).

To investigate if the presence of the phenylsilanol moieties covalently bound to the backbone could alter the hydrophilic/hydrophobic properties of $PhSi_{0.1}S_{0.9}PEEK$, a

conformational search was carried out using a molecular mechanics method using the Hyperchem program. [16]

The conformational exploration was performed on a model with 8 repeat units of $PhSi_{0.1}S_{0.9}PEEK$, varying simultaneously the 4 torsion angles located between the ether linkage next to the sulfonic groups, and the geometric optimization was terminated when the energy difference among successive iteration was lower than 4.2 J/mol. **Figure 4.11** shows the two limit structures that have a difference in energy of 192.5 kJ/mol.

The lower energy conformation has the bulky phenylsilanol group encaged between the hydrophobic chains (**Figure 4.11a**). This particular folded conformation should enhance the hydrophobicity of the macromolecules lowering the hydrophilic/hydrophobic ratio. Moreover, the presence of specific dipolar interactions can help to make the membrane more resistant toward the adsorption of water.

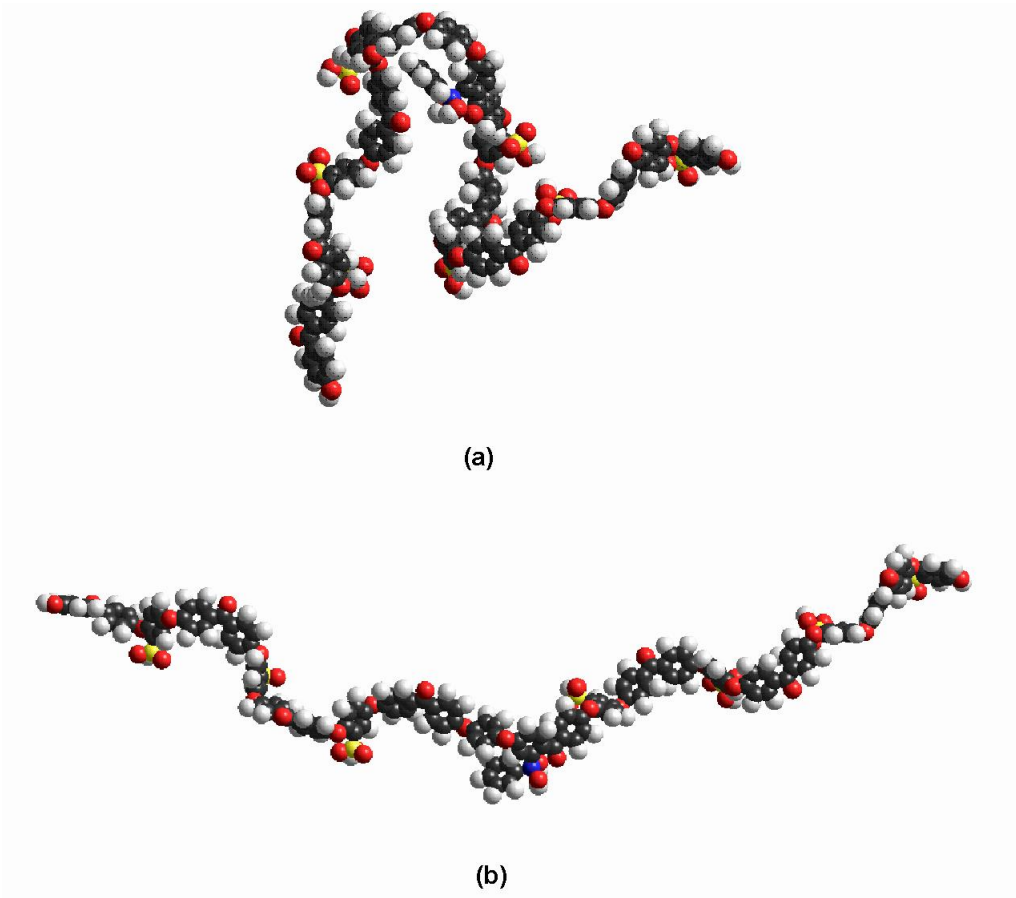

Figure 4.11 - Representation of the two limit structures of $PhSi_{0.1}S_{0.9}PEEK$.

The thermal stability of the polymers was investigated by TGA, using air flow in similarity to real fuel cell conditions. **Figure 4.12** shows the thermogravimetric traces of $S_{0.9}$PEEK, PEEKSO2Cl and $PhSi_{0.1}S_{0.9}$PEEK.

$S_{0.9}$PEEK showed a small continuous mass loss at temperature below 200°C due to the removal of residual solvent bound to the sulfonic acid groups. At higher temperature, two degradation steps were observed, in according to literature data.[17] The first one is mainly associated with the splitting-off of sulfonic acid groups and its starting point falls in the range 250 - 280°C depending on the polymer DS. The second weight loss is mainly due to PEEK aromatic chain scission.

For $S_{0.9}$PEEK, the first degradation step started at about 250°C due to its high DS, whilst the second weight loss was observed in the range 380 - 570°C.

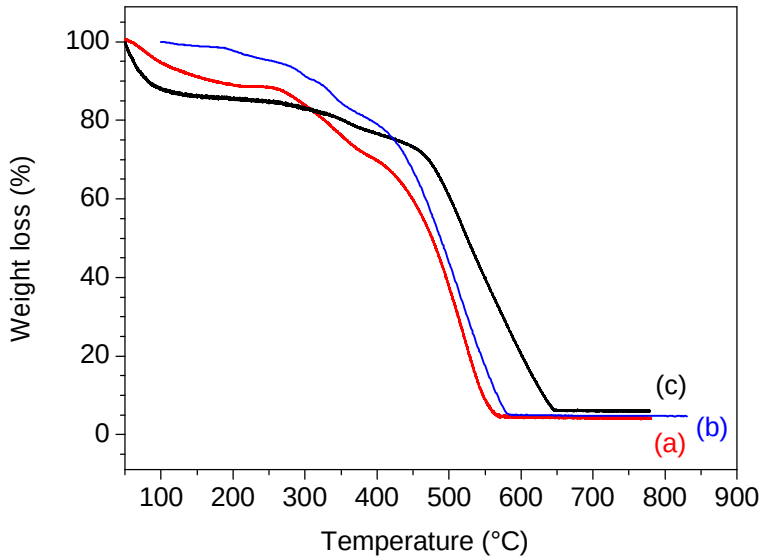

Figure 4.12 - Thermogravimetric curves of (a) $S_{0.9}$PEEK, (b) PEEKSO2Cl and (c) $PhSi_{0.1}S_{0.9}$PEEK.

The thermogram of PEEKSO2Cl showed a similar trend. The splitting-off of the chlorosulfonyl groups started at about 250 °C, whilst the scission of the main chain occurred in the temperature range 380 - 580 °C.

The silylated and sulfonated polymer, $PhSi_{0.1}S_{0.9}$PEEK, showed a continuous mass loss at temperature below 100°C due to the removal of residual water bound to the sulfonic acid groups. A broad first degradation step was observed between 250-400°C,

due to the splitting-off of sulfonic acid groups, whilst the mass loss due to PEEK aromatic chain scission fell in the range 410-650°C. The shift towards higher degradation temperatures with respect to those of $S_{0.9}$PEEK, indicated that the presence of phenylsilanol groups stabilizes the aromatic matrix of the sulfonated polymer.

Membranes made up of pure $PhSi_{0.1}S_{0.9}$PEEK were prepared, but they were too brittle to be used for fuel cell applications. The functionalization with silicon-containing groups has in fact two effects: on one hand it increases the hydrolytic and thermal stability, on the other hand it decreases the processability. [5]

To obtaining membranes with proper flexibility silylated and sulfonated PEEK was used as minor component in blend with $S_{0.5}$PEEK, that was chosen due to its appropriate mechanical properties.

Moreover, the two polymers have a similar chemical structure, so that both π–π and electrostatic interactions were expected to occur in the blend formation easing homogeneous dispersion.

Blend membranes containing 10 and 25 wt.% of $PhSi_{0.1}S_{0.9}$PEEK were prepared and activated.

Their hydration behavior was considered in terms of λ, *i.e.* the number of absorbed water molecules per sulfonic acid group. The λ values were determined by W.U. measurements, after equilibration in saturated water vapour pressure at room temperature. They resulted to be λ = 6.7 for pure $S_{0.5}$PEEK and 25 wt.% blend, and λ = 7.3 for 10 wt.% blend membranes.

The lower water affinity of the 25 wt.% blend with respect to the 10 wt.% blend could be due to the higher content of $PhSi_{0.1}S_{0.9}$PEEK. In fact, as resulted from the conformational analysis, the macromolecules $PhSi_{0.1}S_{0.9}$PEEK tend to have a folded conformation that should make the membrane more resistant toward the adsorption of water.

Proton conductivity (σ) of the membranes was measured, as a function of temperature, at saturated water vapor pressure (100% RH).

As it can be observed in **Figure 4.13**, the σ values of all membranes increased with the increment of temperature, exceeding 0.01 S cm^{-1} above 50 °C.

In particular, the 10 wt.% blend membrane showed the highest conductivity values over the whole investigated temperature range, reaching 0.03 S cm^{-1} between 80°C and

100°C. This trend was consistent with higher hydrophilic nature of 10 wt.% blend with respect to the other membranes.

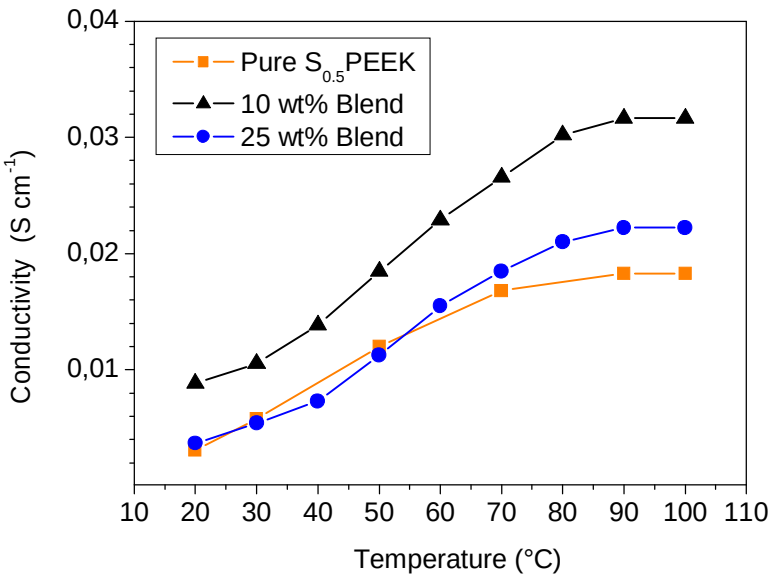

Figure 4.13 - Proton conductivity of pure $S_{0.5}$PEEK and blend membranes at RH=100%.

In conclusion, in our group several synthetic routes have been developed to prepare derivatives of PEEK having sulfonic acid groups and silicon-containing substituents covalently bound to the aromatic chain.

Although successful, the synthetic pathway used to prepare SiSPEEK carrying out the silylation reaction in heterogeneous conditions cannot guarantee reproducible results.[3]

Hence, another synthetic strategy was developed to introduce the silicon-containing functional groups onto aromatic chain of PEEK using homogeneous reaction conditions.[4] The crosslinking through SO_2 moieties, introduced *via* sulfonyl chlorination with chlorosulfonic acid (HSO_3Cl), led to a precursor which solubility in organic solvents allowed to carry out an efficient silylation reaction. However, the formation of SO_2 bridging moieties added a further parameter, that is the degree of cross-linking, that must be considered for the reproducibility of the chemical structure of the products.

In this work, a highly reproducible synthetic pathway was developed, in which the sulfonyl chlorination was carried out by using of thionylchloride ($SOCl_2$), thus avoiding crosslinking reactions. This procedure led to a higher control of chemical structure of the synthesized polymers. Moreover, phenylsilanol instead of silanol moieties were

covalently bound to the backbone of highly sulfonated PEEK because the presence of hydrophobic phenyl group onto the silicon allows further control on the hydrophilic/hydrophobic ratio, allowing the use of a lower amount of electrophilic reactant. However, the degree of silylation of the products must be optimized to obtain electrolytes having proper mechanical proprieties to be used alone as membrane materials for PEMFC applications.

4.2.3 References

1) J.A. Kerres, *J. Membr. Sci.* **2001**, 185, 3.

2) K.D. Kreuer, *J. Membr. Sci.* **2001**, 185, 29.

3) M.L. Di Vona, D. Marani, A. D'Epifanio, E. Traversa, M. Trombetta, S. Licoccia, *Polymer* **2005**, 46, 1754.

4) M.L. Di Vona, D. Marani, C. D'Ottavi, M. Trombetta, E. Traversa, I. Beurroies, P. Knauth, S. Licoccia, *Chem. Mater.* **2006**, 18, 69.

5) D. Marani, M.L. Di Vona, E. Traversa, S. Licoccia, I. Beurroies, P.L. Llewellyn, P. Knauth, *J. Phys. Chem. B* **2006**, 110, 15817.

6) W. Zhang, V. Gogel, K. Friedrich, J. Kerres, *J. Power Sources* **2006**, 155, 3.

7) S.M.J. Zaidi, S.D. Mikhailenko, G.P. Robertson, M.D. Guiver, S. Kaliaguine, *J. Membr. Sci.* **2000**, 173, 17.

8) X. Jin, M.T. Bishop, T.S. Ellis, F.E. Karasz, *British Polymer Journal* **1985**, 17, 4.

9) H.H. Bosshard, R. Mory, M. Schmid, Hch. Zollinger, *Helvetica Chimica Acta* **1959**, 42, 1653.

10) C. Kim, J.G. Choi, T.M. Tak, *J. Appl. Polym. Sci.* **1999**, 74, 2046.

11) B.J. Lindberg, *Acta Chem. Scand.* **1967**, 21, 841.

12) I.K. Adzamli, K. Libson, J.D. Lydon, R.C. Elder, E. Deutsch, *Inorg. Chem.* **1979**, 18, 303.

13) Z. Olejniczak, M. Łęczka, K. Cholewa-Kowalska, K. Wojtach, M. Rokita, W. Mozgawa, *J. Mol. Structure* **2005**, 744, 465.

14) H. Gunzler, H.U. Gremlich, *IR spectroscopy - An introduction*, Wiley, Weinheim (D), **2002**.

15) L.J. Bellamy, *The infrared spectra of complex molecules*, Vol 1, Chapman and Hall, London (UK), **1980**.

16) HyperChem Release 8.0, Hypercube Inc. **2007**.

17) P. Xing, G.P. Robertson, M.D. Guiver, S.D. Mikhailenko, K. Wang, S. Kaliaguine, *J. Membr. Sci.* **2004**, 229, 95.

4.3 $PhSi_{0.2}S_2PPSU$ / $S_{0.5}PEEK$ Blend

Among the reasons considered to focus the attention on polyphenylsulfone, prominent was its solubility in organic solvents that allowed to carry out functionalization reactions in homogeneous conditions, a circumstance hardly met by other polymers.

As for PEEK, the conductivity of PPSU is a function of the degree of sulfonation, but the polymer becomes water-soluble with increasing of DS, preventing its possible application in fuel cells.[1]

However, it was chosen to prepare PPSU with high DS to enhance the proton conductivity, since the swelling was controlled by proper dosage of inorganic moieties covalently bound to the aromatic chain, thus modulating the hydrophilic/hydrophobic ratio in the polymer matrix. Such ratio, in fact, determines conductivity and hydrolytic stability, which balance will eventually be responsible of the electrolyte performance under fuel cell operating conditions.

Silylated and sulfonated polyphenylsulfone ($PhSi_{0.2}S_2PPSU$, DS=2 and DSi=0.2) was then prepared following a versatile and highly reproducible synthetic route, previously developed in our group.[2]

Blends made up of $PhSi_{0.2}S_2PPSU$ and sulfonated PEEK with DS=0.5 ($S_{0.5}PEEK$) were prepared to obtain membranes having good features for fuel cells application.[3] The blending technique, in fact, has the advantage of combining the positive features of each component while being very simple. Moreover, we have shown that when sulfonated PEEK is used as main blend component, the presence of silylated PPSU improves the membrane strength.[4]

4.3.1 Polymers Synthesis

Synthesis of $PhSi_{0.2}S_2PPSU$

PPSU (5 g, 12.5 meq) was dissolved, under nitrogen atmosphere, in anhydrous THF (250 mL) at -60°C. Then, an excess of BuLi (2.5 M in hexane, 25 mL, 62.5 mmol) and TMEDA (9.4 mL, 62.5 mmol) were added and the solution was stirred for 4 h at -60 °C. A solution of $PhSiCl_3$ (0.41 mL, 2.5 mmol) in anhydrous THF (3 mL) was added and the mixture was slowly warmed to room temperature and then kept under reflux for 2 h.

After cooling to RT, the precipitate was filtered off and washed with water until no chlorides were detected, obtaining the purified product $PhSi_{0.2}PPSU$.

Silylated PPSU ($PhSi_{0.2}PPSU$) was added to H_2SO_4 96% (500 mL) and the mixture was kept under stirring at 50 °C for 5 h, then was poured in ice-cold water. The precipitate was filtered off, washed with water to neutral pH and dried under vacuum for 5 h at room temperature, obtaining the final product $PhSi_{0.2}S_2PPSU$. The yield of the reaction was 68%.

The degree of sulfonation was determined by Elemental Analysis (C and S content) and was DS = 2. The same method was used to evaluate the silicon content, which was %Si = 0.95±0.05.

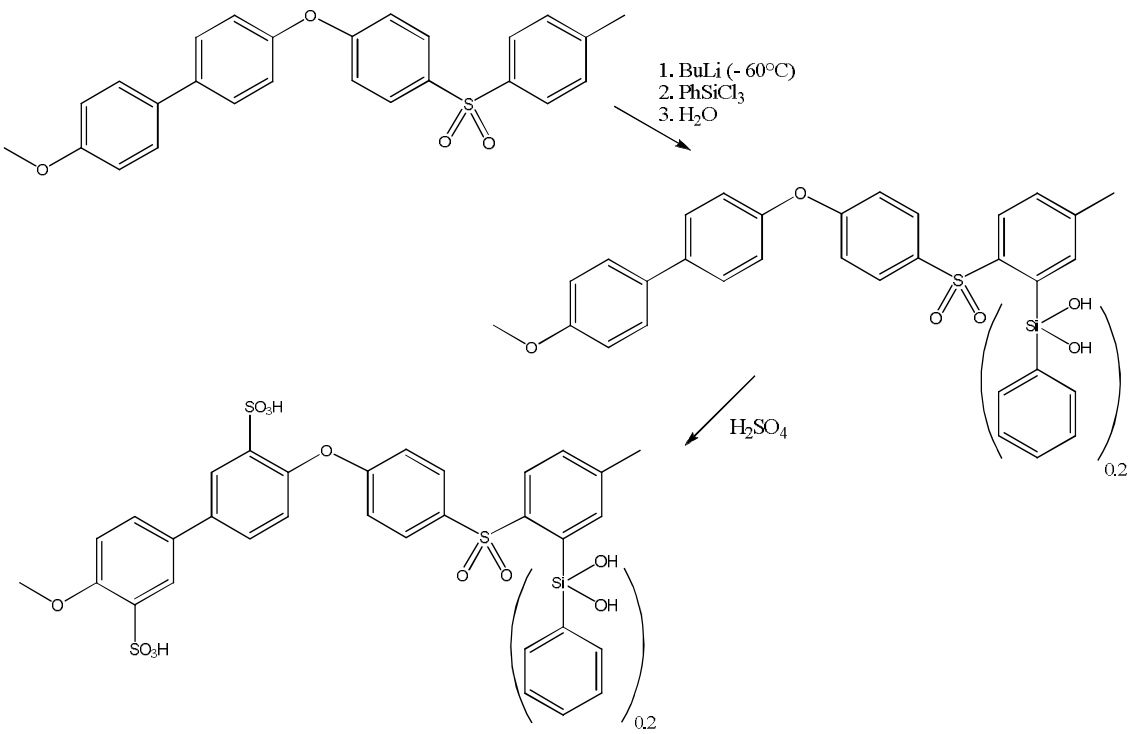

Scheme 4.3 - Synthesis of $PhSi_{0.2}S_2PPSU$.

Synthesis of $S_{0.5}$PEEK

The synthesis of $S_{0.5}$PEEK was carried out following the pathway shown in **Scheme 4.2**. PEEK (5 g, 17.3 meq) was dissolved in H_2SO_4 96% (250 mL) and the solution was stirred at room temperature for 70 hours. The mixture was poured in a large excess of ice-cold water, under continuous stirring, obtaining a white precipitate. After standing overnight, the precipitate was filtered and washed several times with cold water to neutral pH. The sulfonated polymer was then dried under vacuum for 5 h at room temperature. The yield of the reaction was 86%.
The DS of the product was evaluated by ^{1}H NMR spectroscopy and resulted to be 0.5.

4.3.2 Results and Discussion

The polymer $PhSi_{0.2}S_2$PPSU was prepared starting from PPSU and following the two synthetic steps shown in **Scheme 4.3**: *i*) metalation reaction with butyllithium and subsequent substitution by phenyltrichlorosilane, followed by hydrolysis; *ii*) reaction with concentrated sulphuric acid.

Polyphenylsulfone was completely dissolved in THF at T = -60°C. The lithiation of PPSU was thus carried out in homogeneous reaction conditions. Then, the stoichiometric amount of the electrophile, $PhSiCl_3$, was added to achieve the desired amount of phenylsilanol groups bound to the aromatic backbone. Finally, hydrolysis allowed to obtain the product $PhSi_{0.2}$PPSU having hydroxyl groups covalently bound to silicon.

Further functionalization was carried out by reaction of $PhSi_{0.2}$PPSU with concentrated sulphuric acid. Thus, proton conductivity properties were added to the polymer by the introduction of sulfonic acid groups, obtaining $PhSi_{0.2}S_2$PPSU as final product.

NMR and ATR/FTIR analysis of the synthesized polymers were carried out to obtain the structural characterization of products verifying the success of the developed synthetic route.
The labeling of carbons in $PhSi_{0.2}S_2$PPSU repeat units are shown in **Figure 4.14**.

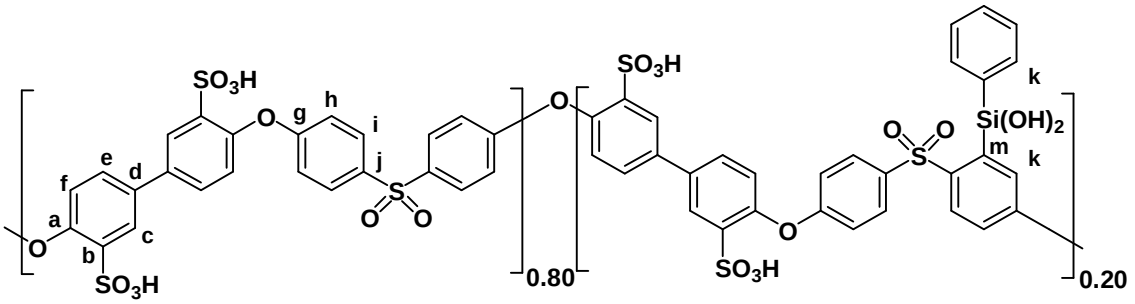

Figure 4.14 - Assignment of the aromatic carbons of $PhSi_{0.2}S_2PPSU$.

Figure 4.15 shows the ^1H NMR spectrum of $PhSi_{0.2}S_2PPSU$. The signal due to H**h** protons is a doublet centered at about 7.0 ppm, shifted upfield because of shielding effect of the sulfonic acid group. On the contrary, the H**c** protons showed a down-field shift due to deshielding effect of the sulfonic acid group in *ortho* position.[1] Moreover, the H**k** protons were shifted downfield by the effect of the silyl substituent on the aromatic ring.[5]

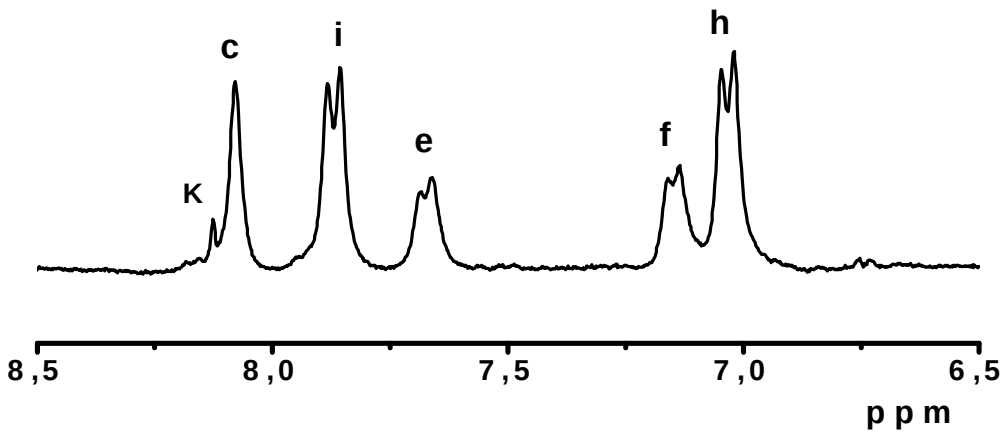

Figure 4.15 - ^1H NMR spectra of $PhSi_{0.2}S_2PPSU$.

The ^{13}C NMR spectrum of $PhSi_{0.2}S_2PPSU$ is shown in **Figure 4.16** and the carbon resonance values with the correspondent assignments are listed in **Table 4.2**.

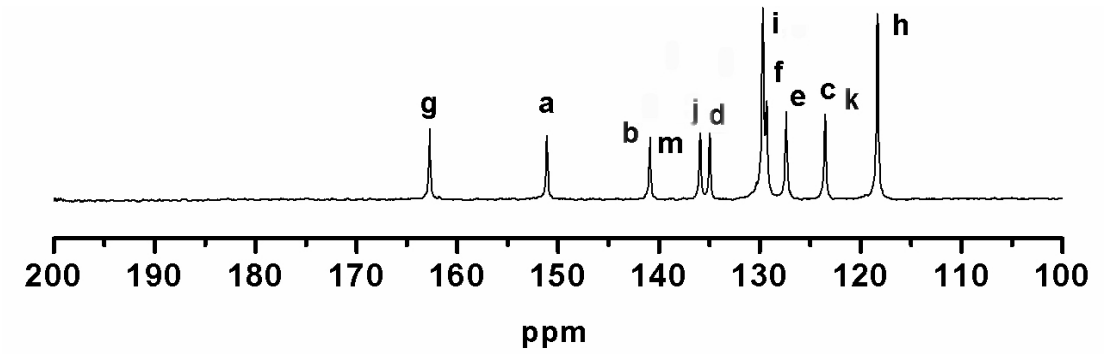

Figure 4.16 - ^{13}C NMR spectra of $PhSi_{0.2}S_2PPSU$.

δ (ppm)	Carbon designation	δ (ppm)	Carbon designation
162.74	g	129.71	i
151.12	a	129.34	f
140.90	b, m	127.39	e
135.93	j	123.54	c, k
134.97	d	118.34	h

Table 4.2 - ^{13}C NMR data of $PhSi_{0.2}S_2PPSU$.

The chemical structure of the polymers was also investigated by ATR/FTIR spectroscopy. **Figure 4.17** shows the spectra of PPSU, $PhSi_{0.2}PPSU$, and $PhSi_{0.2}S_2PPSU$ (traces a-c). All samples showed the characteristic bands of PPSU: 1581 and 1481 cm^{-1} ν (C=C_{Ph}), 1319 cm^{-1} ν_{asym} (S=O), 1218 cm^{-1} ν (C-O), 1144 cm^{-1} ν_{sym} (S=O).

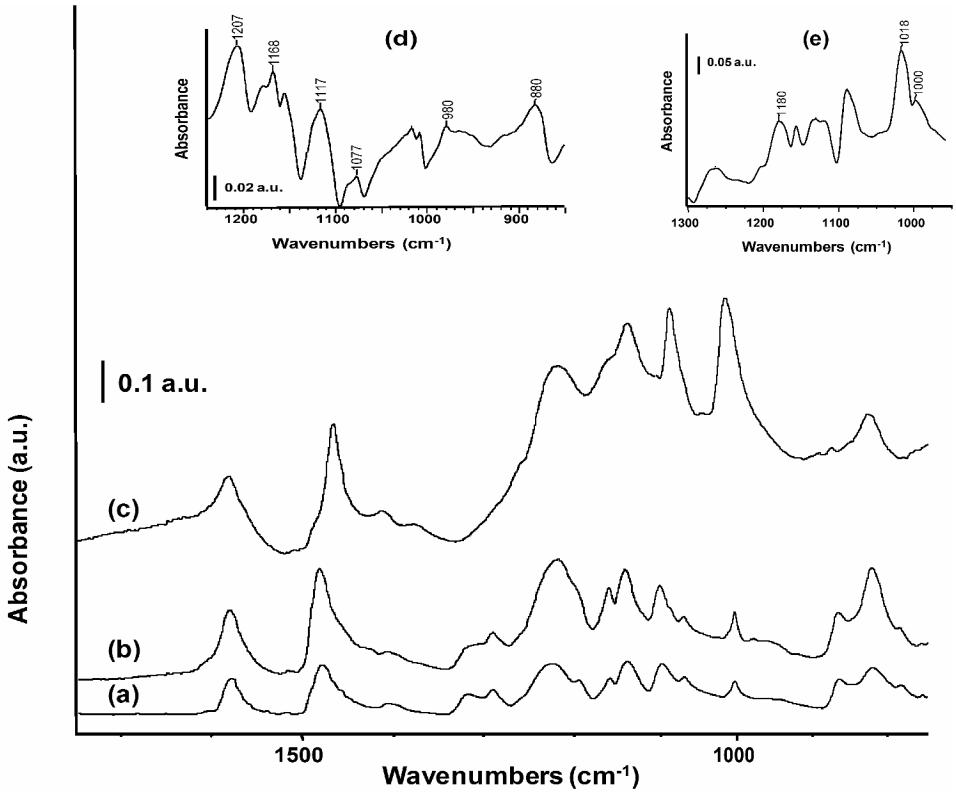

Figure 4.17 - ATR/FTIR spectra of (a) PPSU, (b) $PhSi_{0.2}$PPSU, (c) $PhSi_{0.2}S_2$PPSU, (d)- (e) subtraction results: (d) = (b)-(a) and (e) = (c) – (b).

Figure 4.17d shows the spectrum obtained subtracting the spectrum of PPSU from that of $PhSi_{0.2}$PPSU to highlight the signals characteristic of silicon-phenyl bonds. The bands at 1207 and 1077 cm^{-1} are characteristic of 1,4- and 1,2,4-substituted phenyl rings. Moreover, the absorption at 1168 cm^{-1} supports the presence of 1,2,4- substituted species. [6]

The band at 1117 cm^{-1} is attributed to an in-plane deformation of the ring with some contribution from the stretching of Si-C bond, and the signals related to vibrations of the Si–OH groups are observed at 980 and 880 cm^{-1}. [7,8]

Subtraction of the spectrum of $PhSi_{0.2}$PPSU from that of $PhSi_{0.2}S_2$PPSU is shown in **Figure 4.17e**. The bands due to aromatic sulfonic groups are clearly observed at 1180 cm^{-1} ν_{asym} ($-SO_3H$), 1018 cm^{-1} ν_{sym} ($-SO_3H$), and 1000 cm^{-1} δ ($-SO_3H$).[5]

The very low solubility and poor plastic properties of $PhSi_{0.2}S_2$PPSU in the solvents conventionally used for membrane casting (DMAc, DMSO, DMF etc.) prevented its electrochemical characterization. To achieve the required mechanical

properties it was then mixed with $S_{0.5}$PEEK. The two polymers have a similar chemical structure, so that both π–π and electrostatic interactions are expected to occur in the blend formation easing homogeneous dispersion.

Blend membranes made up of $S_{0.5}$PEEK, and containing 5 and 10 wt.% of $PhSi_{0.2}S_2$PPSU, were prepared by casting from DMAc and activated. Pure $S_{0.5}$PEEK membranes were also prepared and used as reference.

Figure 4.18 shows the ATR/FTIR spectra of 5 and 10 wt.% blend membranes (trace c and d, respectively) compared with the spectra of $S_{0.5}$PEEK (trace b) and $PhSi_{0.2}S_2$PPSU (trace a). In the difference spectra, traces **e** and **f**, the presence of the signal at 1022 cm^{-1}, characteristic of 1,2,4-trisubstituted benzene rings, confirmed the occurrence of π-π interactions between the two blend components.

Moreover, the presence of the asymmetrical stretching vibration of the sulfonic acid group at 1078 cm^{-1} indicates the interaction between the two polymers, probably *via* H-bonding.

As it can be observed, the intensity of both signals is higher in the 10 wt.% blend with respect to the 5 wt.% blend, in agreement with the higher amount of $PhSi_{0.2}S_2$PPSU presents into the first membrane.

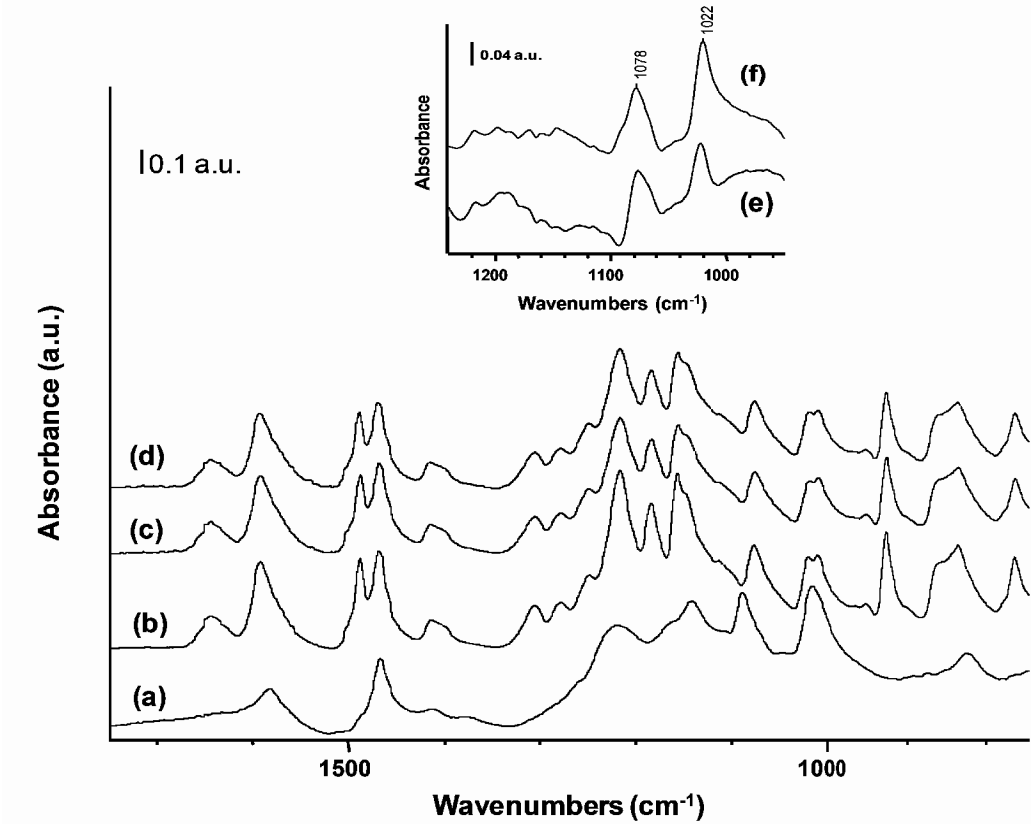

Figure 4.18 - ATR/FTIR spectra of (a) $PhSi_{0.2}S_2PPSU$, (b) $S_{0.5}PEEK$, (c) 5 wt.% blend, (d) 10 wt.% blend and (e,f) subtraction results: (e) = (c)-(b) -(a); (f) = (d)-(b) -(a).

The occurrence of interactions between the two blend components was also investigated by DSC analyses performed on the membranes. **Figure 4.19** shows the DSC thermograms of the pure $S_{0.5}PEEK$ and blend membranes.

The membrane made of pure $S_{0.5}PEEK$ showed a glass transition temperature (T_g) of 186°C, in agreement with literature data.[9] The introduction of $–SO_3H$ groups onto the PEEK backbone results in increment of its T_g from ~150 °C to higher temperature because of the intra- and inter-molecular associations, caused by the formation of strong hydrogen bonds, which reduce the mobility and flexibility of the polymer chain. [10]

An analogous dependence of T_g values on the sulfonation degree was previously observed also for PPSU, being well known that its T_g increases from ~220 °C to higher values with increasing DS.[11] This trend was consistent with the slight T_g increase observed for the blend membranes as a function of their $PhSi_{0.2}S_2PPSU$ content.

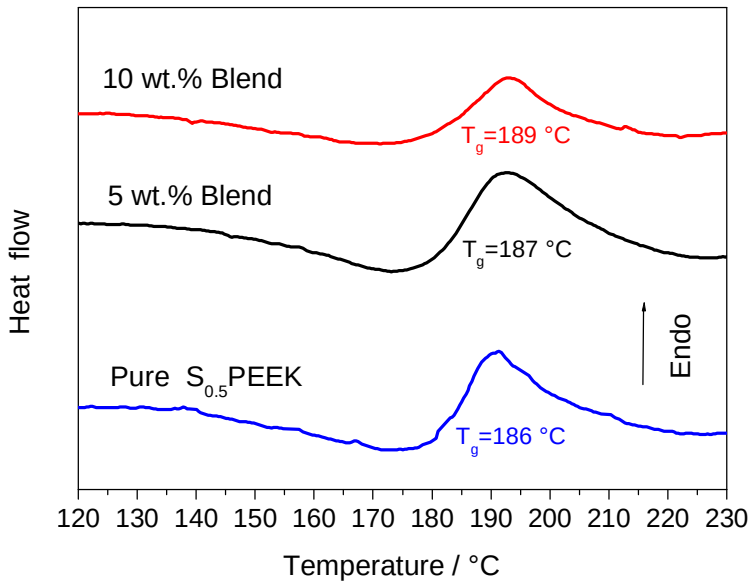

Figure 4.19 - DSC thermograms of pure $S_{0.5}$PEEK and blend membranes.

Further indications about the interactions between the blend components, as well as information on the dimensional stability of the membranes, were obtained analyzing their water and methanol uptake.

The λ value, *i.e.* the uptake of solvent molecules per sulfonic acid group in the membrane, was calculated using the following equation: [12]

$$l = \frac{n_{SOLVENT}}{n_{SO_3H}} = \frac{\left(\frac{(W_{wet} - W_{dry}) \times 100}{W_{dry} \times MW_{solvent}}\right)}{\left(\frac{wt.\%_{S_{0.5}PEEK} \times 0.5}{EW_{S_{0.5}PEEK}} + \frac{wt.\%_{PhSi_{0.2}S_2PPSU} \times 2}{EW_{PhSi_{0.2}S_2PPSU}}\right)} \qquad \textit{(Eq. 4.5)}$$

where W_{wet} and W_{dry} are the weights of wet and dry membranes; $MW_{solvent}$ is the molecular weight of solvent; wt.%$S_{0.5}$PEEK and wt.%$PhSi_{0.2}S_2$PPSU are the weight percentage of $S_{0.5}$PEEK and $PhSi_{0.2}S_2$PPSU, respectively, in the membranes; EW$S_{0.5}$PEEK and EW$PhSi_{0.2}S_2$PPSU are the equivalent weight of the two polymers. This equation takes into account the SO_3H groups of both $PhSi_{0.2}S_2$PPSU and $S_{0.5}$PEEK.

Equilibrium water and methanol uptake values are shown in **Table 4.3**.

	l H_2O	l MeOH
Pure $S_{0.5}$PEEK	17.9	10.9
5 wt.% Blend	16.1	8.2
10 wt.% Blend	14.4	6.1

Table 4.3 - Water and methanol uptake of pure $S_{0.5}$PEEK and blend membranes.

The water uptake of blend membranes resulted to be lower than that of the pure $S_{0.5}$PEEK reference membrane, indicating that the formation of blend modified the water absorption characteristics of the electrolyte.

Moreover, the 5 wt.% blend showed higher water affinity with respect to the 10 wt.% blend. This trend can be explained on the basis of the lower content of $PhSi_{0.2}S_2$PPSU in the latter membrane. The hydroxyl groups of the phenylsilanol moieties -$Si(OH)_2$Ph could cause a double effect: a minor hydration due to the formation of hydrogen bonds with sulfonic acid groups, and a major affinity for water molecules due to their hydrophilicity. The enhanced stability of the 10 wt.% blend towards water absorption indicates the predominance of the first factor.

The influence of $PhSi_{0.2}S_2$PPSU on methanol affinity was studied by evaluating the membrane methanol uptake upon immersion in absolute methanol. The value of methanol uptake decreased with increasing $PhSi_{0.2}S_2$PPSU content in the blend membranes. The blend membranes are then expected to possess a lower methanol permeation rate when exposed to methanol aqueous solution in DMFC.

Proton conductivity (σ) of the membranes was measured by EIS. **Figure 4.20** shows the Arrhenius plots of pure $S_{0.5}$PEEK and blend membranes.

The σ values of the blend membranes were always higher than those of the pure $S_{0.5}$PEEK membrane, in the whole investigated temperature range.

In particular, the 5 wt.% blend membrane showed the highest proton conductivity reaching about 0.1 S cm^{-1} at 100°C.

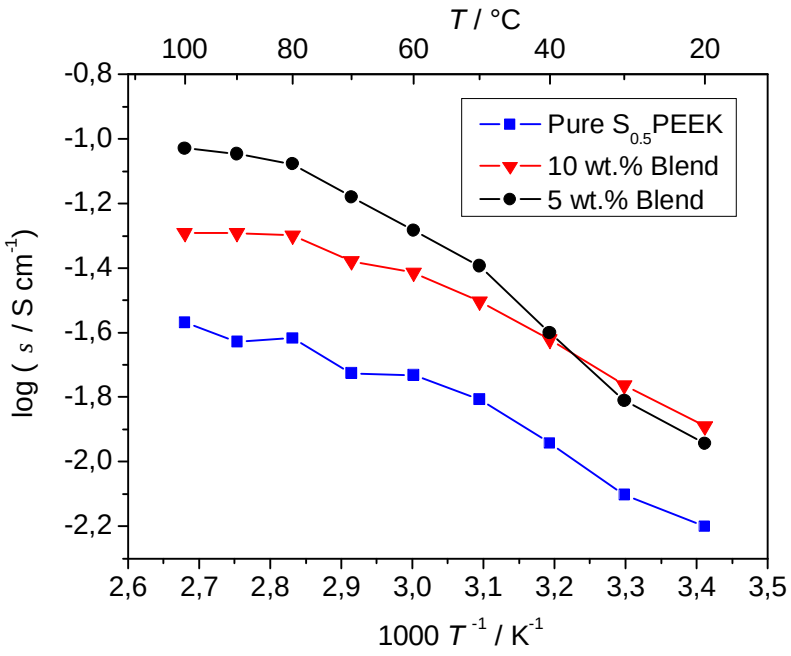

Figure 4.20 - Arrhenius plot of pure $S_{0.5}$PEEK and blend membranes at RH=100%.

Upon MEAs fabrication, pure $S_{0.5}$PEEK and blend electrolytes were tested in a DMFC station. **Figure 4.21** shows the current-voltage (I-V) and power density curves recorded at 100 °C. At this temperature, it was not possible to record the polarization curve of pure $S_{0.5}$PEEK membrane because it underwent a mechanical degradation and eventually dissolved. On the contrary, the blend membranes showed higher stability as expected by the reduced values of solvent uptake.

The OCV of the 10 wt.% blend (0.71 V) was higher than that of the 5 wt.% blend (0.65V) leading to the conclusion that with increasing $PhSi_{0.2}S_2$PPSU content the methanol permeation through the membrane was reduced.

The 5 wt.% blend showed a higher performance than that of 10 wt.% blend, reaching about 450 mA cm^{-2} at 0.2 V that corresponds to a power density higher than 80 mW cm^{-2} (**Figure 4.21**). This behaviour can be explained with an enhanced proton mobility in 5 wt.% blend with respect to 10 wt.% blend, as indicated by the proton conductivity features.

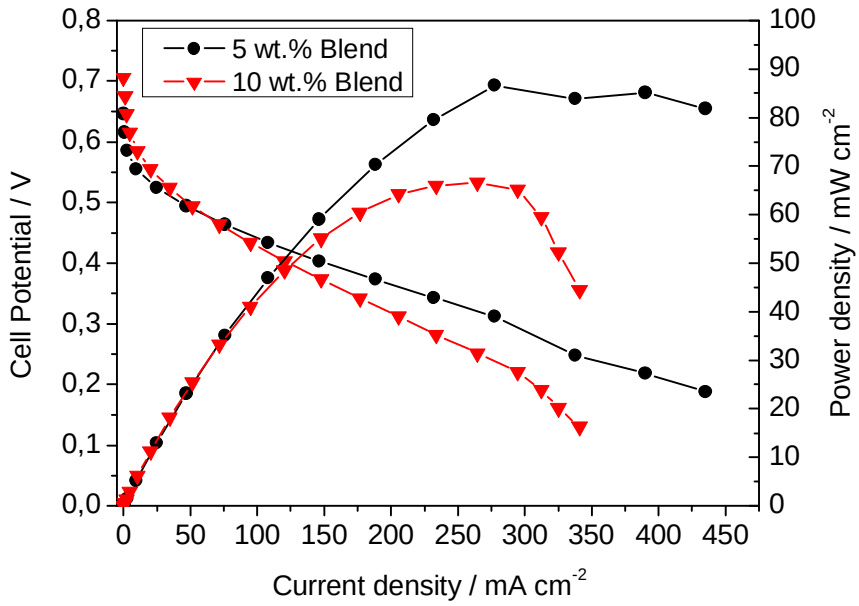

Figure 4.21 - Polarization and Power density curves of blend membranes at 100 °C.

All these results indicate that the interaction between the two physically crosslinked polymers led to change of the blend membrane properties with respect to pure $S_{0.5}$PEEK membrane. The presence of $PhSi_{0.2}S_2$PPSU improved the hydrolytic stability of pure $S_{0.5}$PEEK avoiding its solubilization in aqueous methanol solution at high temperature and the consequent loss in electrochemical performance, as indicated by tests in DMFC at 100°C. In fact, at this temperature, a drop in the mechanical properties for pure $S_{0.5}$PEEK membrane was observed, whilst the blend systems maintained a considerable stability allowing to obtain adequately high power density values.

These features identify $PhSi_{0.2}S_2$PPSU / $S_{0.5}$PEEK blend membranes as promising electrolytes for DMFCs.

4.3.3 References

1) A. Dyck, D. Fritsch, S.P. Nunes, *J. Appl. Polym. Sci.* **2002**, 86, 2820.

2) M. L. Di Vona, A. D'Epifanio, D. Marani, M. Trombetta, E. Traversa, S. Licoccia, *J. Membr. Sci.* **2006**, 279, 186.

3) C. de Bonis, A. D'Epifanio, M.L. Di Vona, C. D'Ottavi, B. Mecheri, E. Traversa, M. Trombetta, S. Licoccia, *Fuel Cells*, DOI: 10.1002/fuce.200800112.

4) E. Sgreccia, M. Khadhraoui, C. de Bonis, S. Licoccia, M. L. Di Vona, P. Knauth, *J. Power Sources* **2008**, 178, 667.

5) Y. Dai, M.D. Guiver, G.P. Robertson, F. Bilodeau, Y.S. Kang, K.J. Lee, J.Y. Jho, J. Won, *Polymer* **2002**, 43, 5369.

6) H. Gunzler, H. U. Gremlich, *IR spectroscopy - An introduction*, Wiley, Weinheim, **2002**.

7) L.J. Bellamy, *The infrared spectra of complex molecules,* Vol 1, Chapman and Hall, London, **1980**.

8) Z. Olejniczak, M. Łęczka, K. Cholewa-Kowalska, K. Wojtach, M. Rokita, W. Mozgawa, *J.Mol. Structure* **2005**, 744, 465.

9) A. Carbone, R. Pedicini, G. Portale, A. Longo, L. D'Ilario, E. Passalacqua, *J. Power Sources* **2006**, 163, 18.

10) P. Xing, G.P. Robertson, M.D. Guiver, S.D. Mikhailenko, K. Wang, S. Kaliaguine, *J. Membr. Sci.* **2004**, 229, 95.

11) H. Sun, N. Venkatasubramanian, M.D. Houtz, J.E. Mark, S.C. Tan, F.E. Arnold, C. Y-C Lee, *Colloid. Polym. Sci.* **2004**, 282, 502.

12) X. Ren, T.E. Sprinter, S. Gottesfeld, *J. Electrochem. Soc.* **2000**, 147, 92.

4.4 PPSU-based Hybrid Electrolyte

The organic-inorganic hybrid polymer HSiSPPSU was prepared by reaction of two polyphenylsulfone derivatives $Si_{0.2}S_2$PPSU and $Si_{0.03}S_{0.05}$PPSU with different degrees of sulfonation and silylation, to obtain the synergic effect between the polymers having different electrical and mechanical properties. [1]

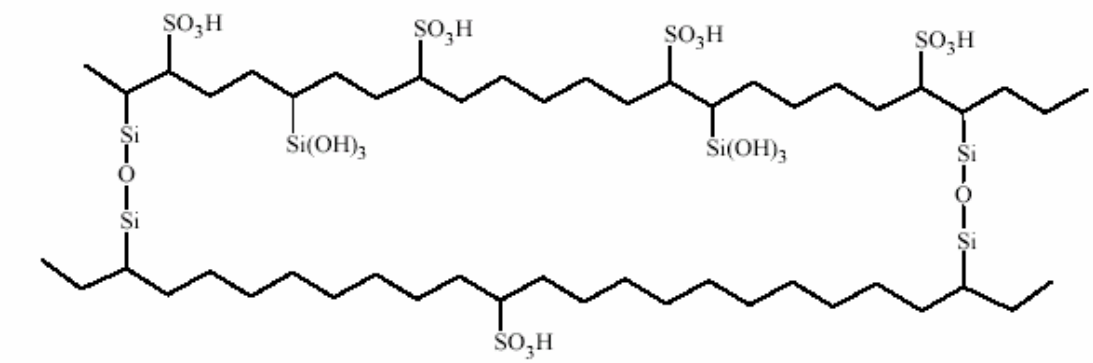

Figure 4.22 - Scheme of covalently crosslinked polymers.

The covalent cross-linking *via* Si–O–Si bonds between the two silylated and sulfonated polymers was expected to enhance morphological stability of HSiSPPSU membrane by modification of the separation between the hydrophilic and hydrophobic domains, maintaining adequate proton conductivity values for PEMFC applications.

4.4.1 Polymers Synthesis

Two silylated and sulfonated derivatives of PPSU were prepared. The organic–inorganic hybrid polymer HSiSPPSU was then synthesized by non-hydrolytic sol–gel reaction. Moreover, sulfonated polyphenylsulfone S_2PPSU was also prepared to be used as reference material for the structural characterization of the products.

Synthesis of $Si_{0.2}S_2$PPSU

PPSU (5 g, 12.5 meq) was dissolved, under nitrogen atmosphere, in anhydrous THF (150 mL), at -60°C. An excess of BuLi (2.5M in hexane, 25 mL, 62.5 mmol) and TMEDA (9.4 mL, 62.5 mmol) were added and the solution was stirred for 2 h at -60°C.

A solution of tetrachlorosilane ($SiCl_4$, 0.29 mL, 2.5 mmol) in anhydrous THF (3 mL) was then added and the mixture was slowly warmed to room temperature and then kept under reflux overnight. After cooling to RT, the precipitate was filtered off and washed with cold water until no chlorides where detected.

Silylated PPSU ($Si_{0.2}$PPSU) was added to H_2SO_4 96% (500 mL) and the mixture was kept under stirring at 50 °C for 5 h, then poured in ice-cold water. The precipitate was filtered off, washed with water to neutral pH and dried under vacuum for 5 h at room temperature, obtaining the final product $Si_{0.2}S_2$PPSU. The yield of the reaction was 65%.

The degree of sulfonation was determined by Elemental Analysis (C and S content) and was DS = 2. The same method was used to evaluate the silicon content, which was %Si = 0.97±0.05.

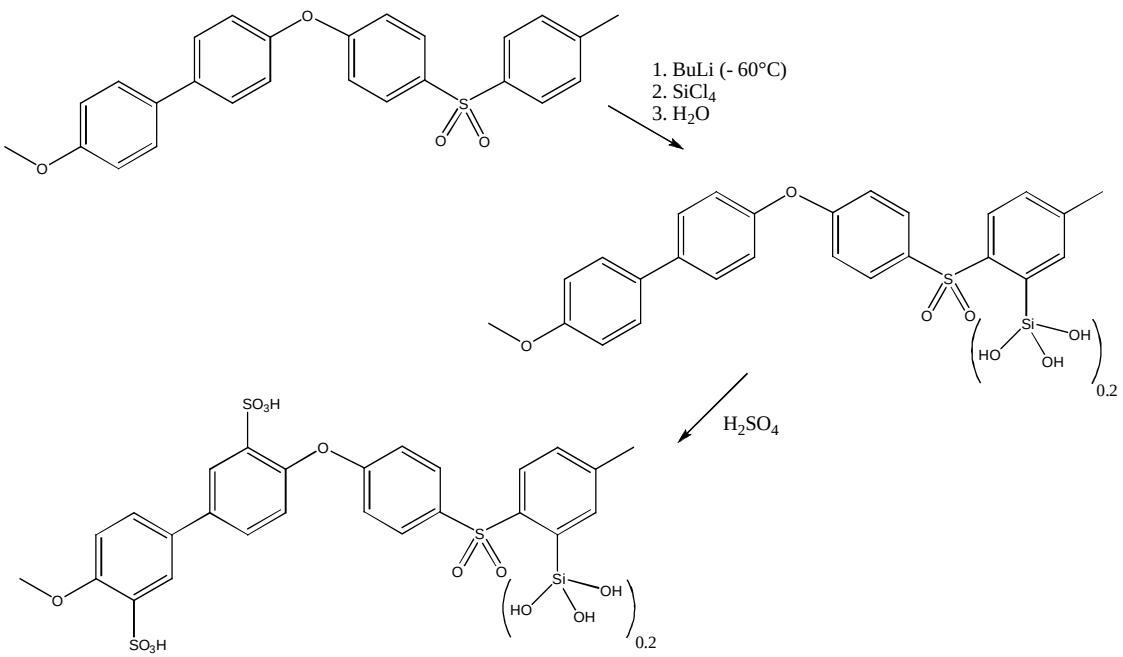

Scheme 4.4 - Synthesis of $Si_{0.2}S_2$PPSU.

Synthesis of $Si_{0.03}S_{0.05}$PPSU

PPSU (5 g, 12.5 meq) was dissolved, under nitrogen atmosphere, in anhydrous CH_2Cl_2 (400 mL). The yellow solution was stirred under reflux for 1 h, then a solution

of trimethylsilyl chlorosulfonate ($ClSO_3Si(CH_3)_3$, 2 mL, 12.8 mmol) in anhydrous CH_2Cl_2 (8 mL) was added dropwise. After 5 h a light brown precipitate separated from the solution. The mixture was kept under reflux for a total of 2 days.

After cooling to -60°C, BuLi (2.5M in hexane, 30 mL, 75 mmol) was added dropwise and the orange solution was kept under stirring at -60°C for 2 h. A solution of $SiCl_4$ (0.04 mL, 0.375 mmol) in anhydrous CH_2Cl_2 (2 mL) was then added and the mixture was slowly warmed to RT, then kept under reflux for 2 h. Absolute methanol (CH_3OH, 500 mL) was added and the solution was kept under stirring for 1 h at RT.

The product was filtered, washed with methanol, then with distilled water until no chlorides were detected. The product was dried under vacuum for 4 h at RT. The yield of the reaction was 46%.

The degree of sulfonation was determined by Elemental Analysis (C and S content) and was DS = 0.05. The same method was used to evaluate the silicon content, which was %Si = 0.21±0.05.

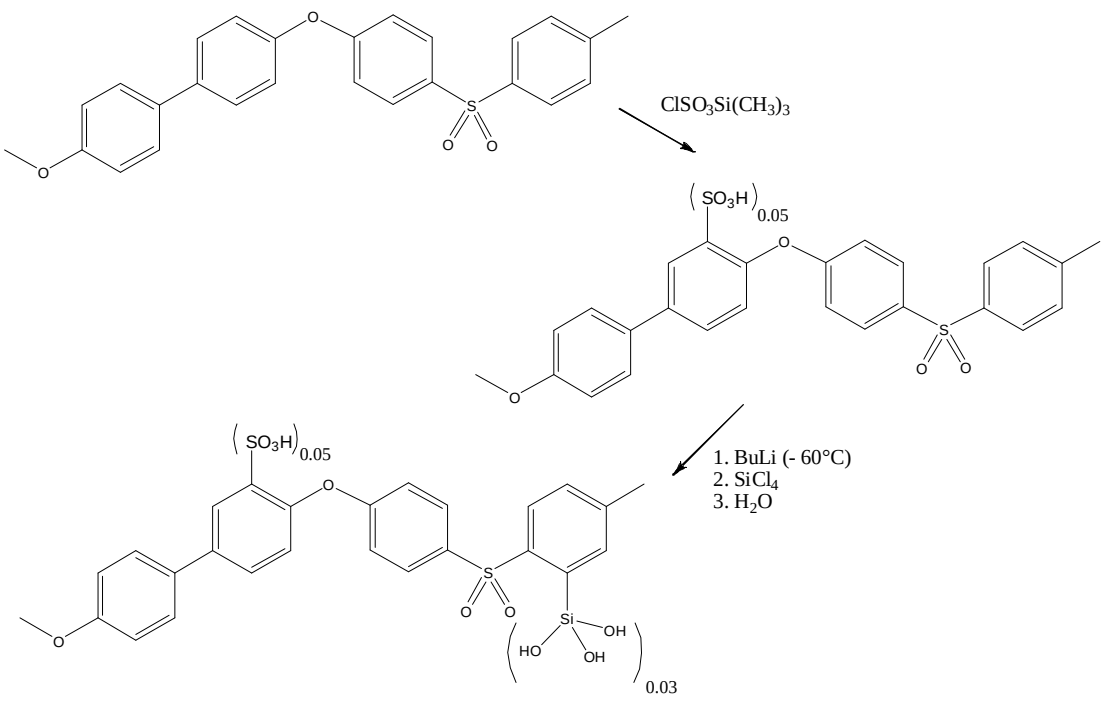

Scheme 4.5 - Synthesis of $Si_{0.03}S_{0.05}$PPSU.

Synthesis of S_2PPSU

PPSU (5 g, 12.5 meq) was dissolved in H_2SO_4 96% (250 mL) and the solution was stirred for 5 hours at 50°C. The mixture was poured in a large excess of ice-cold water, under continuous stirring, obtaining a white precipitate. After standing overnight, the precipitate was filtered and washed several times with cold water to neutral pH. The sulfonated polymer was then dried under vacuum for 5 h at room temperature. The yield of the reaction was 42%.

The DS of the product was evaluated by ^{1}H NMR spectroscopy and resulted to be 2.0.

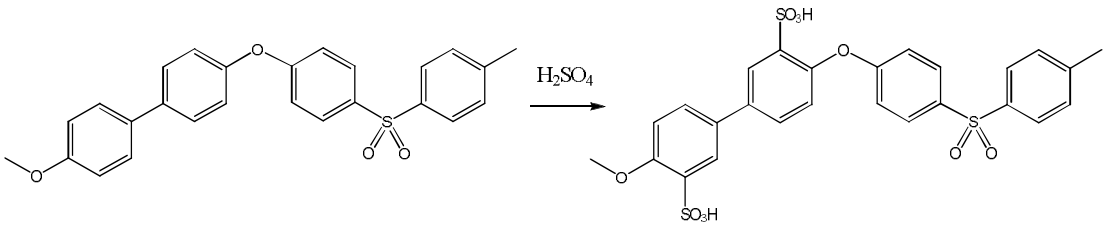

Scheme 4.6 - Synthesis of hybrid polymer S_2PPSU.

Synthesis of HSiSPPSU

The hybrid polymer HSiSPPSU was prepared by reaction of equimolar amounts of $Si_{0.2}S_2$PPSU and $Si_{0.03}S_{0.05}$PPSU in DMAc at 120°C for 2 days, in presence of pyridine. The mixture was dried under vacuum and the residue was washed with water, then dried under vacuum.

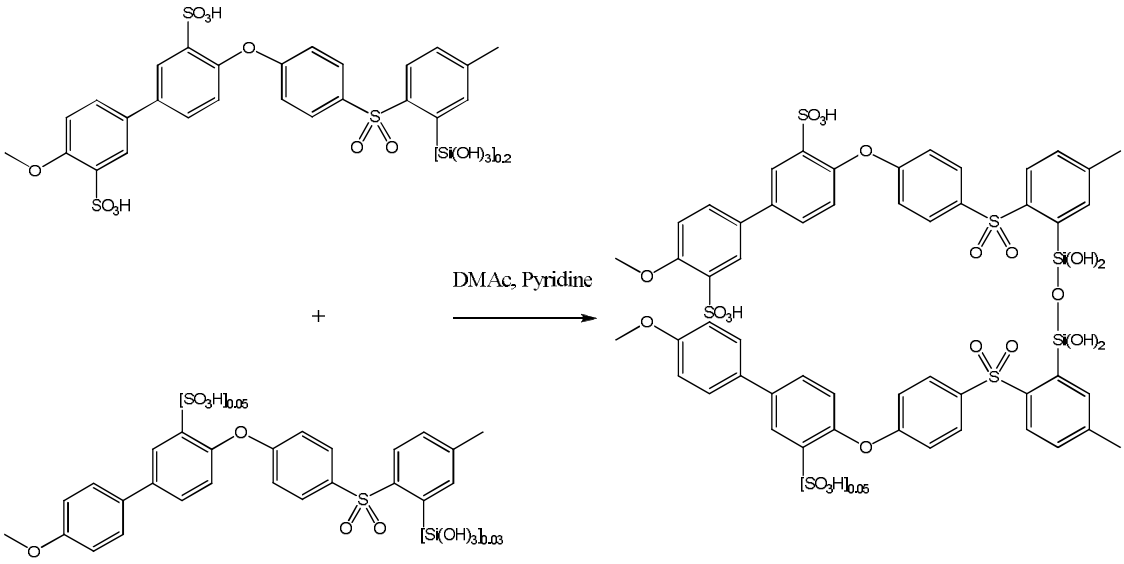

Scheme 4.7 - Synthesis of hybrid polymer HSiSPPSU.

4.4.2 Results and Discussion

Polyphenylsulfone was chosen as starting material because its solubility in organic solvents allows to carry out several functionalization reactions in homogeneous conditions, making it a versatile material from a synthetic standpoint, a condition that is seldom met by other polymeric systems.

Two synthetic pathways were followed to obtain differently silylated and sulfonated PPSU derivatives.

In the first one, PPSU was silylated by reaction with $SiCl_4$, to obtain the desired amount of silanol groups covalently bound to the backbone. Then, $Si_{0.2}$PPSU was sulfonated by reaction with concentrated sulphuric acid up to the maximum degree of sulfonation, obtaining the final product $Si_{0.2}S_2$PPSU.

In the second synthetic route, the use of the mild sulfonating agent $ClSO_3Si(CH3)_3$ allowed a careful control of the degree of sulfonation, and PPSU with a lower DS was obtained. Then, the product was silylated by reaction with $SiCl_4$ and subsequent hydrolysis led to the final product $Si_{0.03}S_{0.05}$PPSU.

Sulfonated polyphenylsulfone was synthesized by reaction of PPSU with concentrated sulphuric acid. **Figure 4.23** shows the ^{1}H NMR spectrum of S_2PPSU,

where the H**e** protons showed a down-field shift due to deshielding effect of the sulfonic acid group in *ortho* position.

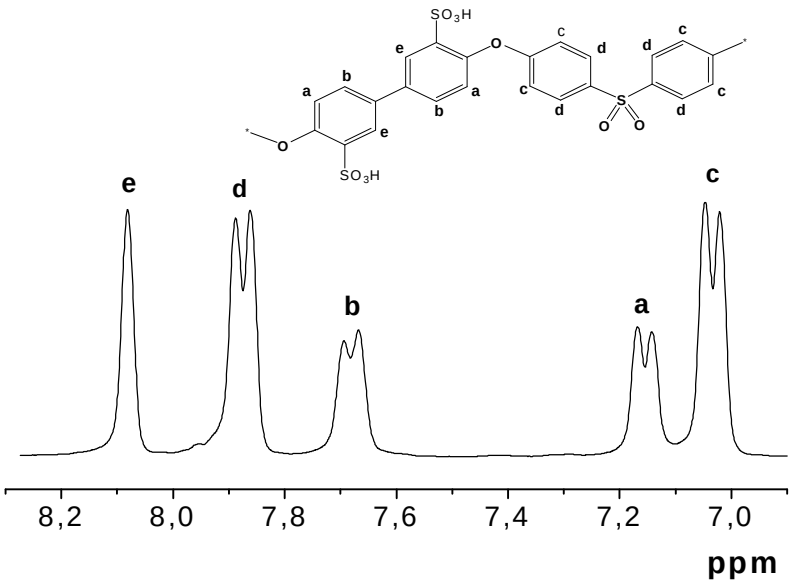

Figure 4.23 - ^{1}H NMR spectrum of S_2PPSU.

Thus, the DS of sulfonated PPSU was evaluated using the following equation: [2]

$$DS = \frac{\left(12 - \frac{4 \times A_{abc}}{A_{de}}\right)}{\left(2 + \frac{A_{abc}}{A_{de}}\right)} \qquad \textit{(Eq. 4.6)}$$

where A_{abc} and A_{de} are the sums of the area of peaks due to a, b, c protons, and d, e protons, respectively.

The structural characterization of PPSU derivatives was performed by ATR/FTIR spectroscopy. **Figure 4.24** shows the spectra of $Si_{0.2}S_2$PPSU and $Si_{0.03}S_{0.05}$PPSU (traces a and b, respectively), compared with that of only sulfonated polyphenylsulfone S_2PPSU (trace c) and that of the starting material PPSU (trace d).

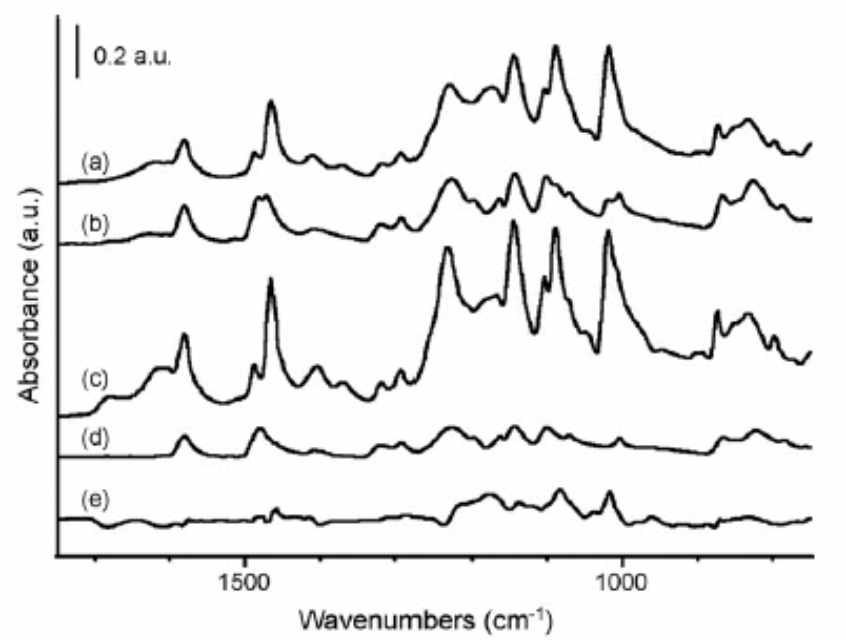

Figure 4.24 - ATR/FTIR spectra of (a) $Si_{0.2}S_2$PPSU, (b) $Si_{0.03}S_{0.05}$PPSU, (c) S_2PPSU, (d) PPSU and (e) = (a)-(c) subtraction spectrum.

All spectra are dominated by PPSU infrared signals, thus, to highlight the differences between products deriving from silylation and sulfonation processes, the spectrum obtained subtracting the signals of S_2PPSU from those of $Si_{0.2}S_2$PPSU is shown in **Figure 4.24e**.

The absorptions at 1138 and 1082 cm^{-1} can be attributed to ring modes of 1,4- and 1,2,4-substituted benzene. The presence of covalently linked silicon is confirmed by the weak signal at 1112 cm^{-1} which is typical of Ph–Si stretching mode.[3] The absorption due to vibrations of the Si–OH groups is observed at about 960 cm^{-1}, [4] while the absence of bands at 1220 and 1090 cm^{-1} confirms the lack of inorganic silicon.[5]

Similar features, although with decreased intensity given the much lower DS and DSi, were observed in the spectrum of $Si_{0.03}S_{0.05}$PPSU (**Figure 4.24b**). The presence of sulfonic groups in $Si_{0.03}S_{0.05}$PPSU is demonstrated by the band at 1165 cm^{-1}. Its lower position and intensity with respect to the bands observed in the spectrum of $Si_{0.2}S_2$PPSU are indicative of a lower sulfonation degree, in agreement with the milder reaction conditions and with elemental analysis results.

The main spectral differences between the two sulfonated and silylated polymers were observed in the region 1150–1000 cm^{-1}: the signals are due to ring modes of polysubstituted benzene and their position and intensities reflect the lower substitution degree of $Si_{0.03}S_{0.05}$PPSU with respect to $Si_{0.2}S_2$PPSU.

Membranes made up of silylated and sulfonated PPSU derivatives were prepared to verify their possible application as polymeric electrolytes. Membranes of $Si_{0.2}S_2$PPSU showed poor mechanical properties, whilst in the case of $Si_{0.03}S_{0.05}$PPSU, conductivity was almost negligible.

It was then chosen to prepare a hybrid polymer by covalent cross-linking, *via* Si–O–Si bridging moieties, between two polymers having different degrees of sulfonation and silylation to merge their conductivity and mechanical properties in an unique material.

The hybrid polymer HSiSPPSU was synthesized by non-hydrolytic sol–gel reaction of $Si_{0.2}S_2$PPSU and $Si_{0.03}S_{0.05}$PPSU, as shown in **Scheme 4.7**.

Figure 4.25a shows the ATR/FTIR spectrum of the condensation product, HSiSPPSU. The spectral features reflect the equimolecular ratio of the two precursors.

The inset in **Figure 4.25d** shows the difference spectrum obtained subtracting the spectra of the precursors (**Figure 4.25 b** and **c**) from that of HSiSPPSU with a subtraction factor equal to 1.

The presence of new components due to Ph–Si stretching signals together with the band at 1030 cm^{-1}, typical of Si–O–Si groups, indicate the formation of inorganic cross-linking between the two different polymers.

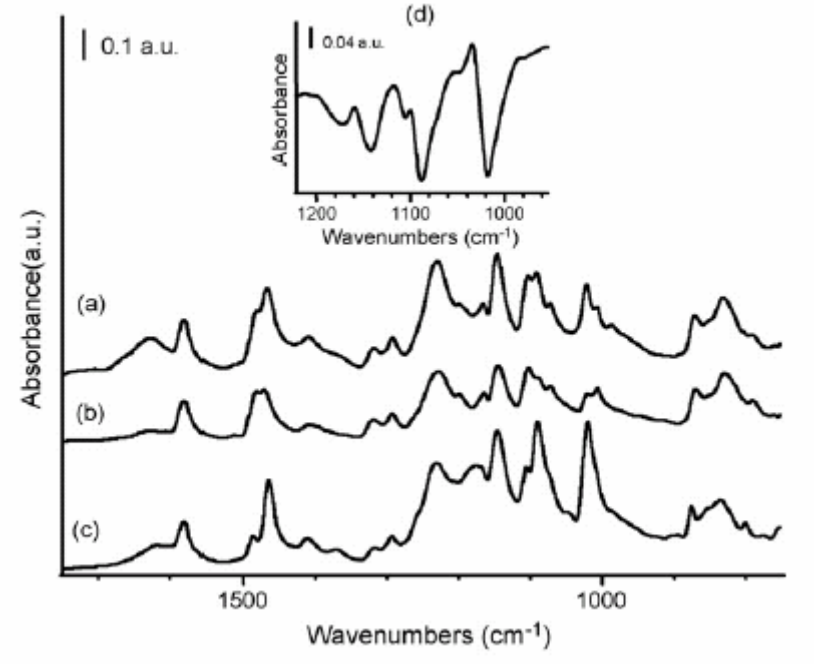

Figure 4.25 - ATR/FTIR spectra of (a) HSiSPPSU, (b) $Si_{0.03}S_{0.05}$PPSU, (c) $Si_{0.2}S_2$PPSU and (d) = (a)-(b)-(c) subtraction spectrum.

The physicochemical properties of the hybrid polymer were suitable for the preparation of flexible and homogeneous membranes.

Their hydration behaviour was considered in terms of λ values that were determined by water uptake measurements. The equilibrium value resulted to be λ = 10.

Conductivity of the membranes was measured under controlled humidity conditions, due to the increasing interest in developing proton-conducting electrolyte for fuel cells operating at high temperatures and low relative humidity values.

Figure 4.26 shows the comparison between the Nyquist plots of HSiSPPSU membrane measured at 110°C at two different relative humidity values, *i.e.* 20% and 50%.

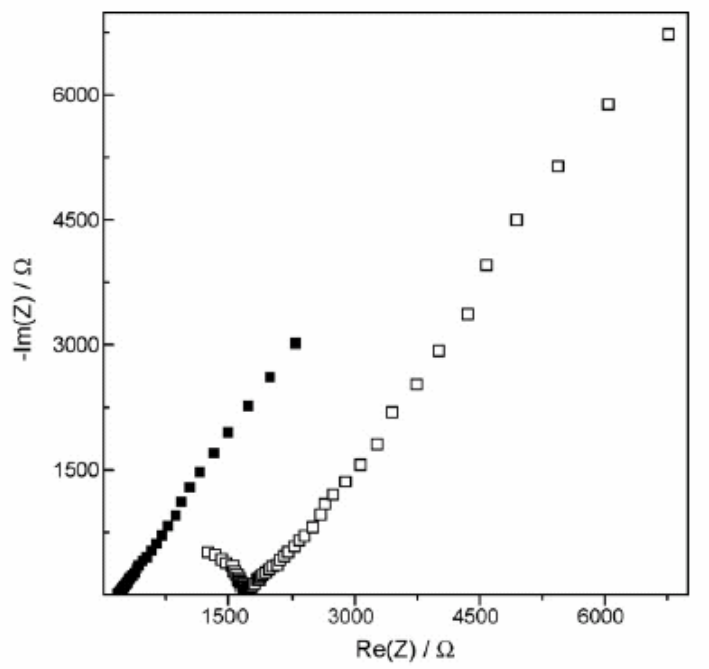

Figure 4.26 - Nyquist plot of HSiSPPSU membrane measured at 20% (□) and 50% (■) RH, at 110°C.

At RH values lower than 50%, the Nyquist plots consisted of two regions: the high-frequency arc due to the bulk of the electrolyte and the low-frequency straight line due to the effect of blocking electrodes.

The diameter of the arc decreased with increasing RH and eventually vanished at RH=50%. Above such RH value only a linear spike was observed. The same trend was observed for the EIS measurements carried out at 130°C.

The disappearance of the arc suggests that continuous water pathways form in the membrane with the increment of RH, and the conductivity increases because the protons displace more easily through the well interconnected liquid phase. At high RH the intermolecular proton transfer is involved in the mobility of protonic charge carriers, indicating that transport of H^+ by Grotthuss mechanism becomes increasingly significant.[6]

The resistance of HSiSPPSU membrane was calculated by a linear fit of the impedance spectra in their linear portion and the conductivity values were then obtained using the ***Eq. 4.3***.

Figure 4.27 shows the conductivity of the membrane as a function of relative humidity, measured at 110 and 130°C.

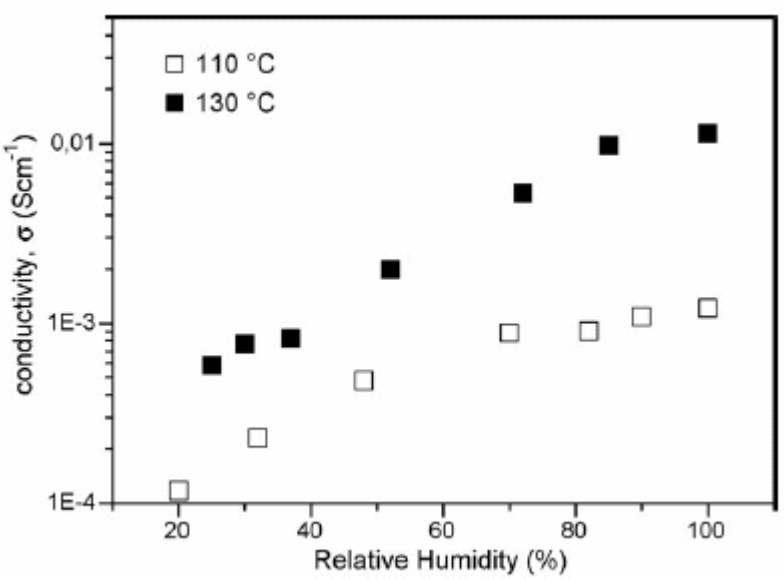

Figure 4.27 - Conductivity as a function of RH of HSiSPPSU membrane at 110 (□) and 130°C (■).

In agreement with the water-assisted conduction mechanism, conductivity increased with increasing of RH values. An increase of conductivity with temperature was also observed in the whole range of investigated RH, probably because of increased chain mobility favouring proton transfer.

The conductivity at 130°C and 100% RH reached 0.01 S cm^{-1}, showing that the hybrid polymer membrane is a suitable candidate for application in PEMFCs operating at T>100°C.

4.4.3 References

1) S. Licoccia, M.L. Di Vona, A. D'Epifanio, Z. Ahmed, S. Bellitto, D. Marani, B. Mecheri, C. de Bonis, M. Trombetta, E. Traversa, *J. Power Sources* **2007**, 167, 79.

2) A. Dyck, D. Fritsch, S.P. Nunes, *J. Appl. Polym. Sci.* **2002**, 86, 2820.

3) L.J. Bellamy, *The Infrared Spectra of Complex Molecules*, Vol. 1, 3rd ed., Chapman and Hall, London, **1980**.

4) Z. Olejniczak, M. Lęcza, K. Cholewa-Kowalska, K. Woitach, M. Rokita, W. Mozgawa, *J. Mol. Struct.* **2005**, 744–747, 465.

5) E. Rodríguez-Castellón, A. Jiménez-López, P. Maireles-Torres, D.J. Jones, J. Rozière, M. Trombetta, G. Busca, M. Lenarda, L. Storaro, *J. Solid State Chem.* **2003**, 175, 159.

6) K.D. Kreuer, *J. Membr. Sci.* **2001**, 185, 29.

5 Conclusions

The primary objective of the present research was the preparation of new proton conducting membranes by the development of suitable procedures for polymers synthesis that allowed to obtain electrolytes having good performance in terms of stability and conductivity.

The main approach proposed in this work was the synthesis of sulfonated aromatic polymers having silicon-containing moieties covalently bound to the backbone. This method allows to modulate the proton conductivity and stability of the electrolyte by the dosage of sulfonic acid groups and inorganic moieties, obtaining materials with desired features for PEMFC application.

A novel synthetic pathway was developed to obtain highly sulfonated PEEK with hydrolytic and thermal stabilities due to the presence of phenylsilanol groups covalently bound to the aromatic chain. The polymer $PhSi_{0.1}S_{0.9}$PEEK was synthesized *via* (i) sulfonation of PEEK, (ii) conversion of SPEEK into sulfonyl chlorinated derivative (PEEKSO2Cl), (iii) silylation, followed by hydrolysis. The solubility of PEEKSO2Cl in organic solvents enabled an efficient and reproducible method to introduce the silicon-containing units into the polymeric structure.

This outlined pathway represents a powerful and versatile tool for synthetic purposes due to the chemical reactivity of functional groups of the products, that can be used to obtain PEEK derivatives having different features. In particular, the ratio between hydrophilic and hydrophobic domains, that determines hydrolytic stability and conductivity of the electrolyte, could be modulate by varying the phenylsilanol groups amount and/or the type of silicon-containing substituent covalently bond to the aromatic chain of sulfonated PEEK.

The structural characterization of $PhSi_{0.1}S_{0.9}$PEEK was carried out by the analysis of ^{1}H NMR, ^{13}C NMR and ATR/FTIR spectra that showed the success of the synthetic route. Thermogravimetric analysis indicated that the presence of phenylsilanol groups stabilizes the aromatic matrix of the sulfonated polyetheretherketone.

Blends of $PhSi_{0.1}S_{0.9}$PEEK and $S_{0.5}$PEEK were prepared using different weight ratios of the two polymers, obtaining membranes with hydrolytic stability and proton conductivity that seems to be promising for PEMFC applications.

The derivative of PPSU having high degree of sulfonation and phenylsilanol moieties covalently bound to the aromatic chain was prepared as membrane material. The synthesis of $PhSi_{0.2}S_2$PPSU was carried out *via* (i) silylation of polyphenylsulfone, followed by hydrolysis, and (ii) sulfonation up to the maximum DS. The solubility of PPSU in organic solvents enabled an direct and reproducible method to bind the silicon-containing moieties to the polymeric structure.
Blends of $S_{0.5}$PEEK and $PhSi_{0.2}S_2$PPSU were prepared using different weight ratios of the two polymers. The formation of physically crosslinked polymers allowed to obtain electrolytes with higher hydrolytic stability and increased proton conductivity with respect to those of pure $S_{0.5}$PEEK membrane. The synergic effect of the two polymers might be related to the modification of the hydrophilic/hydrophobic separation in the blend membranes that makes easier proton transfer.
Blend membranes showed also better performance in DMFC, where a reduced methanol permeability was observed. Moreover, at temperature values as high as 100°C, pure $S_{0.5}$PEEK membrane underwent a mechanical degradation and eventually dissolved, whilst the blend systems maintained a considerable stability allowing to obtain adequately high power density values. In particular, remarkable performance was observed for 5 wt.% blend membrane, indicating that it is a promising electrolyte for DMFCs operating at intermediate temperatures.

Another point of interest was the synthesis of the organic-inorganic hybrid polymer HSiSPPSU, where the aromatic chains of two PPSU derivatives were covalently crosslinked *via* inorganic moieties, to obtain the synergic effect of polymers having different electrical and mechanical properties.
The condensation of the two differently silylated and sulfonated polyphenylsulfone: $Si_{0.2}S_2$PPSU and $Si_{0.03}S_{0.05}$PPSU, was carried out by non-hydrolytic sol-gel reaction between the silanol groups that led to the formation of Si-O-Si bonds, as demonstrated by ATR/FTIR analysis.

The electrochemical characterization of HSiSPPSU membranes by EIS showed adequately high conductivity values to make the hybrid polymer a suitable candidate for application as electrolyte in PEMFCs operating at $T > 100$°C.

Therefore, the electrolytes based on functionalized polyetheretherketone and/or polyphenylsulfone are not only interesting low-cost alternative materials, they may also help to reduce the problems associated with methanol crossover in DMFCs and decrease of conductivity at temperature over 80°C, demonstrating the main role played by chemistry in the preparation of membrane materials for PEMFC applications.

List of Acronyms

AFC	Alkaline Fuel Cell
ATR/FT	Attenuated Total Reflectance Fourier Transform
DMFC	Direct Methanol Fuel Cell
DS	Degree of Sulfonation
DSC	Differential Scanning Calorimetry
DSi	Degree of Silylation
EIS	Electrochemical Impedance Spectroscopy
MCFC	Molten Carbonate Fuel Cell
MEA	Membrane Electrode Assembly
NMR	Nuclear Magnetic Resonance
OIPs	Organic-Inorganic Polymers
ORMOSILs	Organic-Modified Silicates
PAFC	Phosphoric Acid Fuel Cell
PBI	Polybenzimidazole
PEEK	Polyetheretherketone
PEM	Proton Exchange Membrane
PEMFC	Proton Exchange Membrane Fuel Cell
PFSA	Perfluorosulfonic Acid
PPSU	Polyphenylsulfone
PSF	Polysulfone
PTFE	Polytetrafluoroethylene
SOFC	Solid Oxide Fuel Cell
SPEEK	Sulfonated Polyetheretherketone
TGA	Thermogravimetric Analysis

List of Schemes

List of Tables

List of Figures

List of Papers

I. C. de Bonis, A. D'Epifanio, M. L. Di Vona, C. D'Ottavi, B. Mecheri, E. Traversa, M. Trombetta, S. Licoccia, *Proton Conducting Hybrid Membranes Based on Aromatic Polymers Blends for Direct Methanol Fuel Cell Applications*, Fuel Cells, DOI: 10.1002/fuce.200800112.

II. C. de Bonis, A. D'Epifanio, B. Mecheri, M. L. Di Vona, M. Trombetta, E. Traversa, S. Licoccia, *Hybrid Membranes based on Aromatic Polymer Blends for Fuel Cell Applications*, Solid State Ionics **2008**, edited by E. Traversa, T. Armstrong, K. Eguchi, M.R. Palacin (Mater. Res. Soc. Symp. Proc. Vol. 1126, Warrendale, PA, 2009), S12-04.

III. E. Sgreccia, M. Khadhraoui, C. de Bonis, S. Licoccia, M. L. Di Vona, P. Knauth, *Mechanical Properties of Hybrid Proton Conducting Polymer Blends Based on Sulfonated PolyEtherEtherKetones*, Journal of Power Sources **2008**, 178, 667.

IV. S. Licoccia, M. L. Di Vona, A. D'Epifanio, Z. Ahmed, S. Bellitto, D. Marani, B. Mecheri, C. de Bonis, M. Trombetta, E. Traversa, *SPPSU-Based Hybrid Proton Conducting Polymeric Electrolytes For Intermediate Temperature PEMFCs*, Journal of Power Sources **2007**, 167, 79.

Riassunto

Le celle a combustibile con membrane a scambio protonico (PEMFCs) sono alternative sorgenti di energia che offrono numerosi vantaggi come l'alta efficienza, l'alta densità di potenza e la bassa emissione d'inquinanti. Esse sono impiegate nelle macchine ad idrogeno e nei dispositivi elettronici quali computer e cellulari alimentati con metanolo. La diffusione su larga scala di queste tecnologie punta sullo sviluppo di membrane a scambio protonico di nuova generazione, il cui costo di produzione sia compatibile con un mercato di massa. Tali conduttori protonici devono esibire una buona conducibilità, stabilità chimica e termica.

Nel presente lavoro, diverse strategie sono state impiegate per la preparazione di materiali a conduzione protonica a partire dai polimeri termoplastici aromatici: *polietereterchetone* (PEEK) e *polifenilsolfone* (PPSU). Di particolare rilevanza è la funzionalizzazione di tali polimeri mediante l'introduzione sulla catena aromatica di gruppi solfonici e gruppi contenenti silicio. Infatti, questo approccio sintetico permette di controllare la microstruttura del polimero, modulando il rapporto tra la fase idrofila e quella idrofoba, da cui dipendono fortemente le prestazioni dell'elettrolita.

Diversi tipi di membrane sono state preparate impiegando: PEEK solfonato (SPEEK) e/o PPSU solfonato, variamente funzionalizzati con gruppi contenenti silicio, al fine di ottenere l'effetto sinergico derivante dalla combinazione di polimeri aventi diverse conducibilità protonica e caratteristiche meccaniche.

I sistemi *ibridi* sono stati preparati mediante la reazione *sol-gel* che ha portato alla formazione dei legami covalenti Si-O-Si tra due derivati del PPSU diversamente funzionalizzati. Le membrane *blend* sono state invece preparate mescolando, durante il processo di *casting*, derivati del PEEK e/o PPSU. La caratterizzazione dei materiali ha riguardato l'analisi della struttura dei polimeri sintetizzati e delle proprietà chimico-fisiche ed elettrochimiche delle membrane. Risultati molto positivi sono stati ottenuti dai test eseguiti sulle membrane in un prototipo di cella a combustibile operante a metanolo diretto.

Parole chiave: celle a combustibile; membrane a scambio protonico; polimeri termoplastici aromatici; sintesi; risonanza magnetica nucleare; spettroscopia infrarossa; spettroscopia d'impedenza elettrochimica.